75

Copy

[redacted] NASA TM X-561

NASA TM X-561

[redacted]

Declassified by authority of NASA Classification Change Notices No. 113 dated 1/24/67

TECHNICAL MEMORANDUM

PERFORMANCE CHARACTERISTICS OF THE LITTLE JOE LAUNCH VEHICLE

By Ronald Kolenkiewicz and John C. O'Loughlin

Manned Spacecraft Center
Houston, Texas

[redacted] hibited by law.

NATIONAL AERONAUTICS AND SPACE ADMINISTRATION

WASHINGTON September 1962

[redacted]

1D

NATIONAL AERONAUTICS AND SPACE ADMINISTRATION

TECHNICAL MEMORANDUM X-561

PERFORMANCE CHARACTERISTICS OF THE LITTLE JOE LAUNCH VEHICLE*

By Ronald Kolenkiewicz and John C. O'Loughlin

SUMMARY

A summary of performance data is given for the first five Project Mercury Little Joe flights. Some of these data are compared with calculated performance characteristics and are shown to be in good agreement. Curves showing calculated maximum performance characteristics for the Little Joe launch vehicle are presented over a wide range of take-off weights, launch angles, and staging times as an aid in the prediction of performance parameters of the Little Joe launch vehicle when used in future projects.

INTRODUCTION

Little Joe is the designated name of the solid-propellant launch vehicle that was designed by the National Aeronautics and Space Administration to test the Project Mercury spacecraft at certain critical conditions that would be encountered on the exit phase of an earth-orbiting mission. As used in the Project Mercury flight-test program the launch vehicle was conceived as a simple and relatively inexpensive means for determining full-scale Project Mercury spacecraft aerodynamics and proving systems concepts. The launch vehicle is capable of propelling a full-scale Project Mercury spacecraft to speeds up to a Mach number of 6; hence, most of the critical orbital-launch abort conditions can be simulated. Satisfactory performance results have been attained by the first five flights made by the launch vehicle in the Project Mercury program. As a result of its success in this program, it is felt that the launch vehicle or a scaled-up version could be utilized in future areas of research and development. These areas of research and development could include a space trainer for astronauts as well as a check-out for landing, control, navigational, and abort systems.

---

*Title, Unclassified.

[redacted]

The purpose of this paper is to summarize some of the performance characteristics of the launch vehicle, both calculated and actual, so that an estimate of its performance can be made for future projects.

DESCRIPTION OF LAUNCH VEHICLE

The launch vehicle is fin stabilized and consists of a cluster of solid-fuel rocket motors. The spacecraft is attached to the launch
vehicle by means of an adapter. Figures 1 and 2 show the launch vehi- S
cle, the adapter, and a simulated Project Mercury spacecraft. 22

The propulsion system for the launch vehicle nominally consists of a cluster of eight solid-fuel rocket motors – four main motors and four auxiliary motors. The four main motors are either Thiokol Castor (XM-33E2) or Thiokol Pollux (XM-33E4) rocket motors, and the four auxiliary rocket motors are Thiokol Recruit motors (XM-19E1-C12). The general arrangement of the rocket cluster is shown in figure 3, and typical performance characteristics of the solid-fuel rocket motors are shown in figures 4 to 6.

Depending on the mission to be performed, there are four launch-vehicle configurations which are classified by the number and type of rocket motors used. The motors used in the configurations are presented in table I. The four configurations are made possible by the fact that Castor and Pollux motors have the same physical dimensions but the Castor motors have a greater impulse than the Pollux motors. (See figs. 4 and 5.) The ignition sequence for the launch vehicle is the firing of two main motors and four auxiliary motors at take-off and the remaining two main motors (for the type II and type IV vehicles) at a preset time (staging time) after take-off. Both the main and auxiliary rocket motors used in the launch vehicle have canted nozzles. These canted nozzles direct the thrust vector of the motors through the mean center of gravity of the vehicle, and therefore minimize any destabilizing moments that would be caused by motor failure or time differences in ignition and burnout. The cant angle on the main motors is 11° measured through the center line at station 496.8, and the cant angle on the auxiliary motors is 12° measured through the center line at station 529.4. (See fig. 3.)

The launch vehicle is aerodynamically stabilized by means of four fins. The launch vehicle and the spacecraft shown in figure 1 were designed to have static stability for Mach numbers between 0.0 and 6.0. Wind-tunnel data for this configuration up to Mach number 6.86 are given in reference 1. The thrusting and coasting drag parameter obtained from flight-test and wind-tunnel data is shown in figure 7. These data were corrected for base effects by using flight-test data.

The launch vehicle has large fins to insure static stability at a Mach number of 6.0. As a result, the launch vehicle is extremely stable at the lower Mach numbers. This extreme stability causes difficulty at launch since the vehicle tends to weathercock into the wind and go off course. In order to eliminate some of this weathercocking as well as to decrease the flight-path angle dropoff, the launch vehicle is accelerated rapidly by igniting two main motors and four auxiliary motors at take-off. Even with the high acceleration at take-off, the launch vehicle is sensitive to winds during the first moments of flight. A wind-correction method described in reference 2 has been used successfully
S on all of the launch-vehicle flights.
22

RESULTS AND DISCUSSION OF TRAJECTORY DATA

Flight Test

A summary of five flight tests of the Little Joe launch vehicle given in table II includes a list of the figure numbers of the various performance parameters obtained from these tests. The general configuration dimensions for the first four flights were similar to the configuration shown in figure 1. The fifth flight had an additional 18-inch-long adapter between the launch vehicle and the spacecraft in order to accommodate the retrorocket package of the production Project Mercury spacecraft. In the figures presented, the performance parameters for the flight tests were terminated when the spacecraft was separated from the launch vehicle. Note that this was not necessarily launch-vehicle burnout. In general, the data presented in figures 8 to 38 for the first five launch-vehicle flights are: altitude as a function of horizontal range and time histories of altitude, velocity, Mach number, dynamic pressure, and longitudinal acceleration. The exceptions include flight 1, which had no accelerometer and hence no longitudinal acceleration data, and flight 3, in which roll-rate and noise-level data were obtained and presented in figures 25 and 26. The first five flights include all of the launch-vehicle configurations listed in table I. Results of flight 1 are contained in reference 3.

Comparison of Flight Results With Calculated Results

Prior to each launch-vehicle flight a trajectory was calculated. These calculations were carried out on the IBM 704 electronic data processing machine and were essentially the numerical integration of the equations of motion for a point mass in a plane under the influence of gravity, thrust, and drag.

[redacted]

Only the calculations for type I and II launch vehicles are considered in this report since these vehicles exceed the performance of type III and IV launch vehicles, respectively. The only reason for using type III and IV launch vehicles is the fact that Castor rocket motors were not available at the time of some of the flights. Performance of type III and IV launch vehicles can be matched by type I and II launch vehicles by adding some ballast.

The flight-test data are shown in figures 19 to 23 to agree very well with the calculated data for flight 3 (type II launch vehicle). For flight 5 (type I launch vehicle), the flight-test data also agree S
very well with the calculated data as shown in figures 33 to 37. 22

Performance Estimates

Results of calculated data which give performance estimates for the type I and type II launch vehicles are given in figures 39 to 63. The maximum values of the trajectory parameters are given as a function of take-off weight, launch angle, and (in the case of type II launch vehicle) staging time. The trajectory parameters considered are: altitude, velocity, Mach number, dynamic pressure, and longitudinal load factor. Table III presents the range of staging times, take-off weights, and launch angles for which these performance estimates were made. The weight and balance for the type I and type II launch vehicles are given in table IV. The performance estimates are based upon the weights given in table IV, the thrusts given in figures 4 and 6, and the drag parameter given in figure 7. The figures showing performance estimates for the Little Joe type I and II launch vehicles are self explanatory and may be used in planning future projects utilizing the launch vehicles.

CONCLUDING REMARKS

The comparisons of calculated and flight-test data for the Little Joe launch vehicle have been shown to agree very well. On the basis of this agreement, more data have been calculated over a wide range of take-off weights, launch angles, and staging times and were presented as curves showing maximum performance characteristics, an aid in the planning of future projects utilizing the launch vehicles.

Manned Spacecraft Center,
National Aeronautics and Space Administration,
Langley Air Force Base, Va., February 26, 1962.

[redacted]

REFERENCES

1. Moseley, William C., Jr., and Smith, Robert P.: A Compilation of the Longitudinal Stability Characteristics of the Mercury Capsule-Booster Configurations. NASA TM X-560, 1962.

2. Rose, James T., and Rose, Rodney, G.: A Rapid Method of Estimating Launcher Setting To Correct for the Effects of Wind on the Trajectory of an Unguided Fin-Stabilized Rocket Vehicle. NASA TM X-492, 1961.

3. Royall, John F., Jr., and English, Roland D.: Investigation of Flight Performance of Little Joe Booster for Project Mercury. NASA TM X-298, 1960.

[redacted]

TABLE I.- LITTLE JOE LAUNCH-VEHICLE CONFIGURATIONS

Launch-vehicle type	Main motors	Auxiliary motors	Little Joe flight	Date launched
I	2 Castor	4 Recruit	5	Nov. 8, 1960
II	4 Castor	4 Recruit	3	Dec. 4, 1959
III	2 Pollux	4 Recruit	2	Nov. 4, 1959
III	2 Pollux	4 Recruit	4	Jan. 21, 1960
IV	4 Pollux	4 Recruit	1	Oct. 4, 1959

PRECEDING PAGE BLANK NOT FILMED.

[redacted]

TABLE II.- SUMMARY OF FIVE FLIGHT

Flight	Launch-vehicle type	Nominal zero wind launcher setting		Actual launcher setting		Wind conditions	Nominal rocket motor ignition sequence		Actual rocket motor ignition sequence		Weight	
		True azimuth, deg	Elevation, deg	True azimuth, deg	Elevation, deg		t, sec	Rocket motor	t, sec	Rocket motor	Take-off, lb	Burnout, lb
1	IV	110	80	94	78	Given in ref. 2	0	2 Pollux 4 Recruit	0	2 Pollux 4 Recruit	41,347	12,092
									[a]9	1 Pollux		
							25	2 Pollux	[a]18	1 Pollux		
2	III	135	75	110	76	Given in ref. 2	0	2 Pollux 4 Recruit	0	2 Pollux 4 Recruit	26,750	11,431
3	II	140	82	157	78	Given in ref. 2	0	2 Castor 4 Recruit	0	2 Castor 4 Recruit	43,554	12,540
							23	2 Castor	22.8	2 Castor		
4	III	135	77.1	135	70	Given in ref. 2	0	2 Pollux 4 Recruit	0	2 Pollux 4 Recruit	26,993	11,663
5	I	135	82.5	145	80.5		0	2 Castor 4 Recruit	0	2 Castor 4 Recruit	39,457	23,338

[a]Actual ignition sequence erratic because heat from the first two Pollux motors ignited the remaining Pollux motors; this difficulty was corrected in later flights.

[redacted]

DECL[redacted]FIED

S-22

TESTS OF LITTLE JOE LAUNCH VEHICLE

Center-of-gravity station		Figure numbers for -							
Take-off, in.	Burnout, in.	Altitude range	Altitude time history	Velocity time history	Mach number time history	Dynamic-pressure time history	Longitudinal-acceleration time history	Roll-rate time history	Other data presented
390.3	375.6	8	9	10	11	12	No instrumentation	No instrumentation	
388.8	325.28	13	14	15	16	17	18	No instrumentation	
392.0	374.0	19	20	21	22	23	24	25	Noise-level data, 26
391.5	329.5	27	28	29	30	31	32	Poor data	
378.5	—	33	34	35	36	37	38	Poor data	

[redacted]

[redacted]

TABLE III.- CALCULATED TRAJECTORIES FOR LITTLE JOE

TYPE I AND TYPE II LAUNCH VEHICLES

Launch-vehicle type	Staging time, sec	Take-off weight, lb	Launch angle, deg	Data figures
I	Not applicable	24,000 to 49,000	70, 75, 80, 85	39 to 43
II	19	40,000 to 50,000	70, 75, 80, 85	44 to 48
II	23	40,000 to 50,000	70, 75, 80, 85	49 to 53
II	27	40,000 to 45,000	70, 75, 80, 85	54 to 58
		45,000 to 50,000	80, 85	
II	31	40,000 to 45,000	70, 75, 80, 85	59 to 63
		45,000 to 50,000	80, 85	

S
22

[redacted]

DEC[redacted]FIED

TABLE IV.- WEIGHT AND BALANCE FOR LITTLE JOE COMPONENTS

Component	Weight, lb	Center-of-gravity station,[a] inches
Castor motor, loaded	8,785	403
Castor motor, empty	1,333	445
Recruit motor, loaded	364	485
Recruit motor, empty	100	487
Booster airframe	2,425	483

Weight Breakdown for Little Joe Type I Vehicle	
Component	Weight, lb
2 Castor motors, loaded	17,570
2 Castor motors, empty	2,666
4 Recruit motors, loaded	1,456
Booster airframe	2,425
Total take-off weight[b]	24,117

Weight Breakdown for Little Joe Type II Vehicle	
Component	Weight, lb
4 Castor motors, loaded	35,140
4 Recruit motors, loaded	1,456
Booster airframe	2,425
Total take-off weight[b]	39,021

[a] The forward end of the launch-vehicle airframe is at station 302. (See fig. 3.)

[b] Except for spacecraft and adapter.

[redacted]

[redacted]

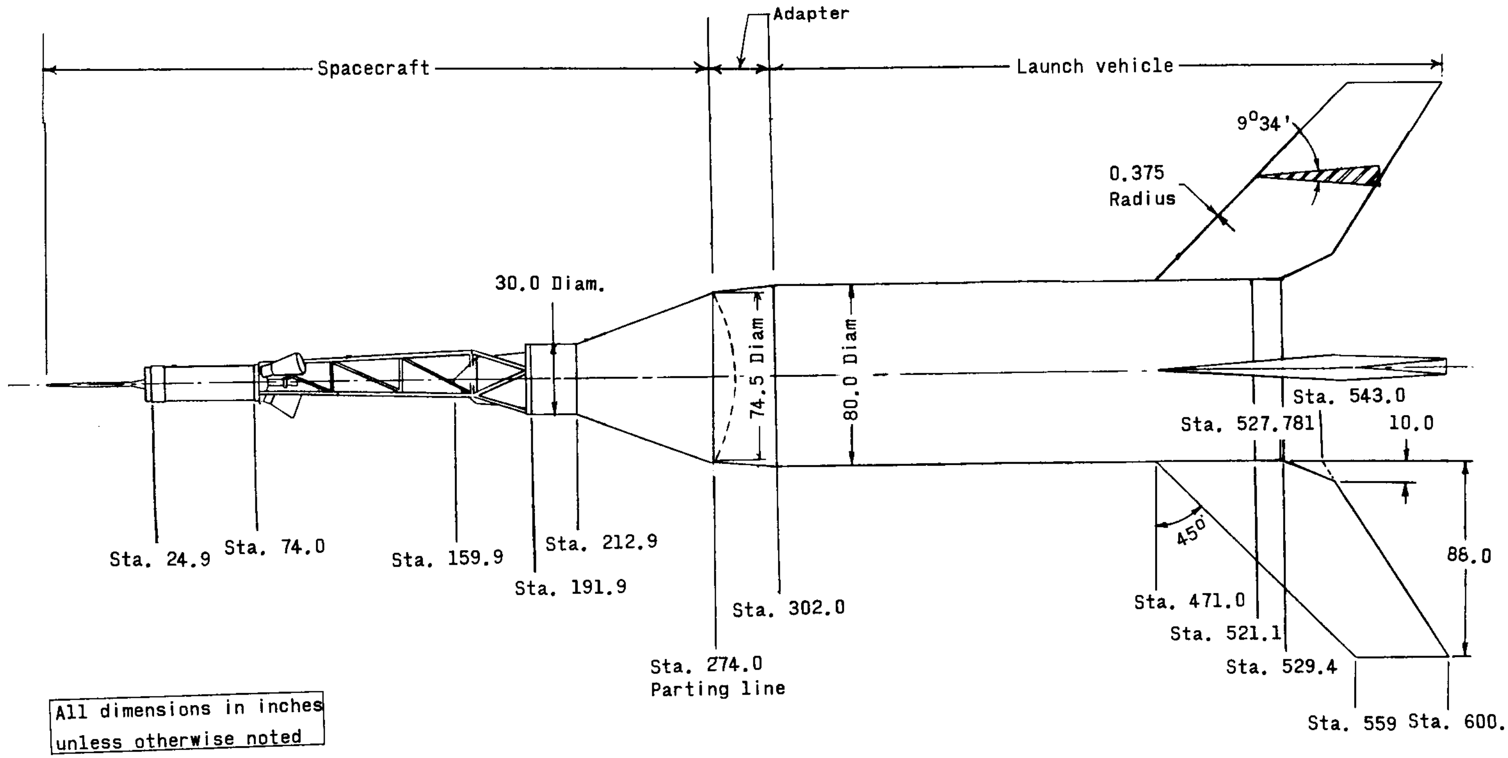

Figure 1.- General arrangement of Mercury Little Joe configuration with a simulated Project Mercury spacecraft. When the production Project Mercury spacecraft is used, the adapter has to be lengthened 18 inches in order to accommodate the retrorocket package.

[redacted]

S-22

Figure 2.- Little Joe ready for launch. G-61-29

[redacted]

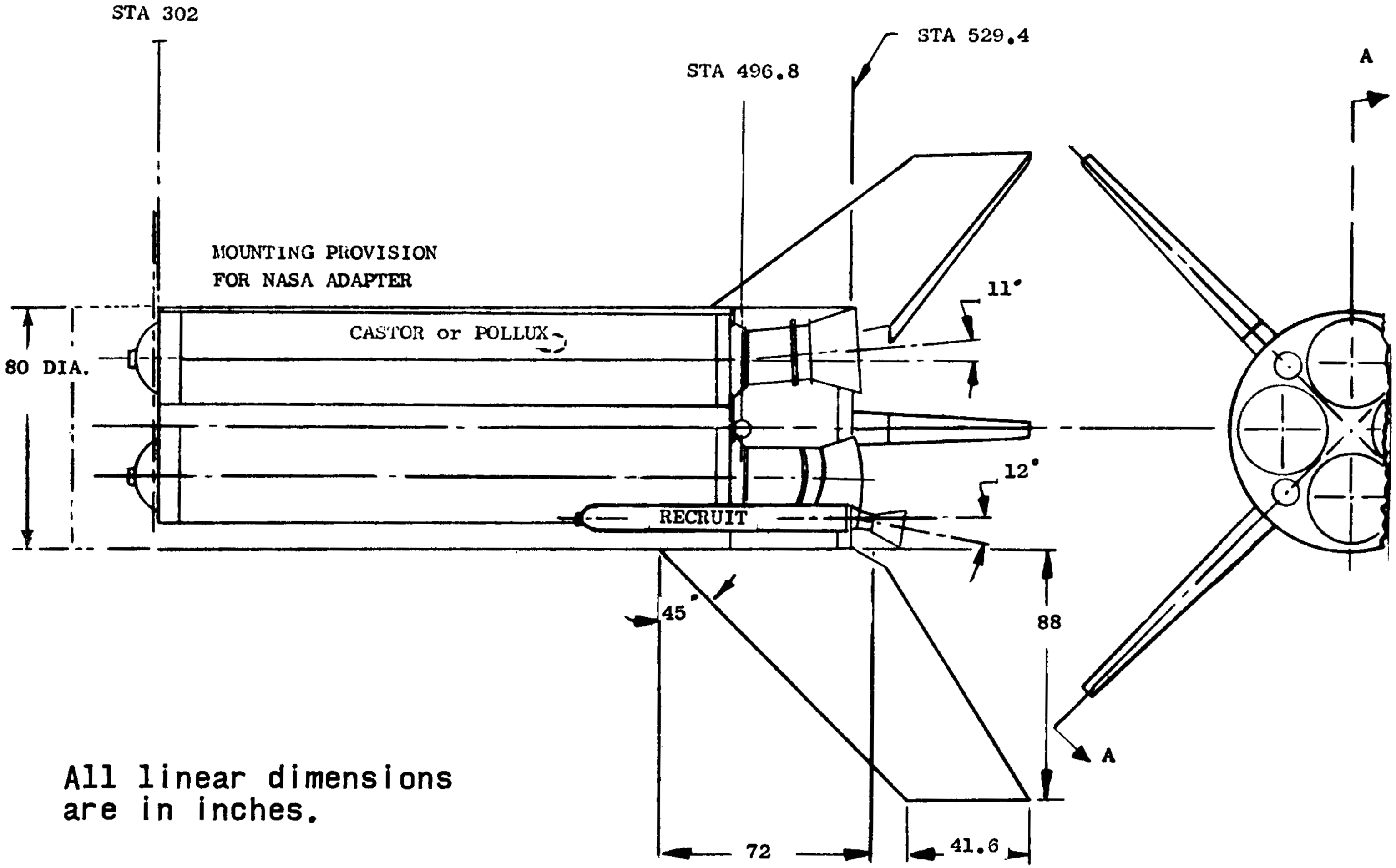

All linear dimensions
are in inches.

SECTION A-A

Figure 3.- General arrangement of the rocket cluster for Little Joe launch vehicle.

[redacted]

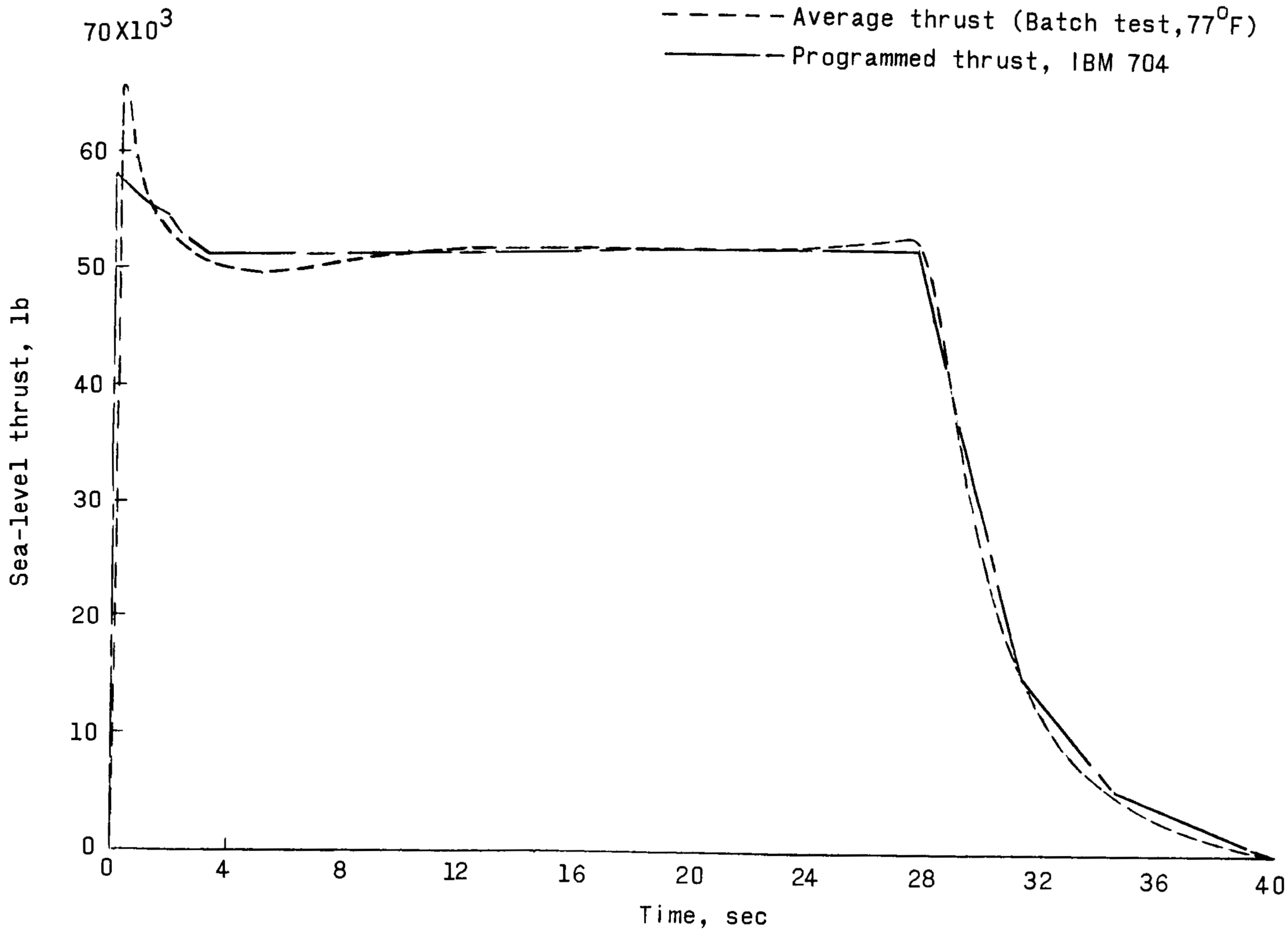

Figure 4.- Time history of sea-level thrust for one Castor rocket motor with an effective exit area of 2.69 sq ft.

[redacted]

[redacted]

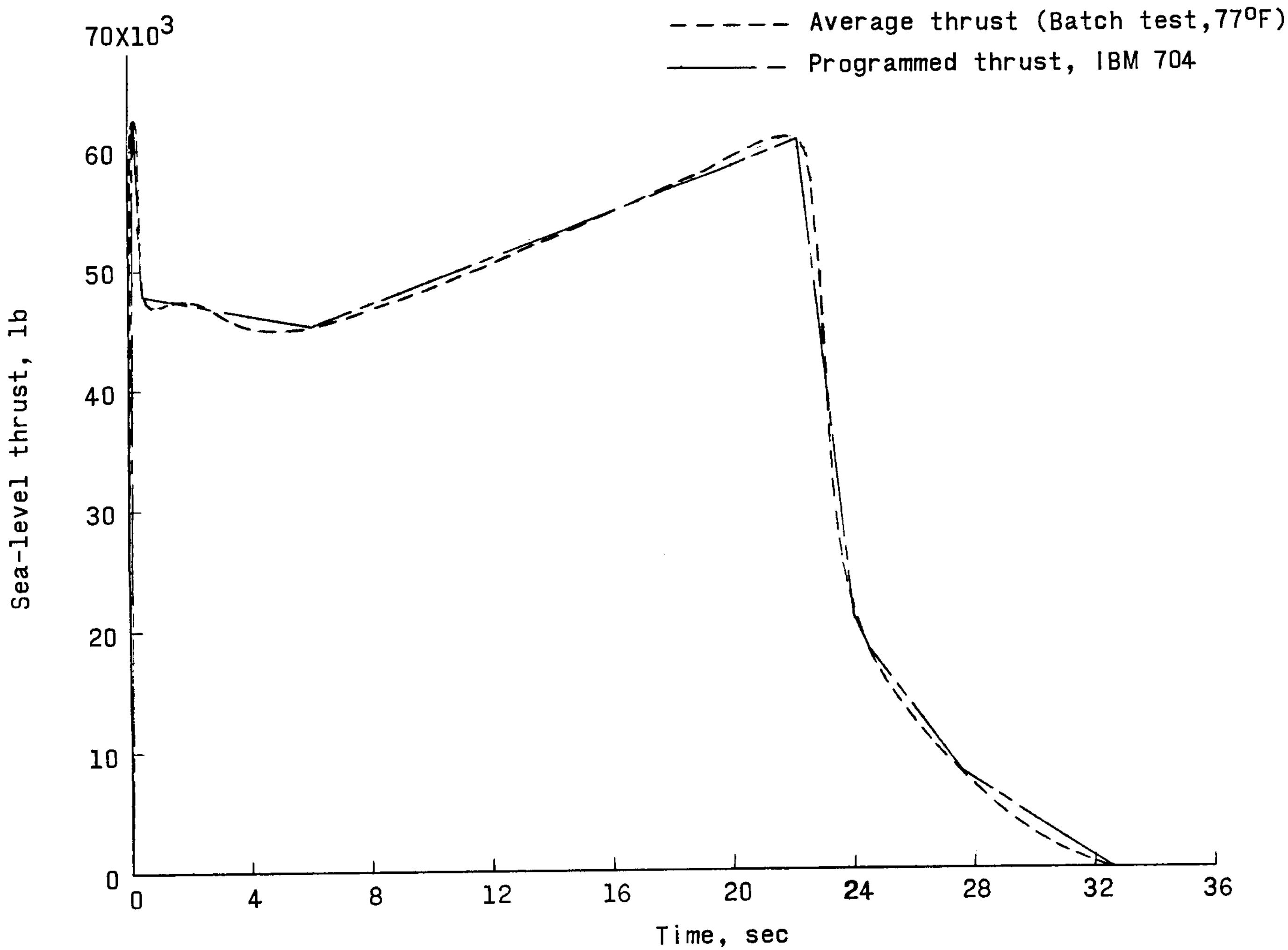

Figure 5.- Time history of sea-level thrust for one Pollux rocket motor with an effective exit area of 2.27 sq ft.

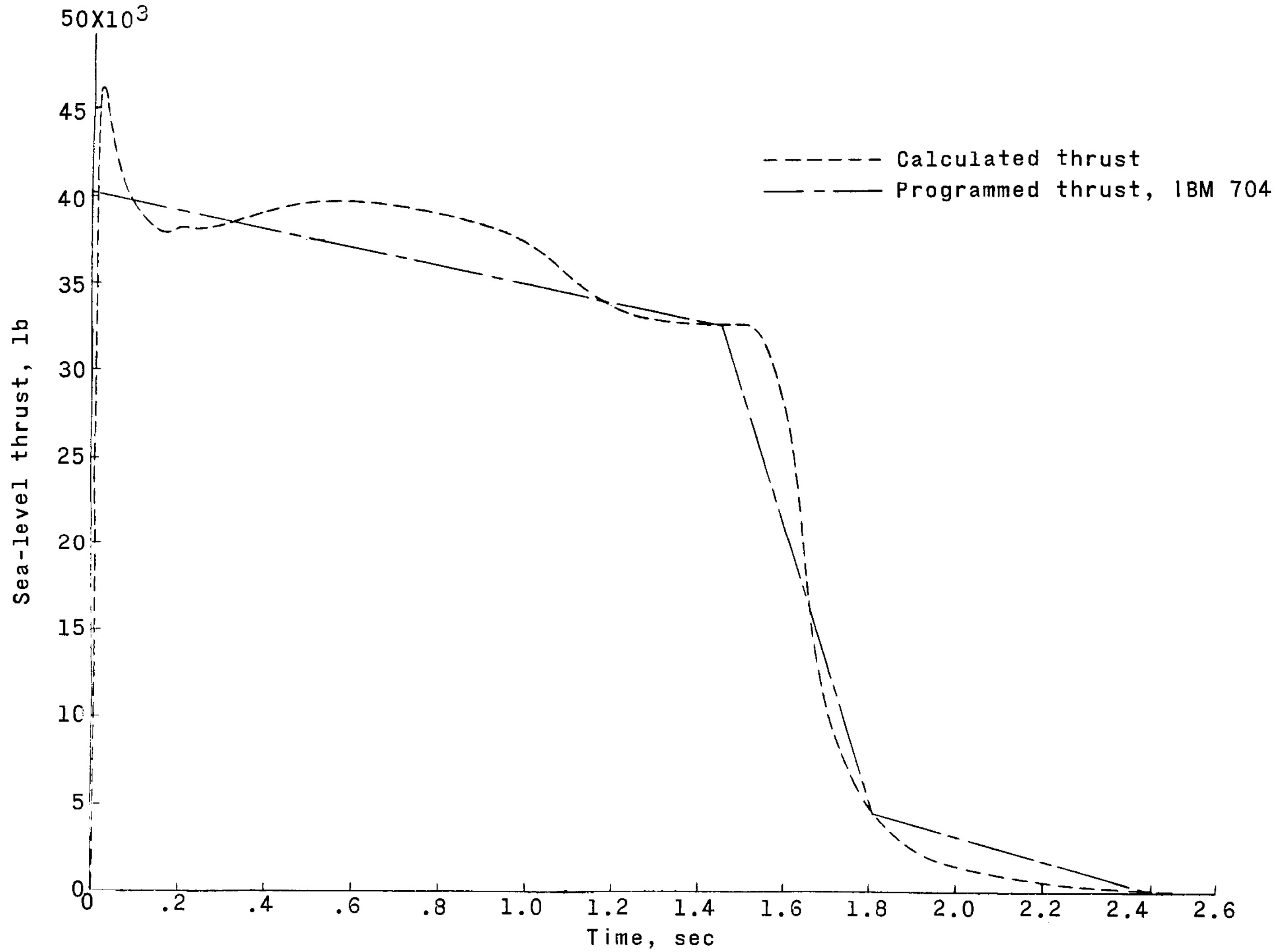

Figure 6.- Time history of sea-level thrust for one Recruit rocket motor with an effective exit area of 0.894 sq ft.

[redacted]

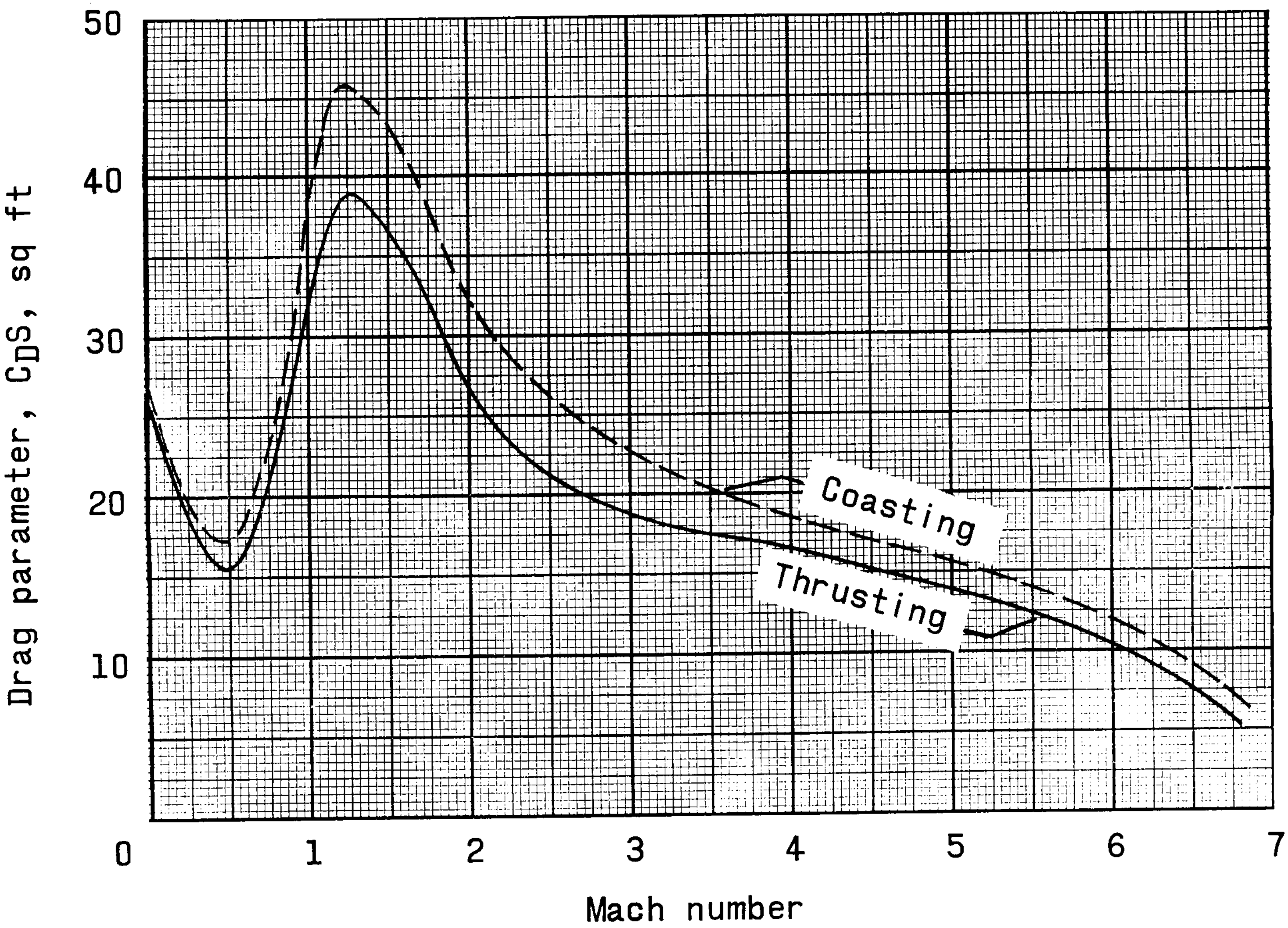

Figure 7.- Drag parameter as a function of Mach number for Little Joe (obtained from a combination of wind-tunnel and flight-test data).

[redacted]

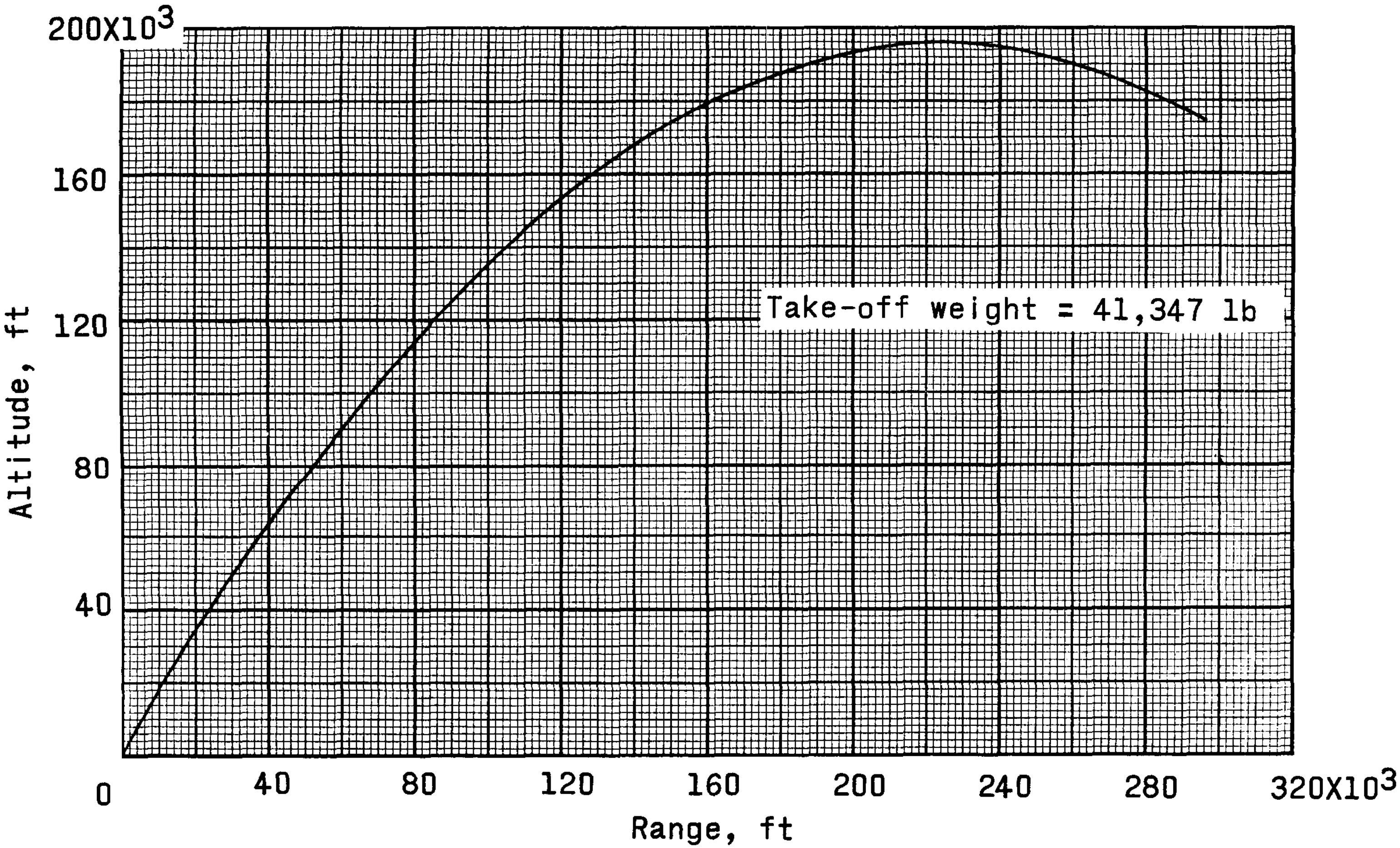

Figure 8.- Altitude as a function of horizontal range for Little Joe flight 1.

[redacted]

[redacted]

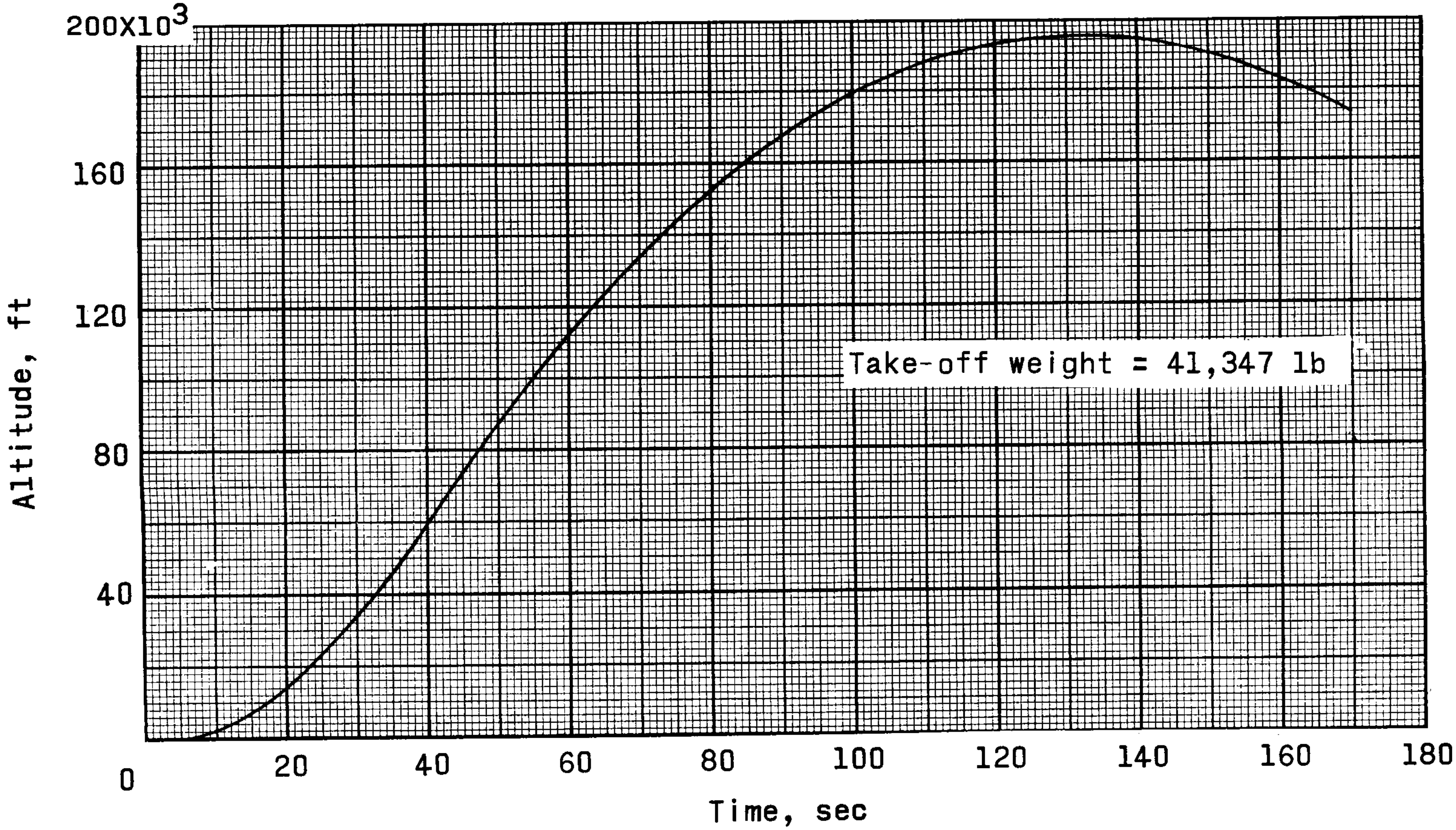

Figure 9.- Altitude time history for Little Joe flight 1.

[redacted]

[redacted]

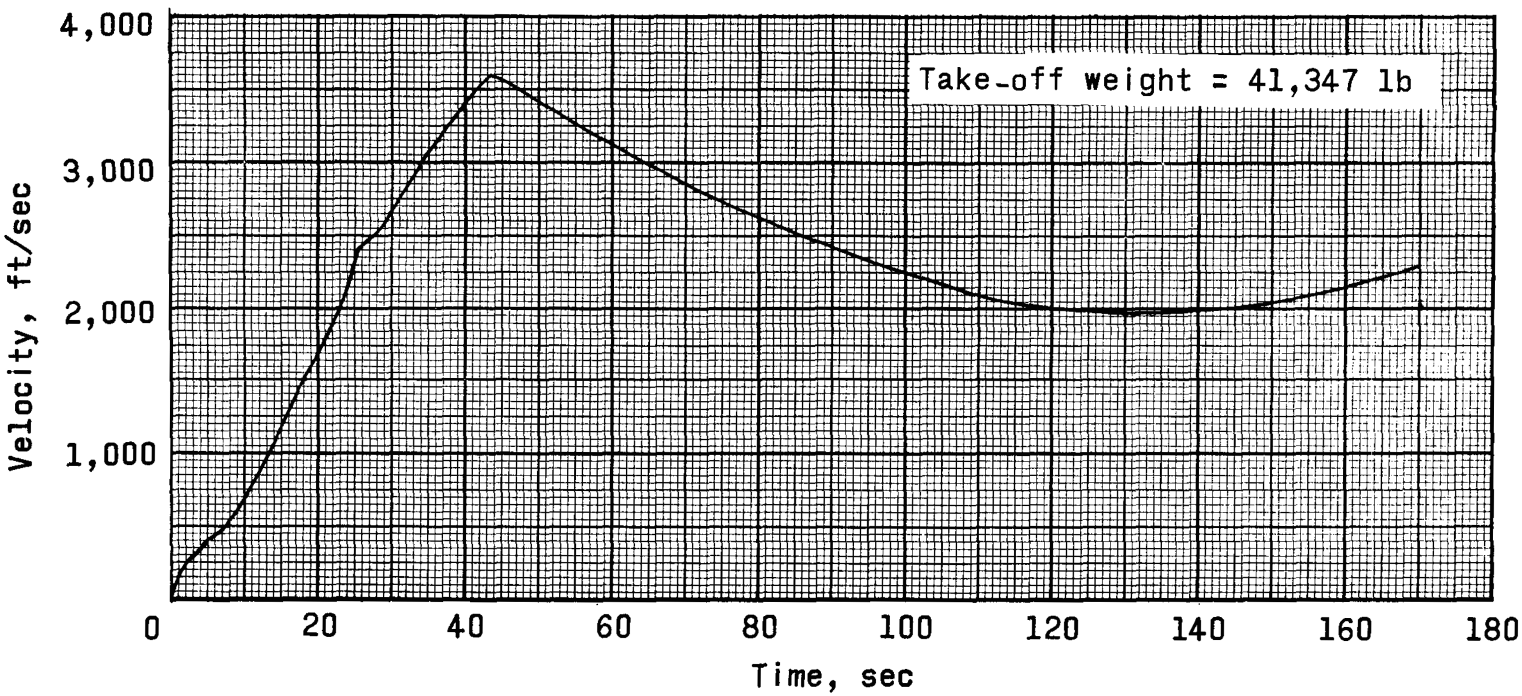

Figure 10.- Earth-fixed velocity time history for Little Joe flight 1.

[redacted]

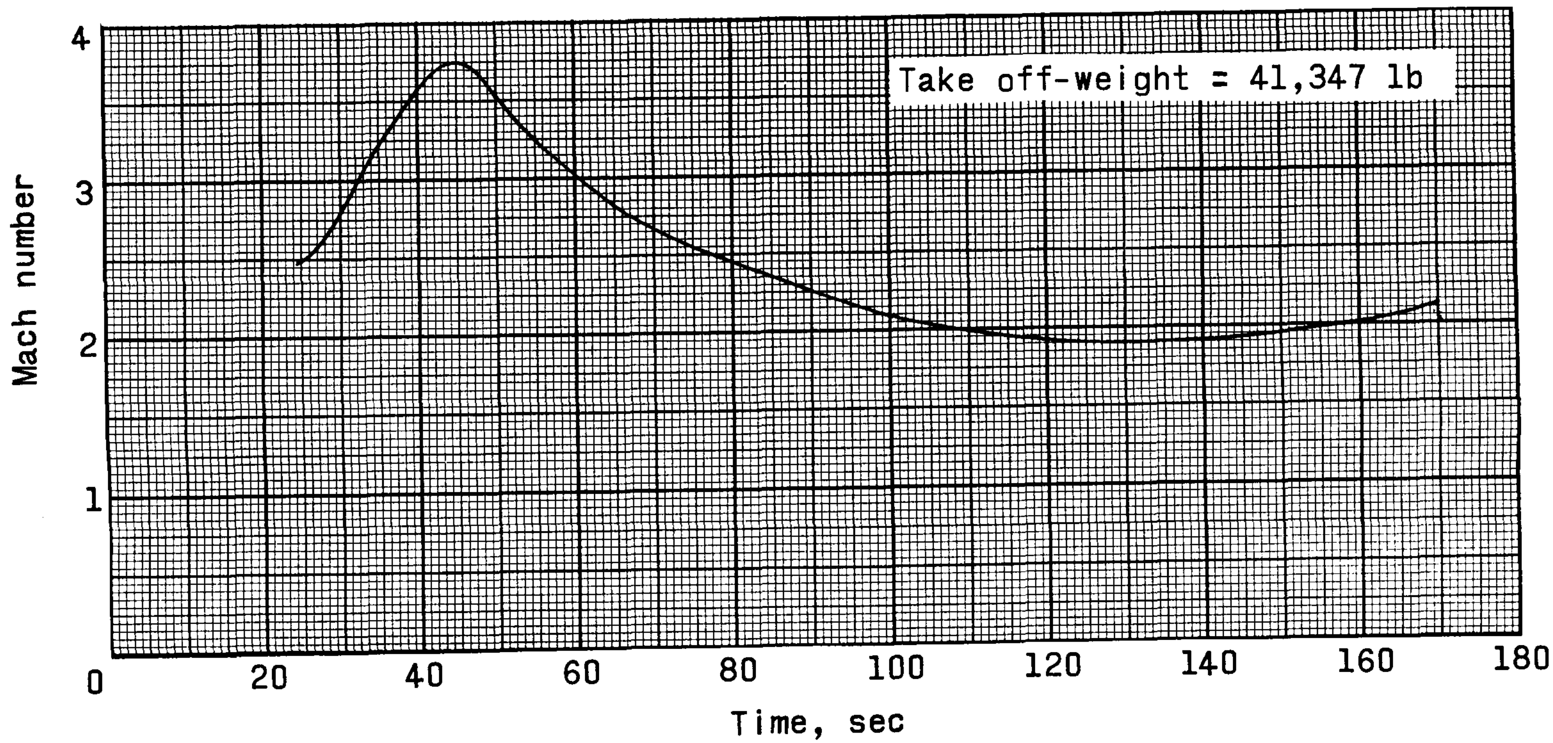

Figure 11.- Mach number time history for Little Joe flight 1.

[redacted]

DEC[redacted]IFIED

S-22

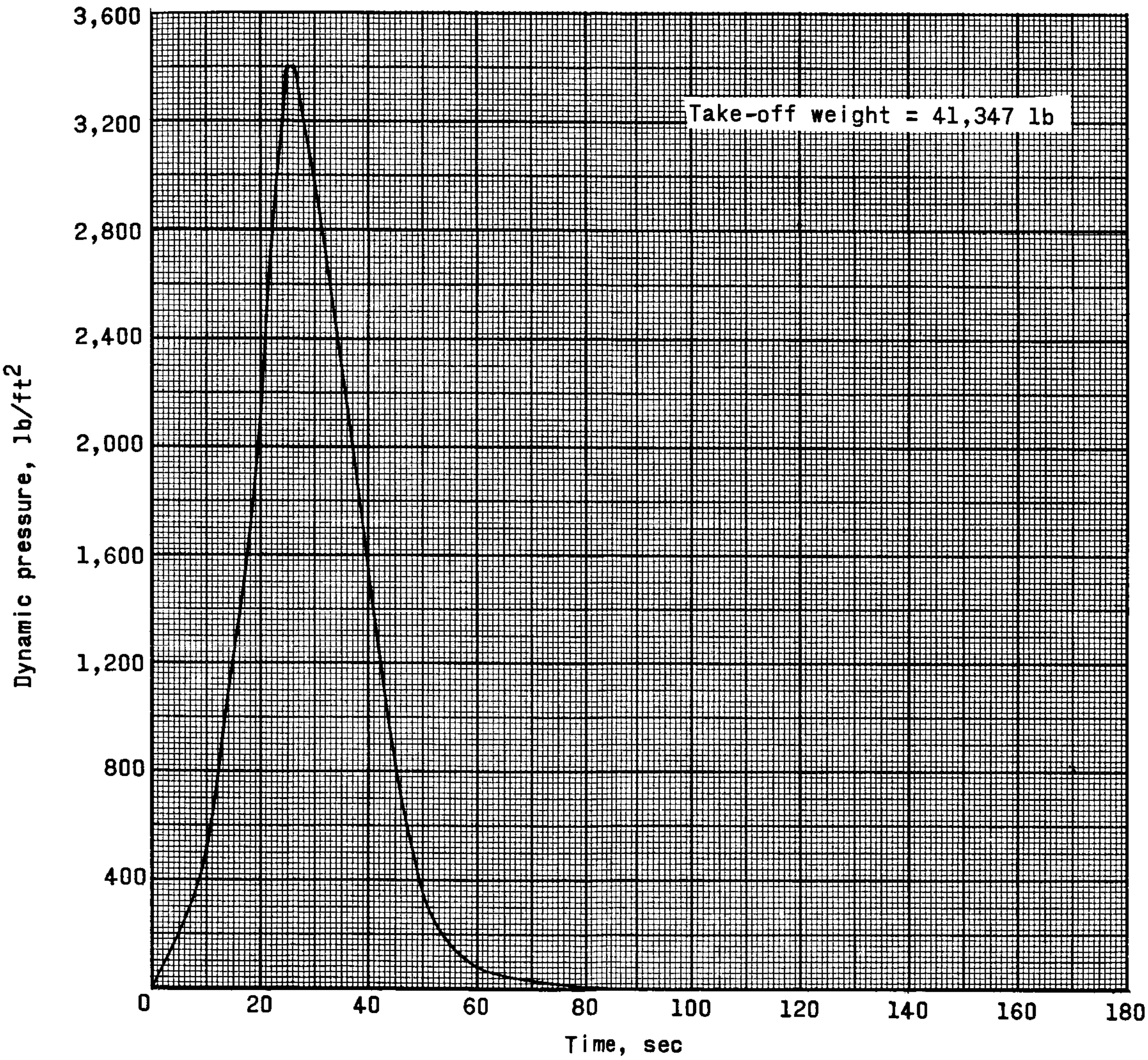

Figure 12.- Dynamic-pressure time history for Little Joe flight 1.

[redacted]

[redacted]

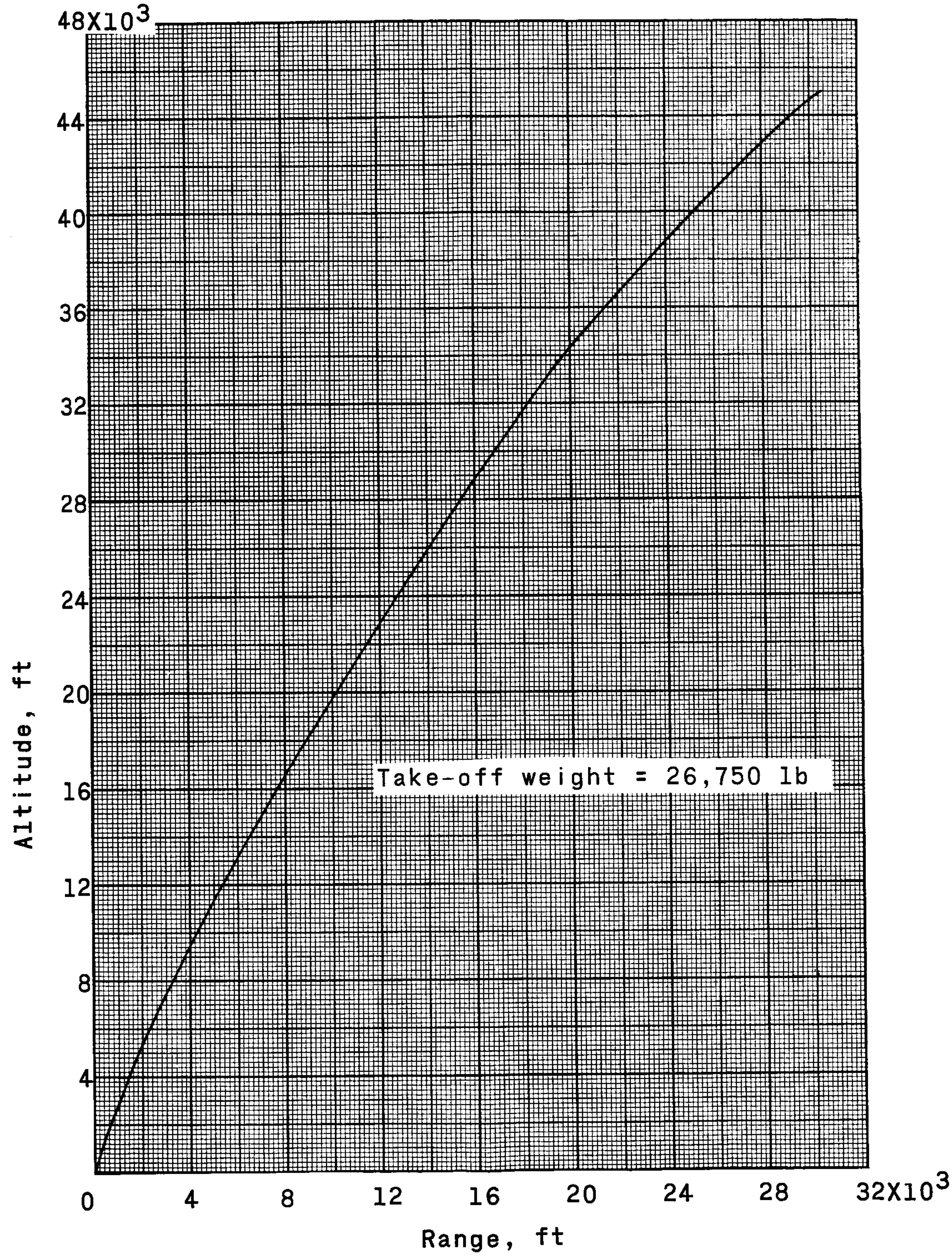

Figure 13.- Altitude as a function of horizontal range for Little Joe flight 2.

S-22

[redacted]

S-22

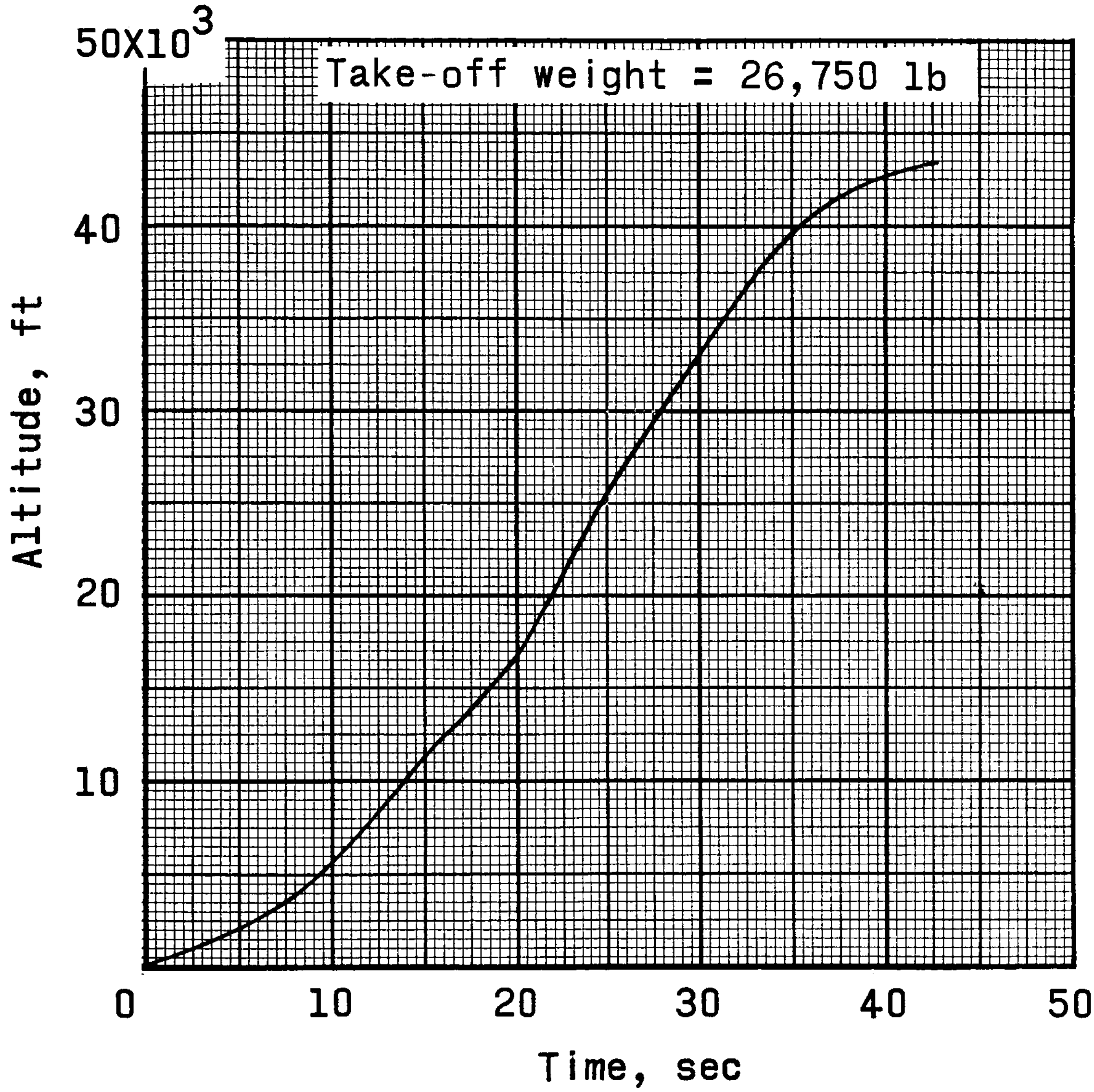

Figure 14.- Altitude time history for Little Joe flight 2.

[redacted]

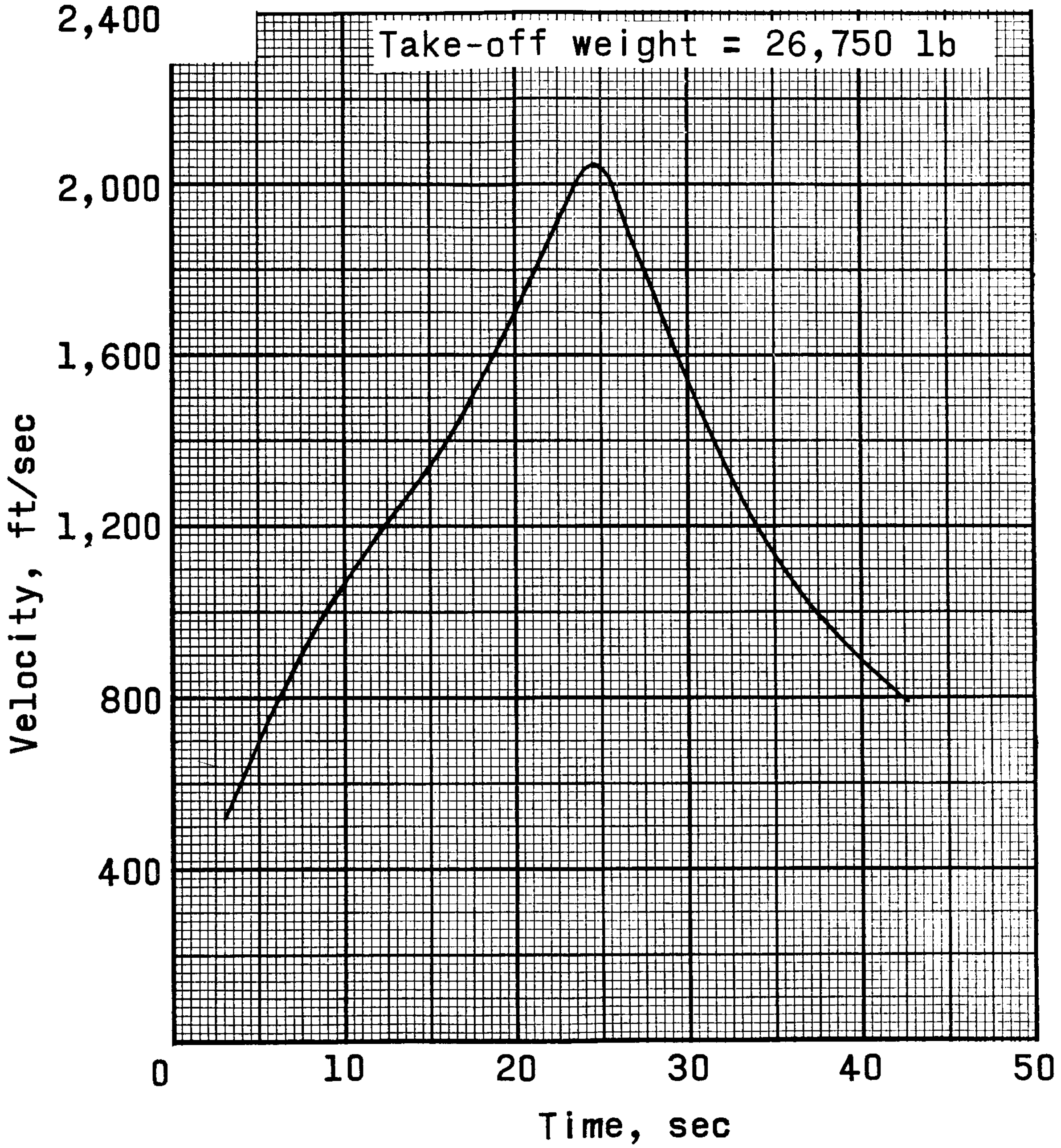

Figure 15.- Earth-fixed velocity time history for Little Joe flight 2.

S-22

[redacted]

S-22

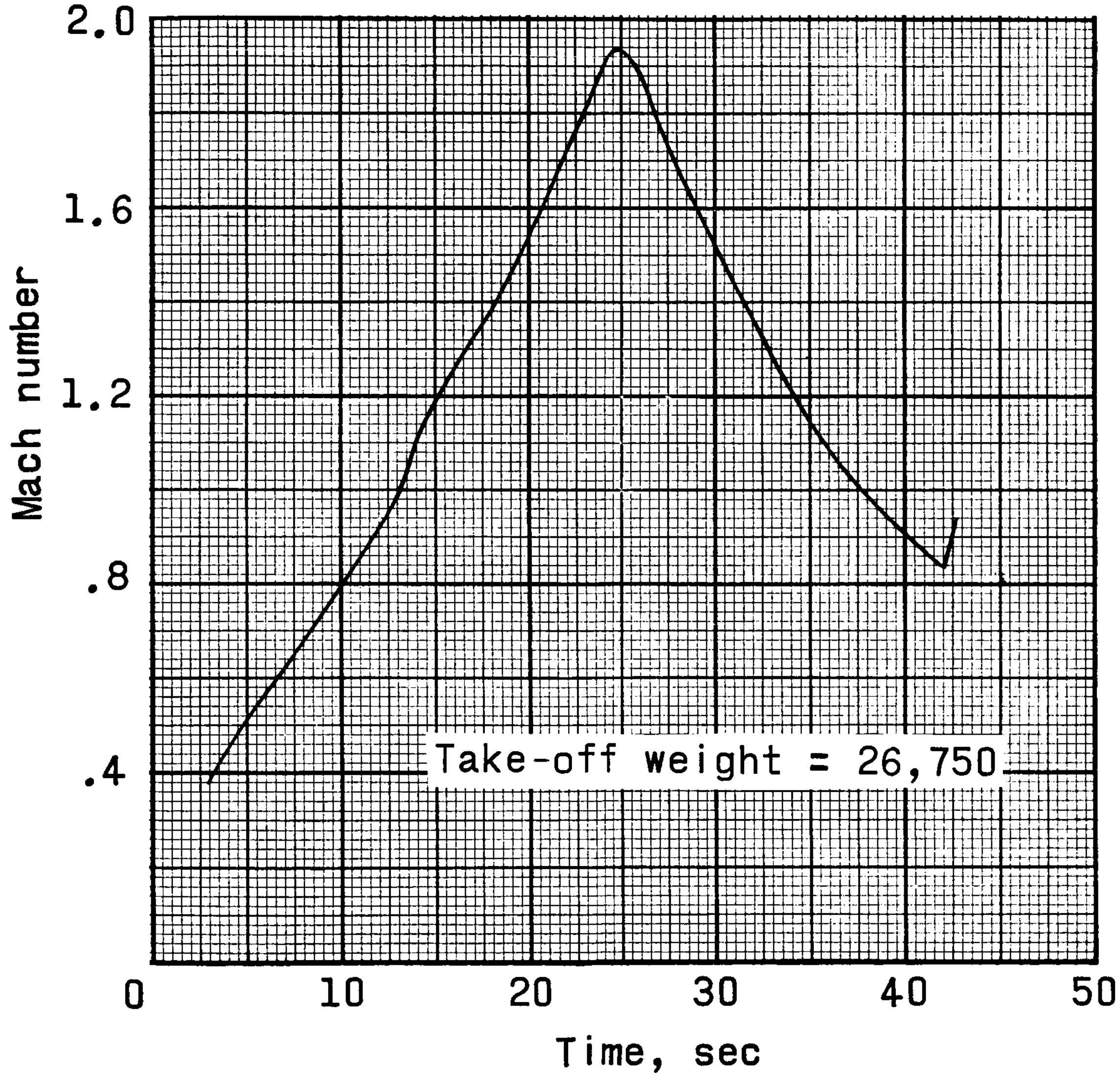

Figure 16.- Mach number time history for Little Joe flight 2.

[redacted]

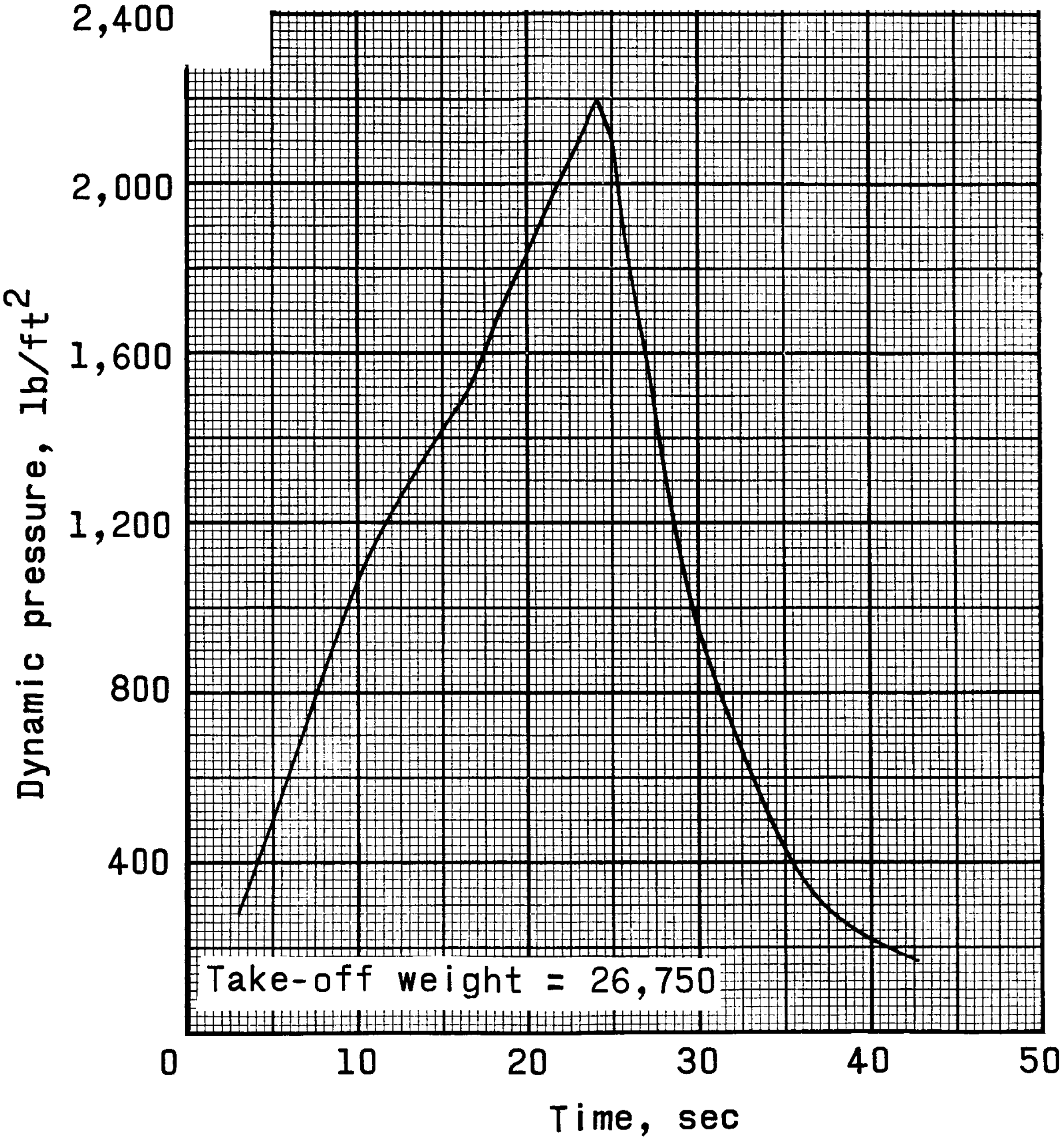

Figure 17.- Dynamic-pressure time history for Little Joe flight 2.

S-22

[redacted]

S-22

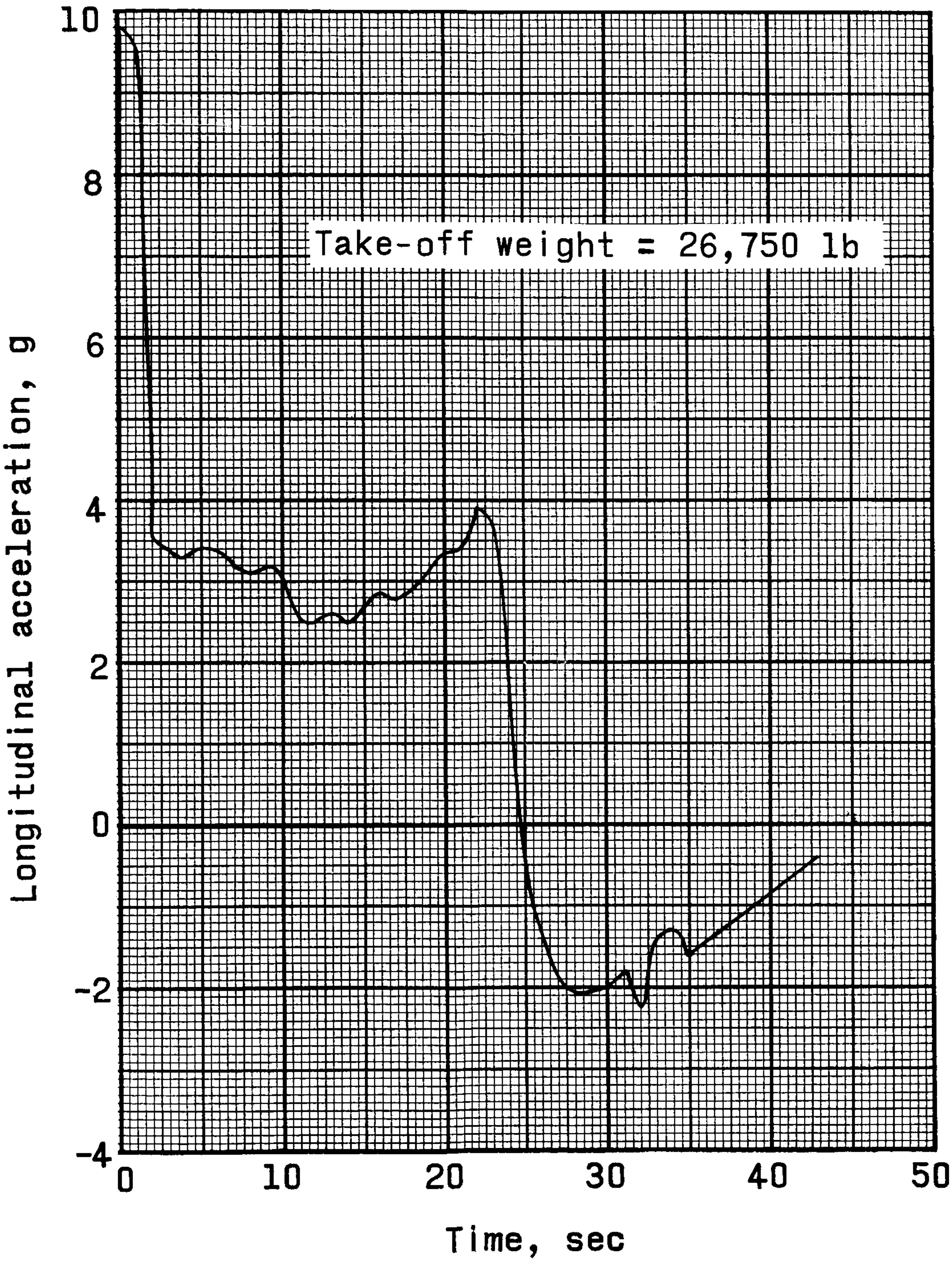

Figure 18.- Longitudinal-acceleration time history for Little Joe flight 2.

[redacted]

S-22

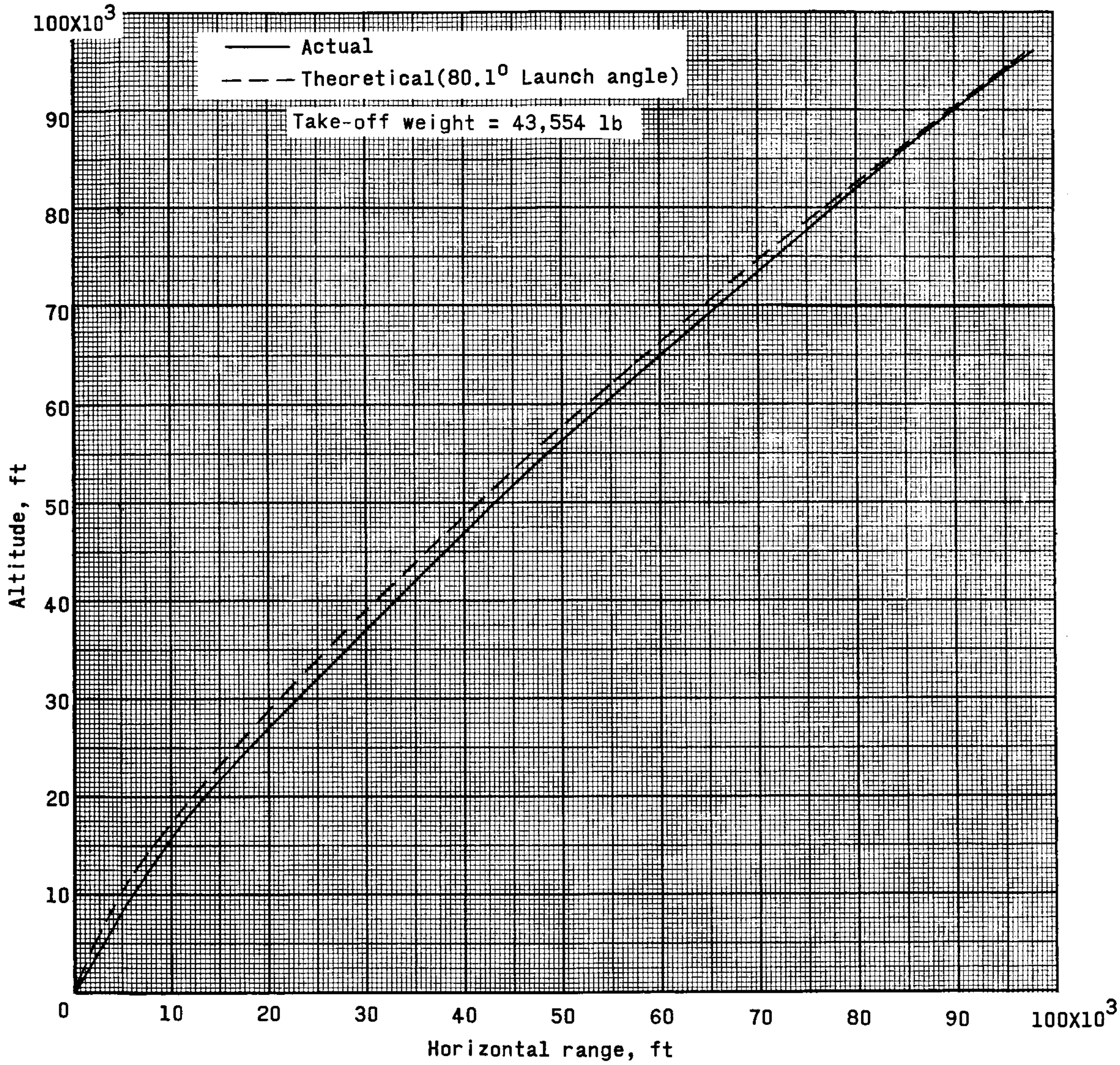

Figure 19.- Altitude as a function of horizontal range for Little Joe flight 3.

[redacted]

S-22

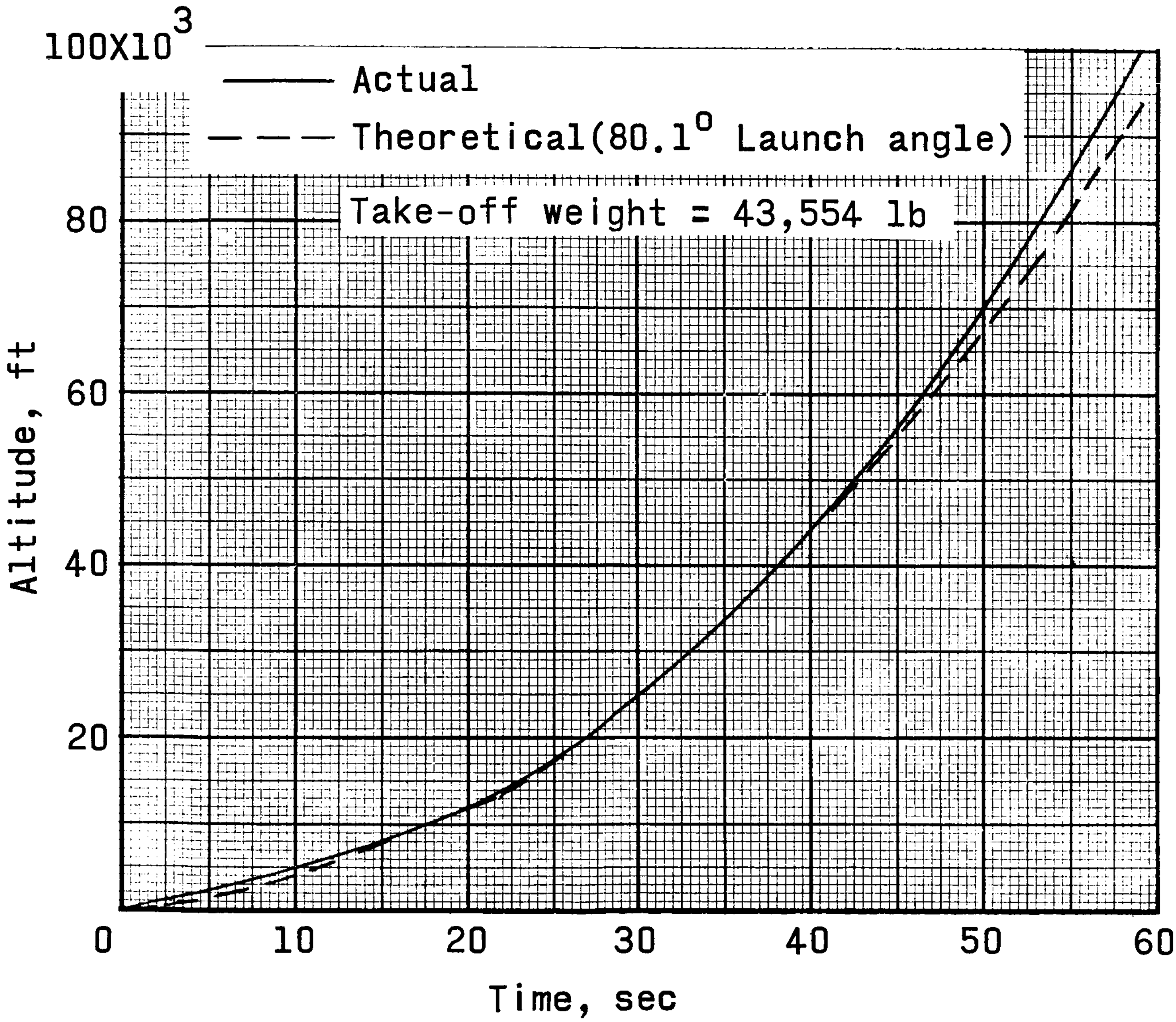

Figure 20.- Altitude time history for Little Joe flight 3.

[redacted]

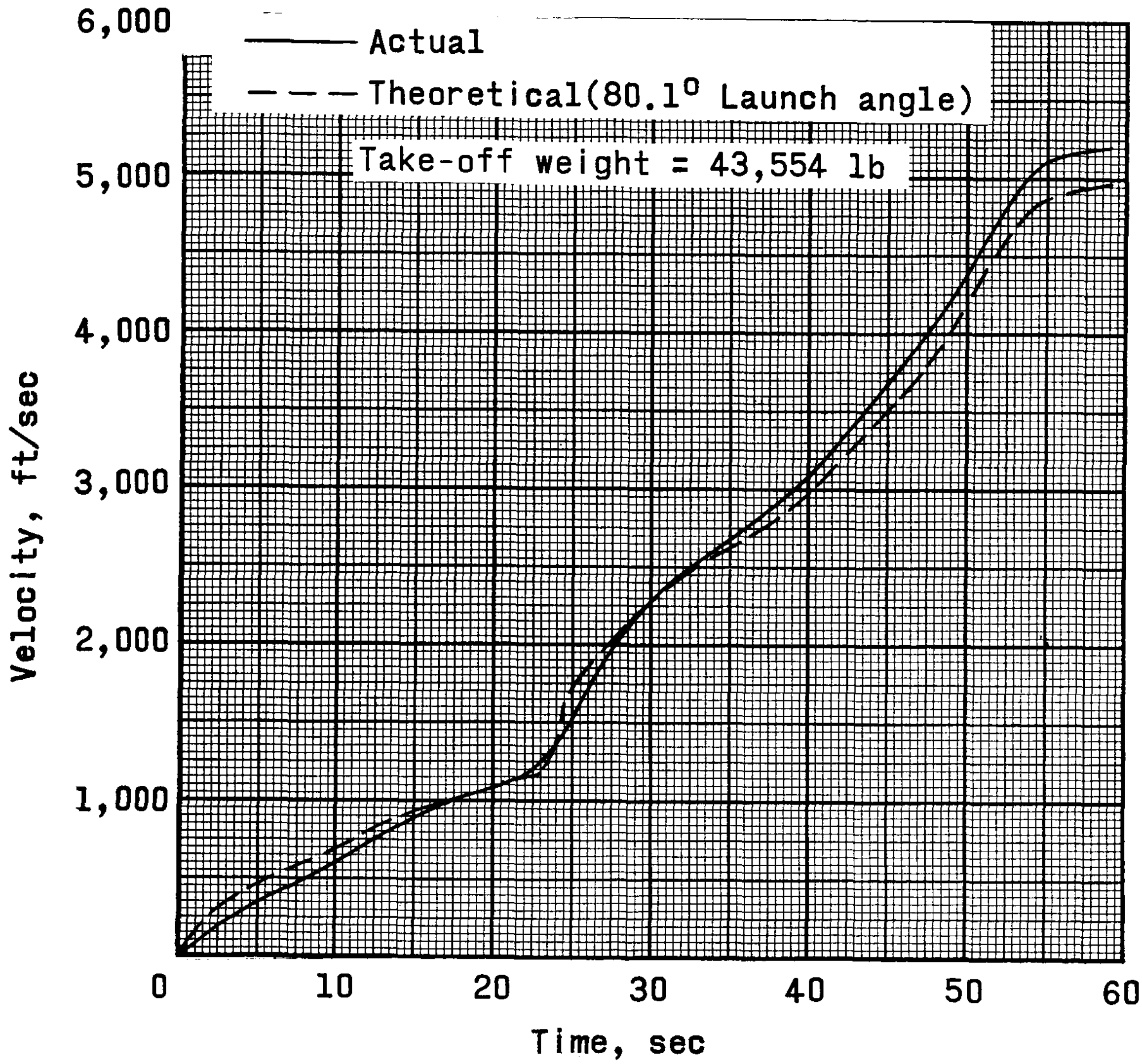

Figure 21.- Velocity time history for Little Joe flight 3.

S-22

S-22

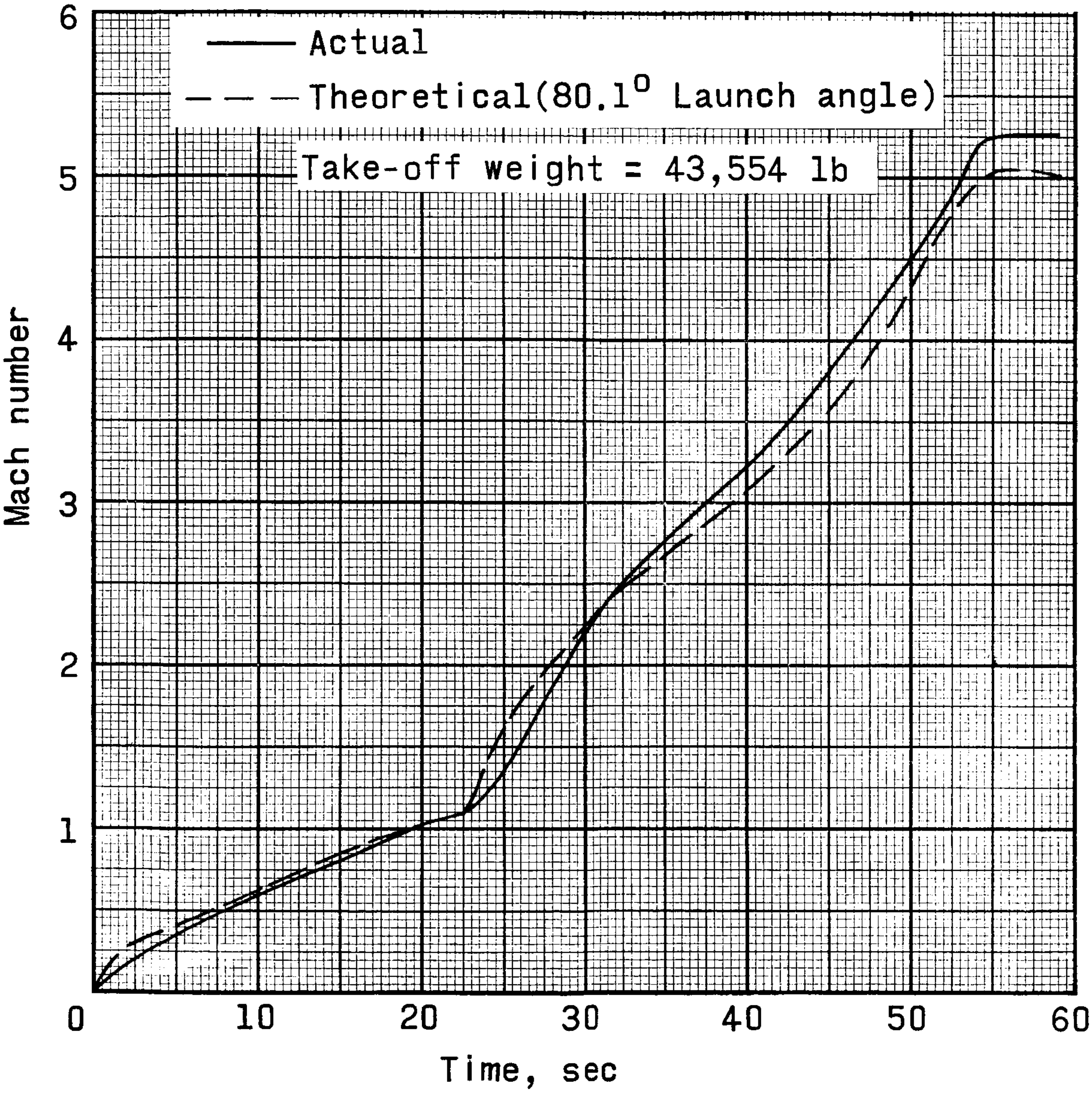

Figure 22.- Mach number time history for Little Joe flight 3.

[redacted]

[redacted]

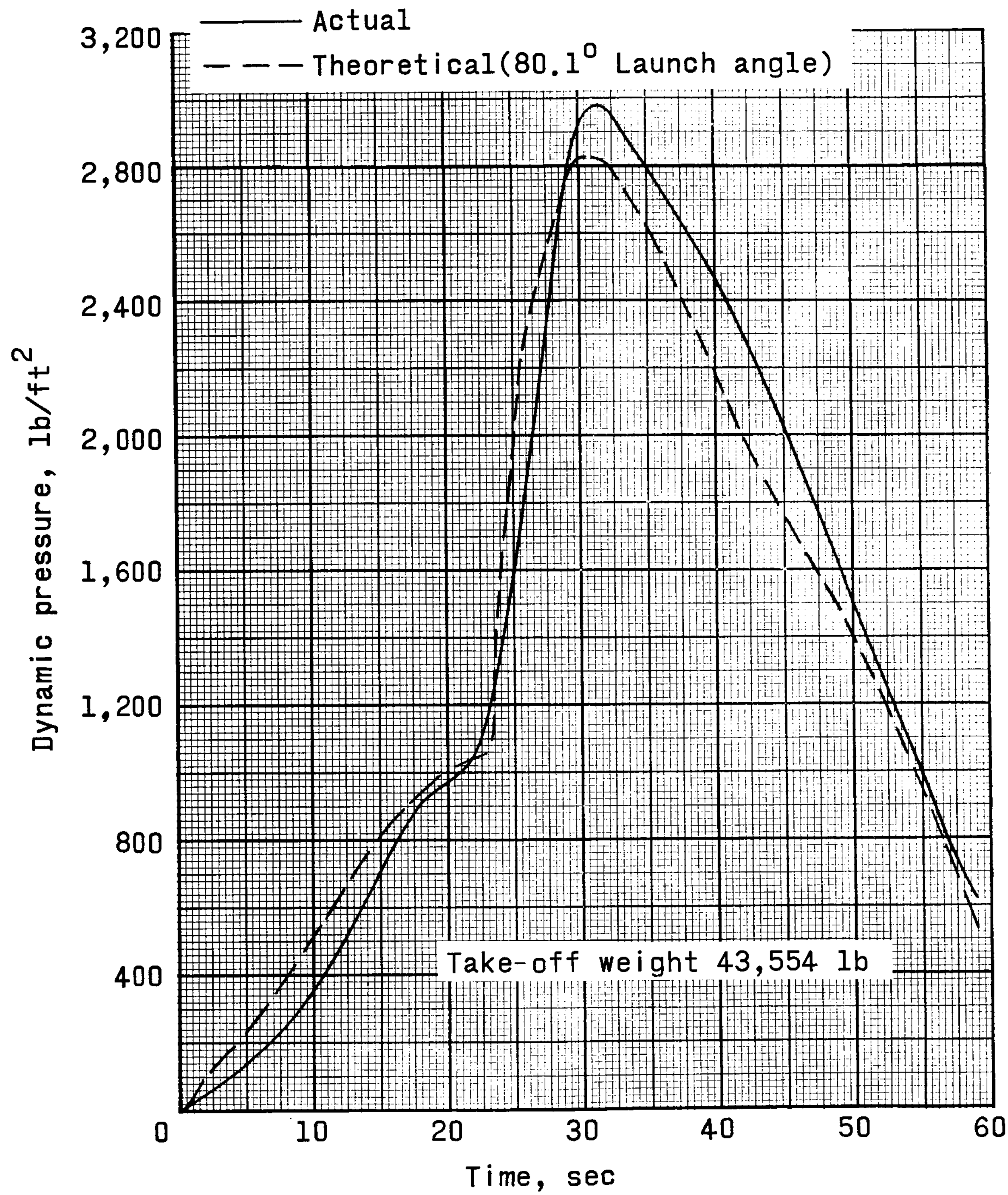

Figure 23.- Dynamic-pressure time history for Little Joe flight 3.

S-22

[redacted]

S-22

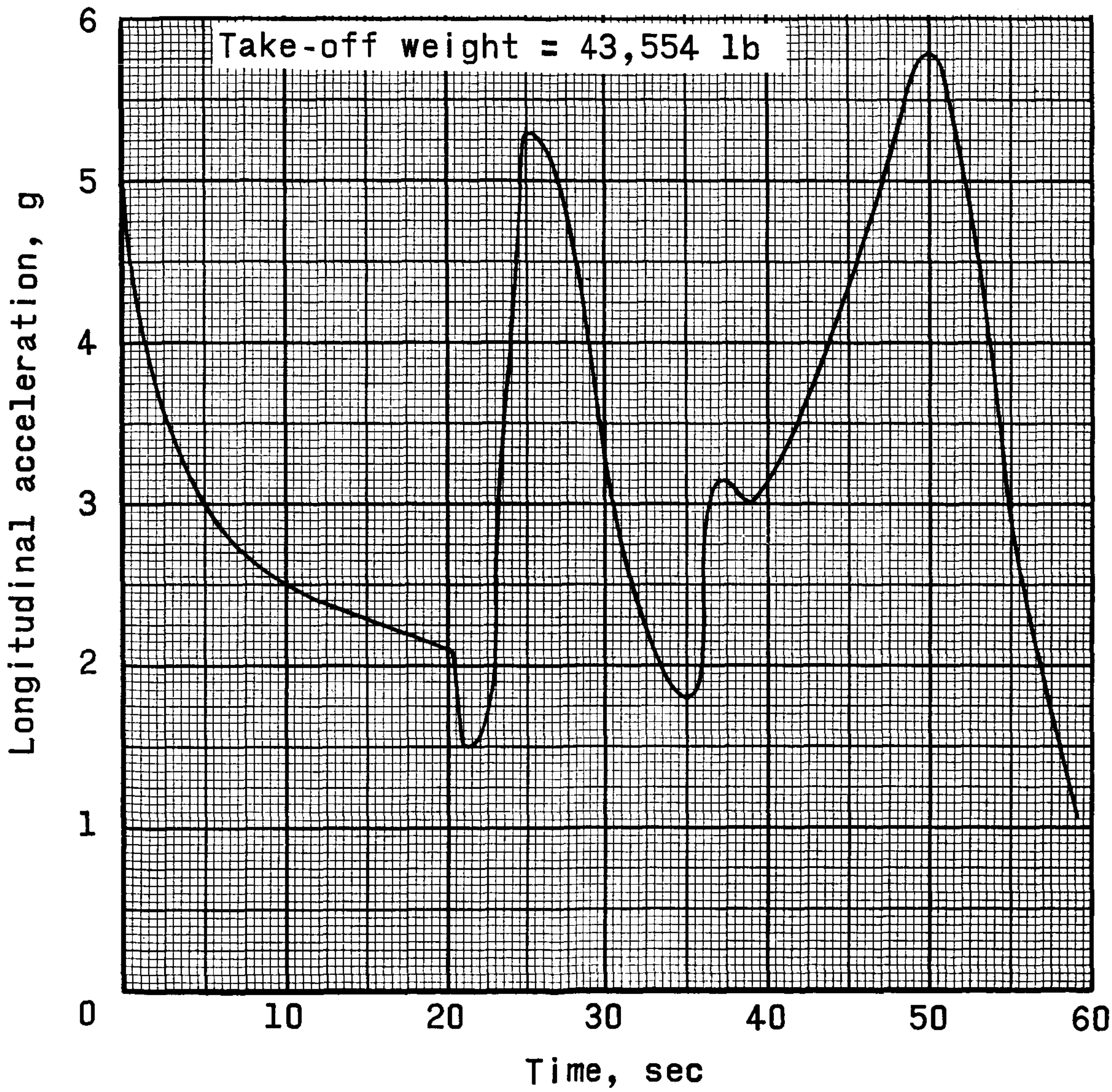

Figure 24.- Longitudinal-acceleration time history for Little Joe flight 3.

[redacted]

[redacted]

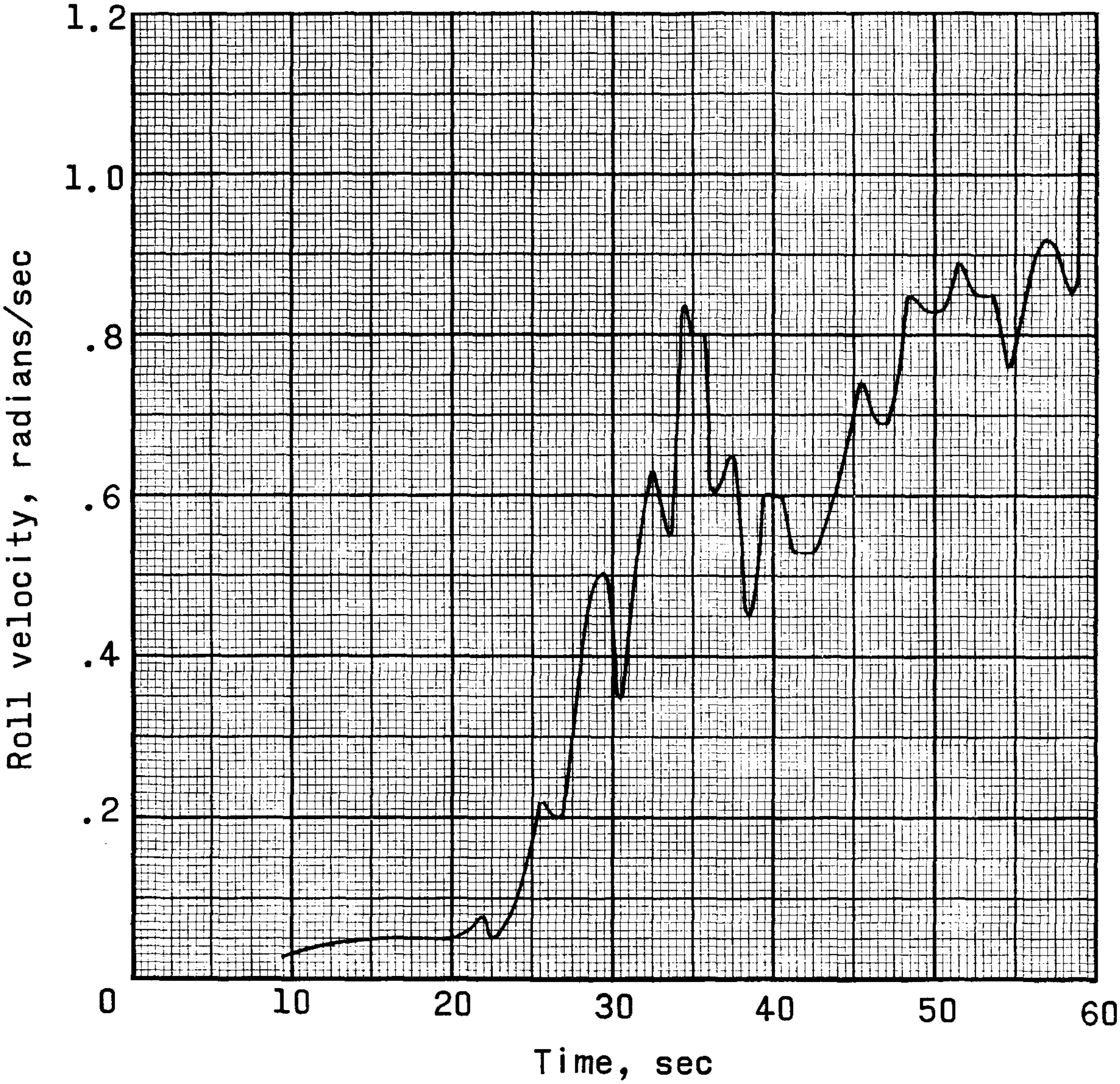

Figure 25.- Roll-velocity time history for Little Joe flight 3.

S-22

[redacted]

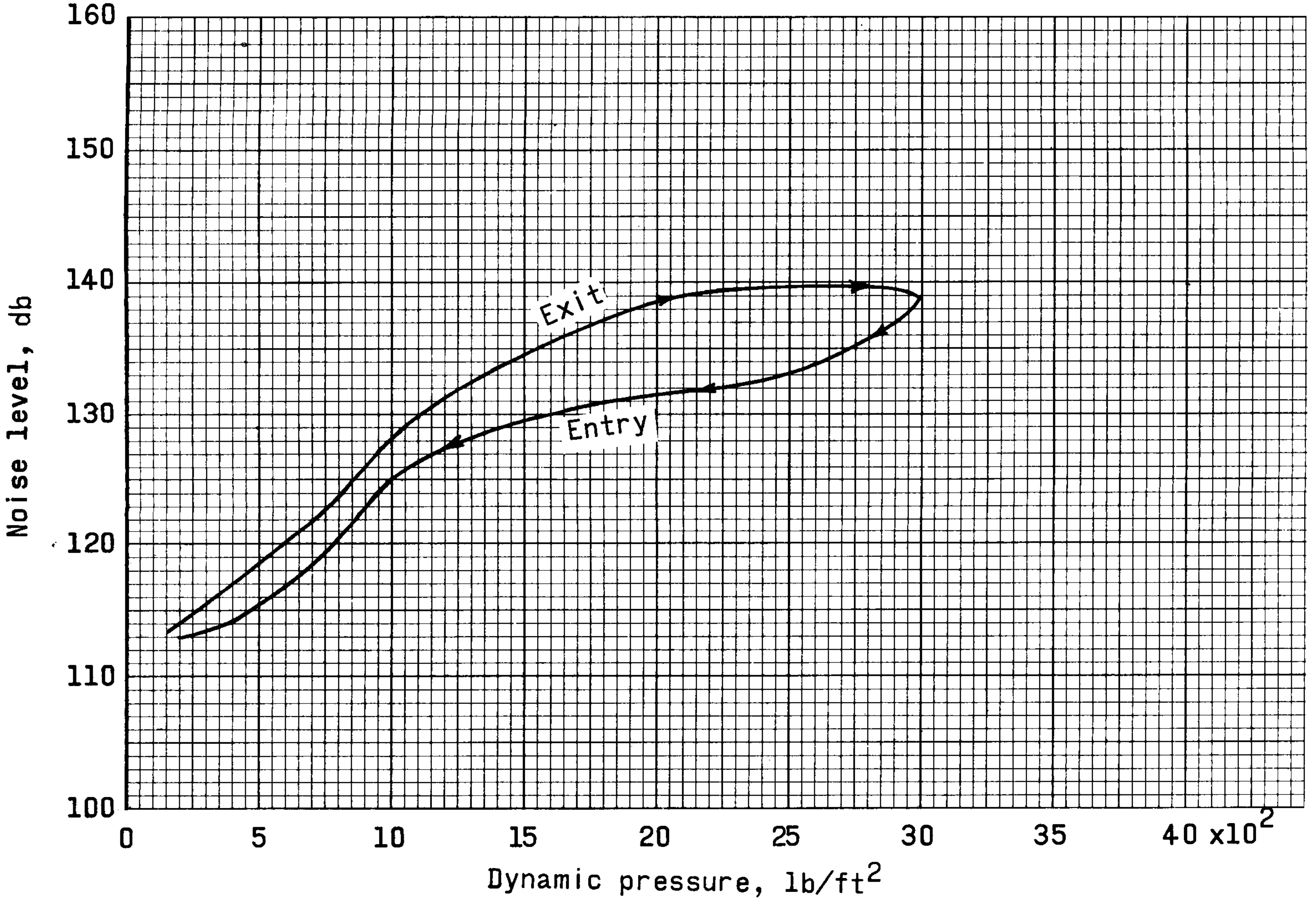

Figure 26.- Effects of dynamic pressure on the internal noise level within the conical payload for Little Joe flight 3.

[redacted]

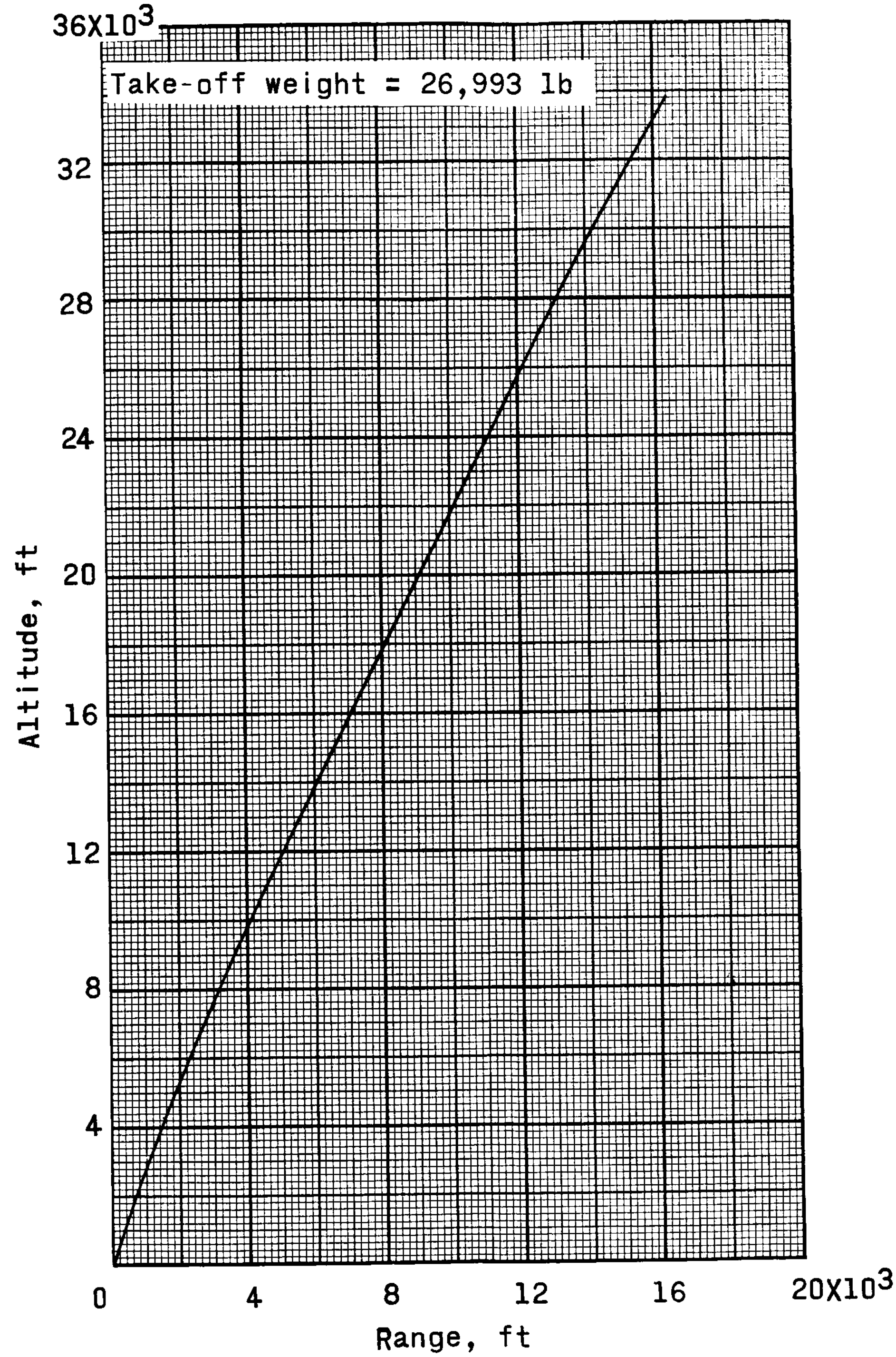

Figure 27.- Altitude as a function of horizontal range for Little Joe flight 4.

[redacted]

S-22

S-22

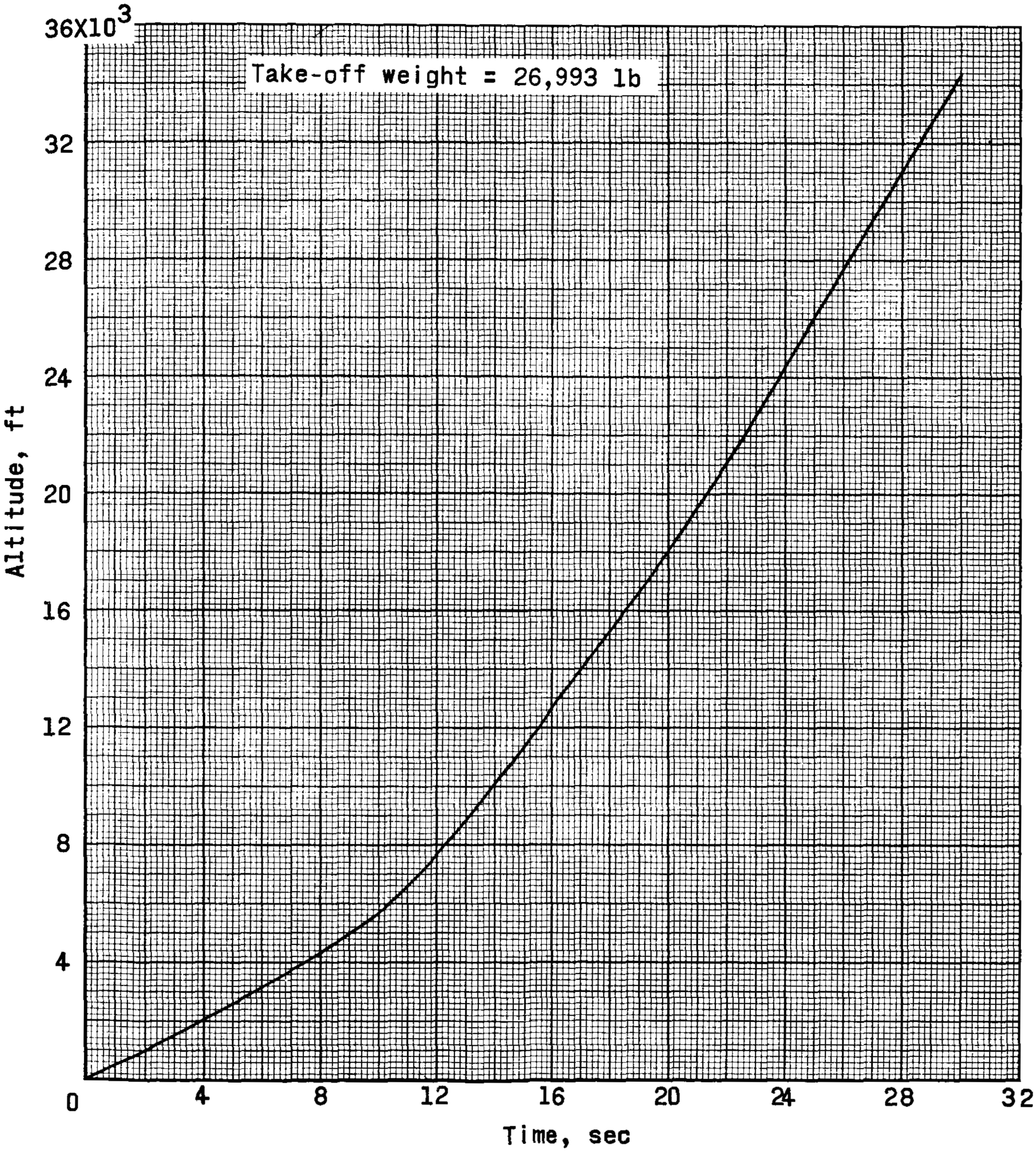

Figure 28.- Altitude time history for Little Joe flight 4.

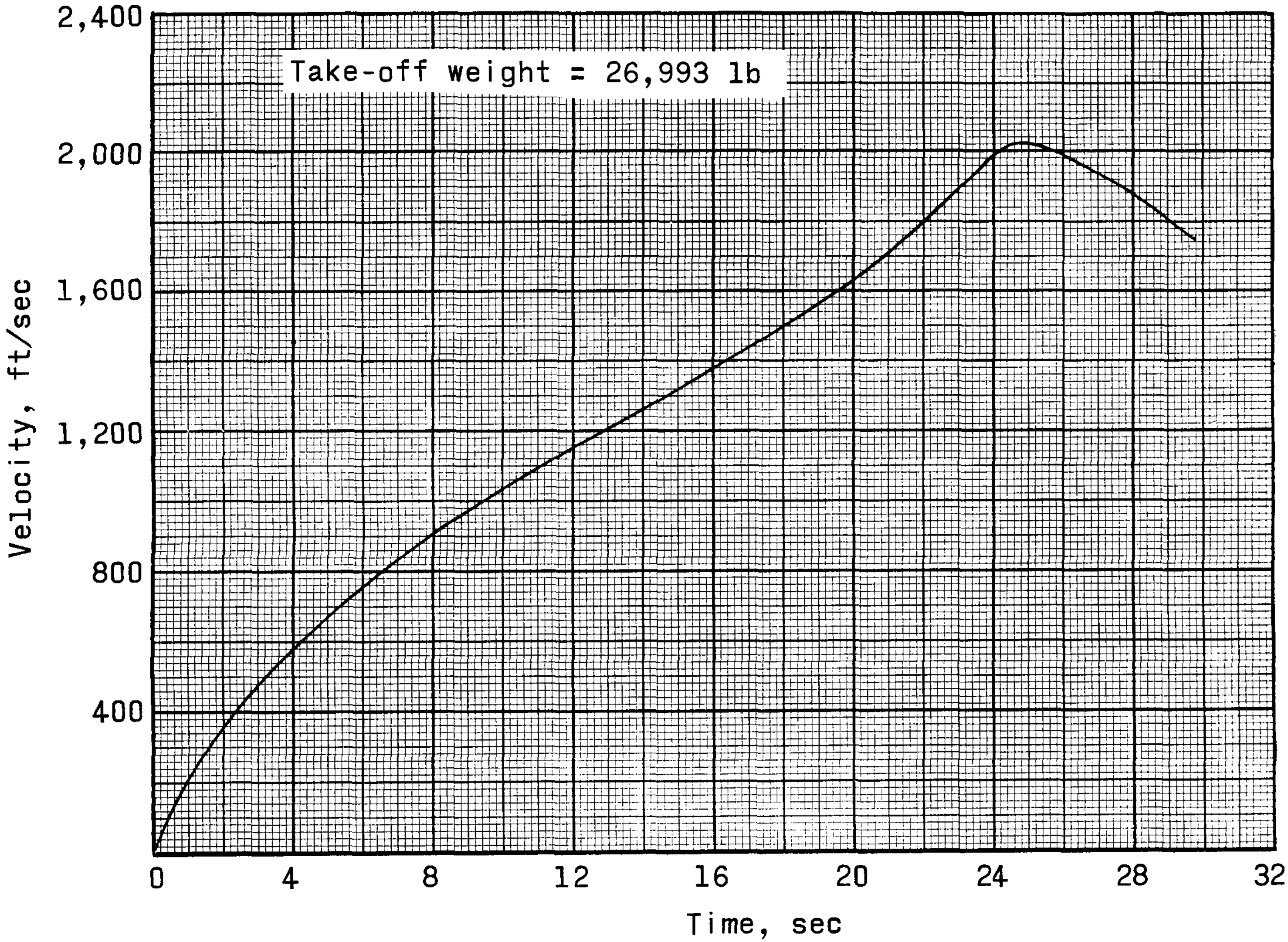

Figure 29.- Velocity time history for Little Joe flight 4.

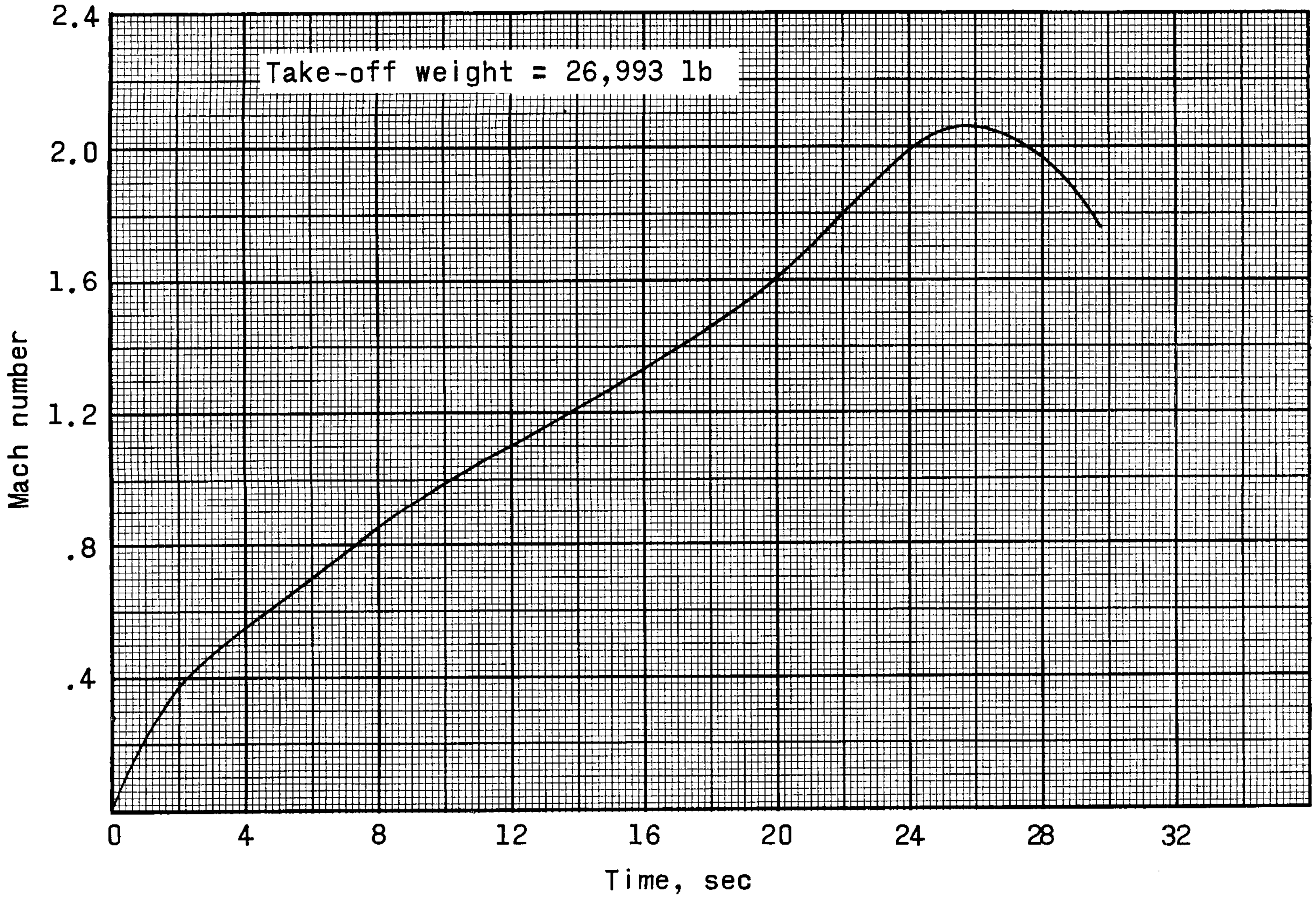

Figure 30.- Mach number time history for Little Joe flight 4.

[redacted]

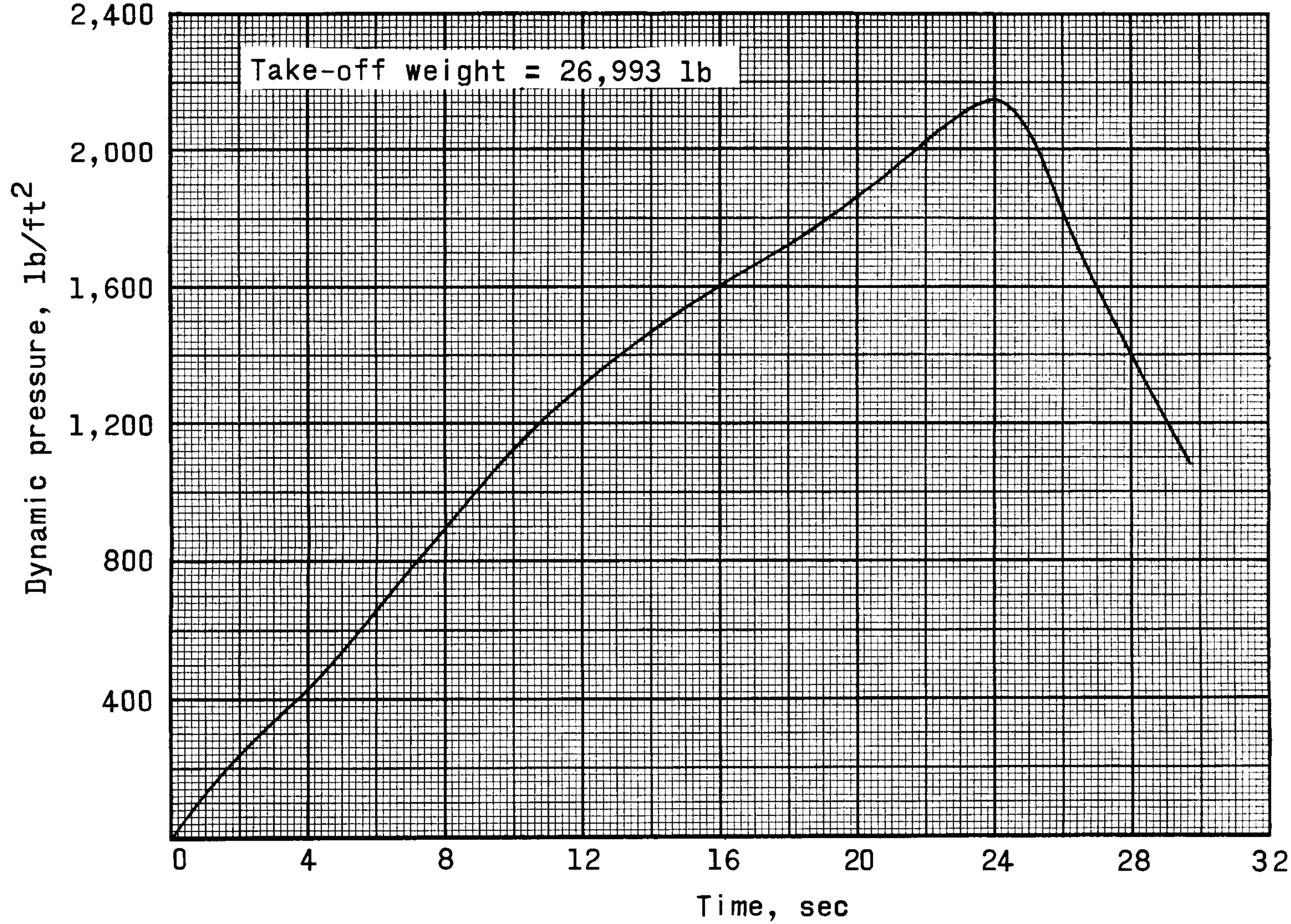

Figure 31. - Dynamic-pressure time history for Little Joe flight 4.

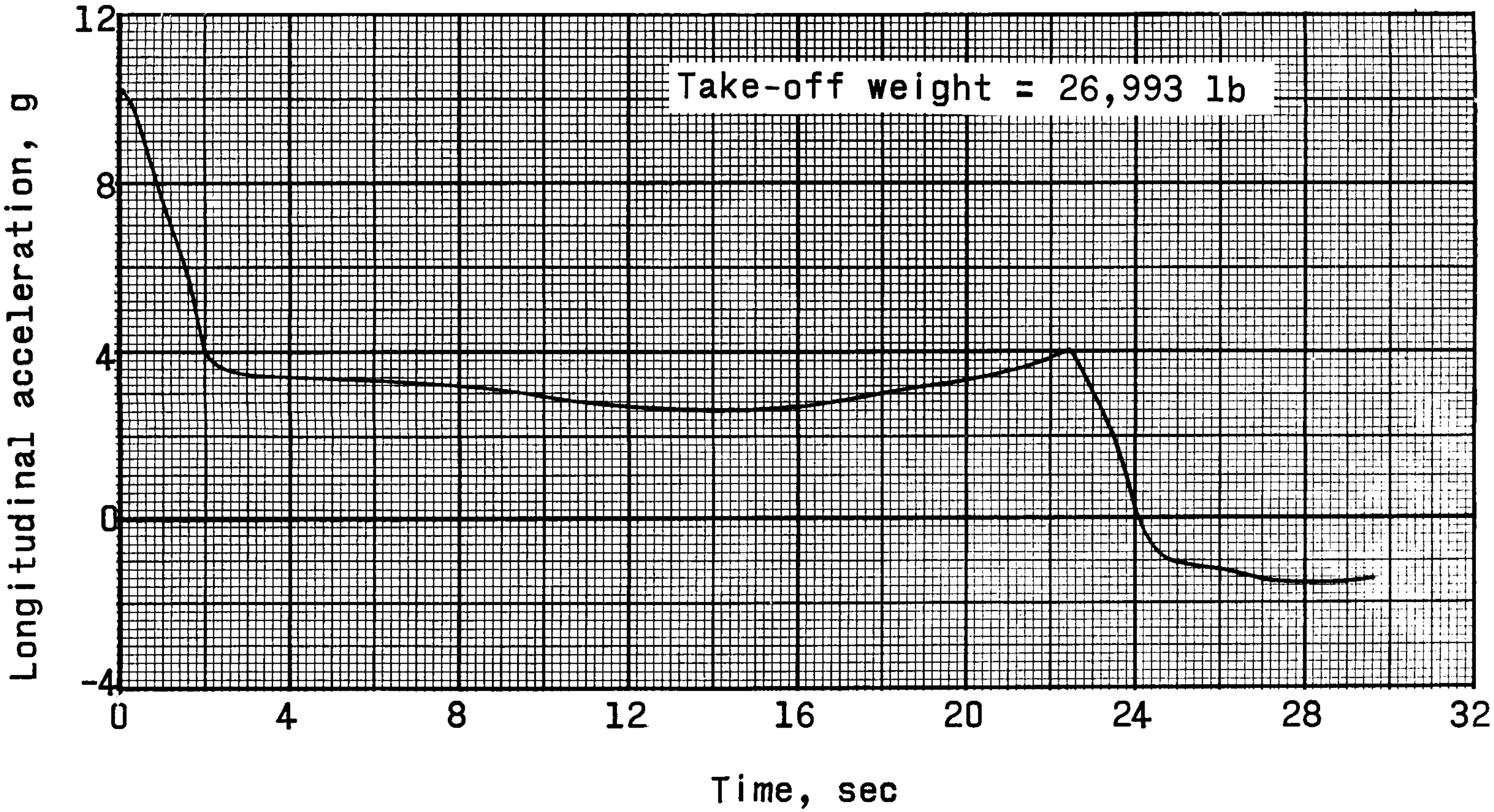

Figure 32.- Longitudinal-acceleration time history for Little Joe flight 4.

[redacted]

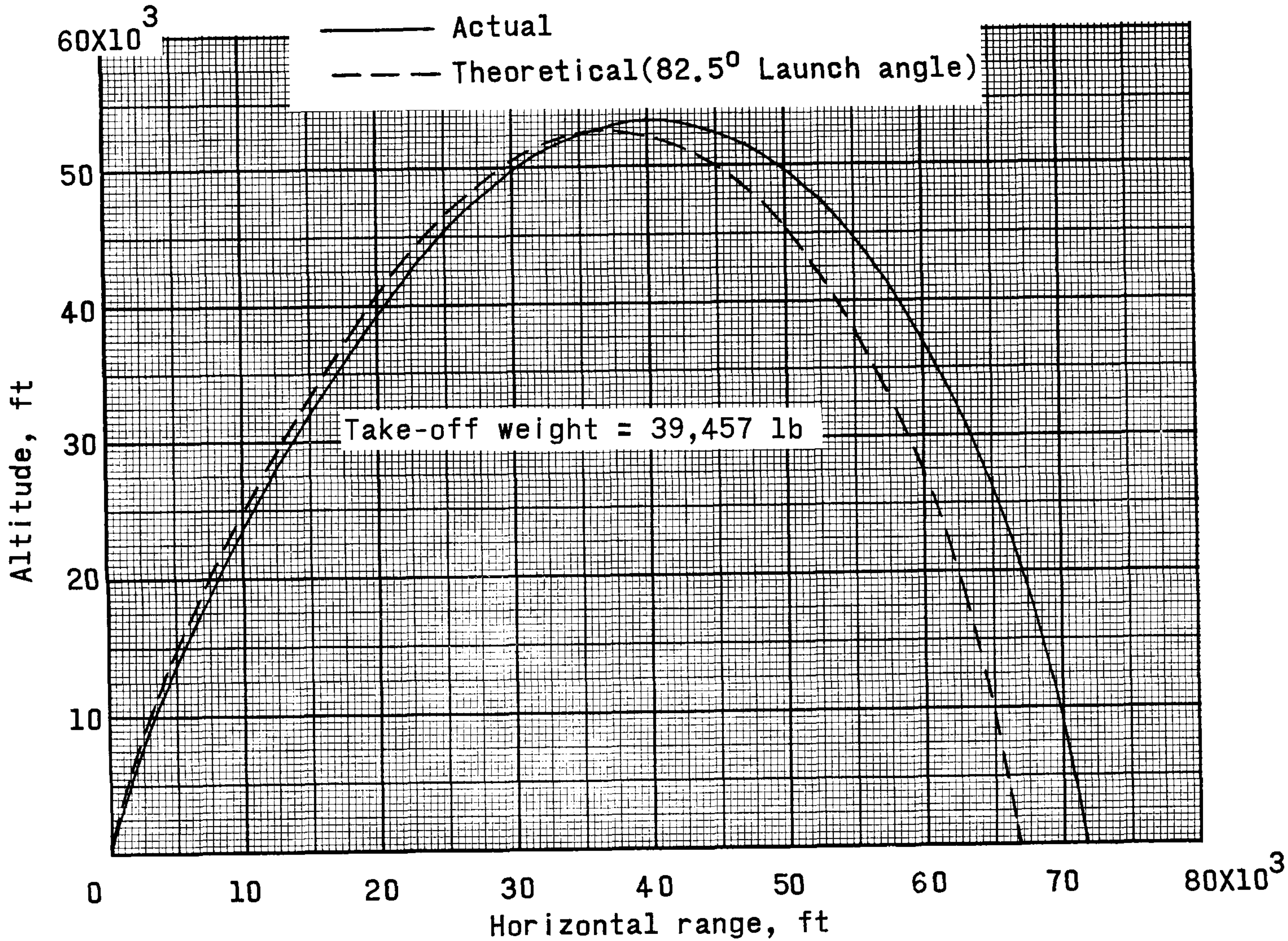

Figure 33.- Altitude as a function of horizontal range for Little Joe flight 5.

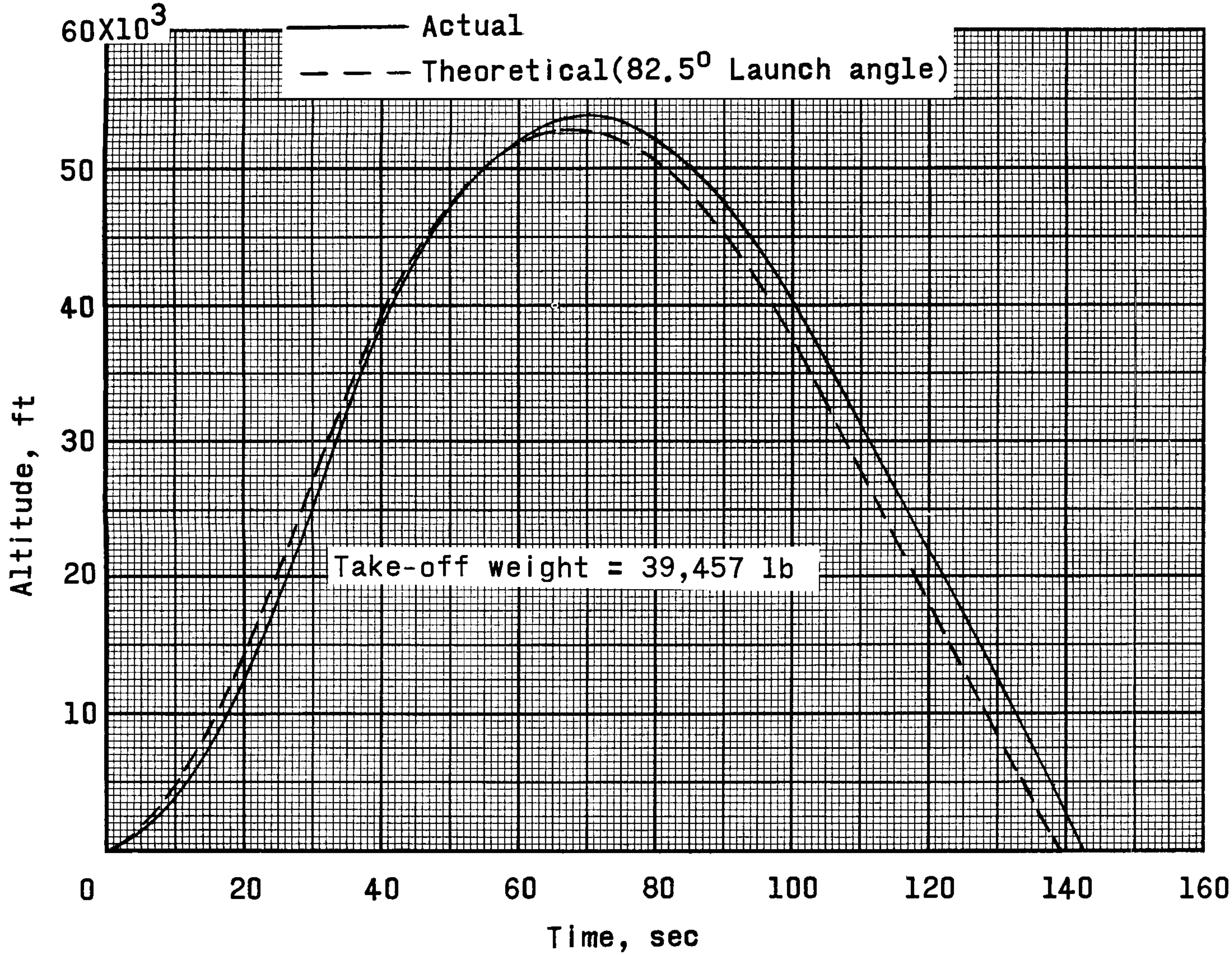

Figure 34.- Altitude time history for Little Joe flight 5.

DEC[redacted]SIFIED

[redacted]

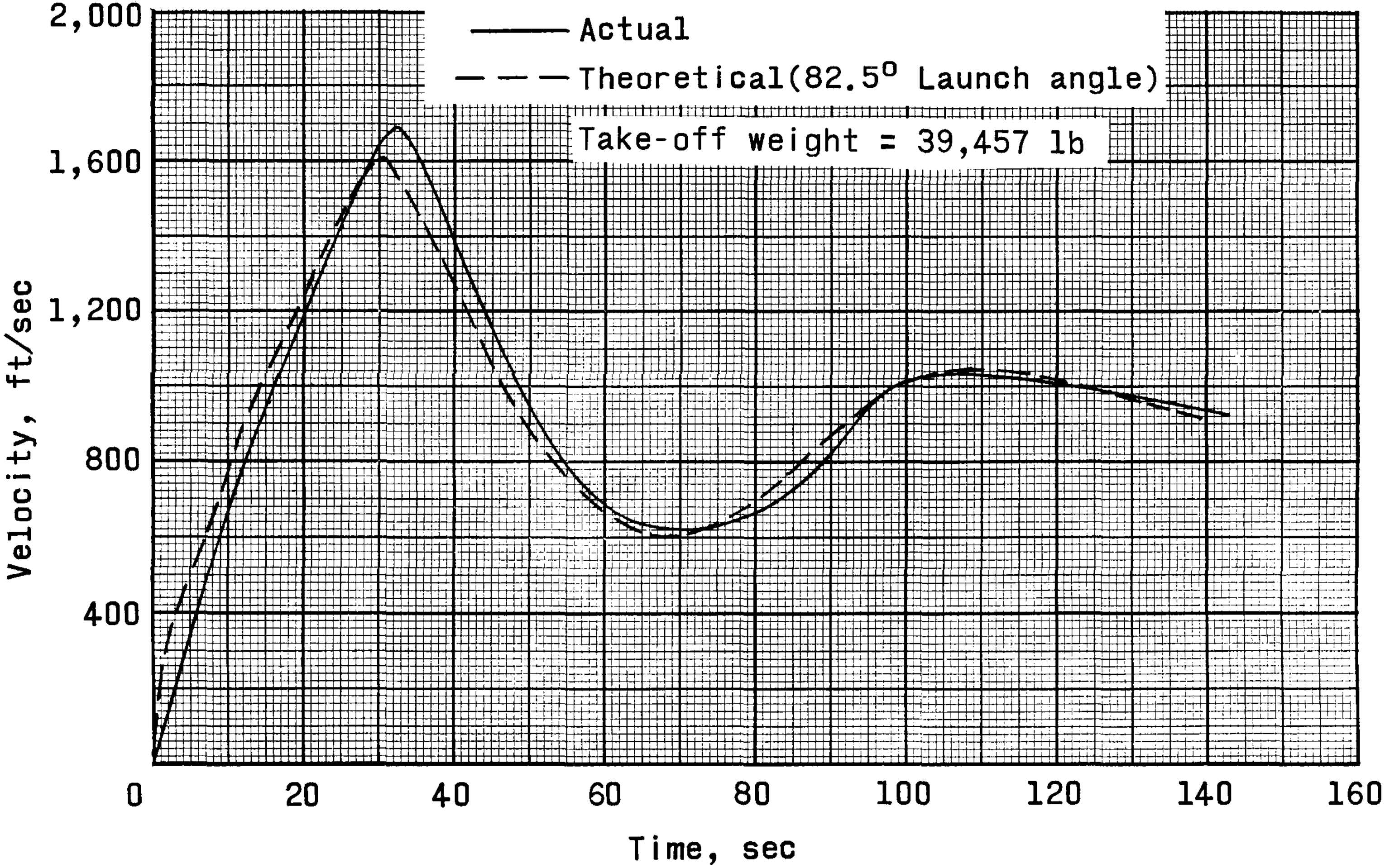

Figure 35.- Velocity time history for Little Joe flight 5.

[redacted]

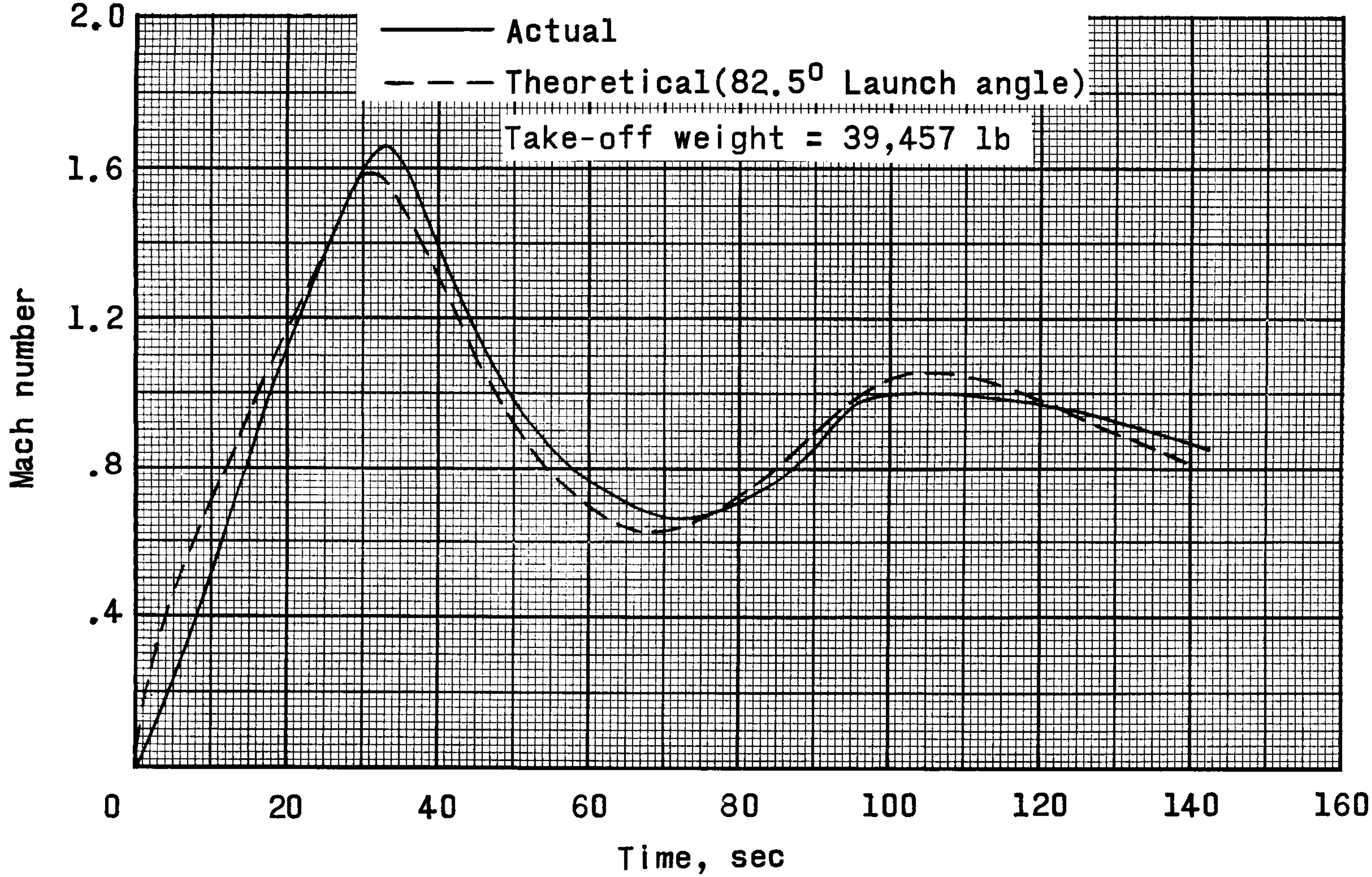

Figure 36.- Mach number time history for Little Joe flight 5.

[redacted]

[redacted]

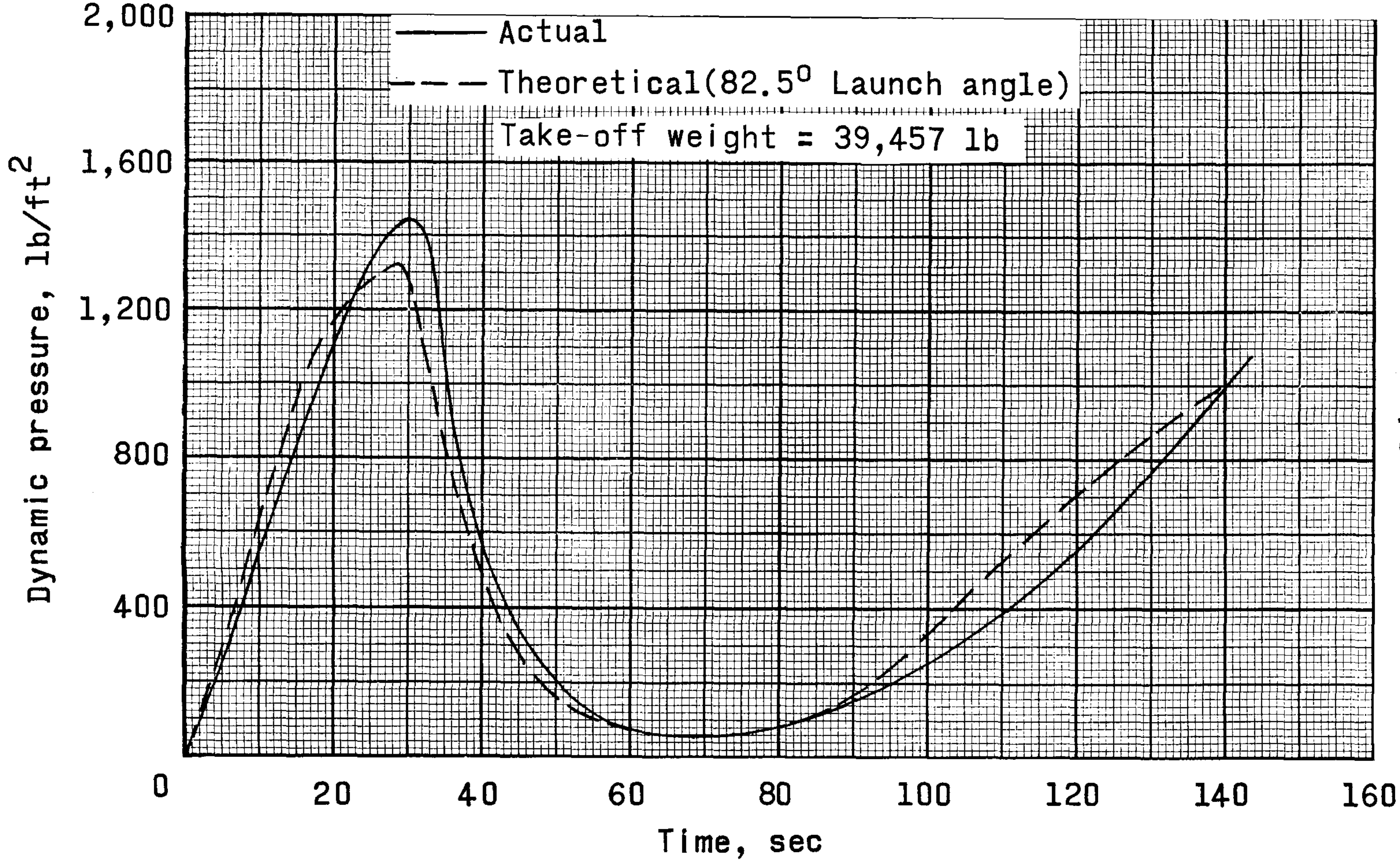

Figure 37.- Dynamic-pressure time history for Little Joe flight 5.

[redacted]

S-22

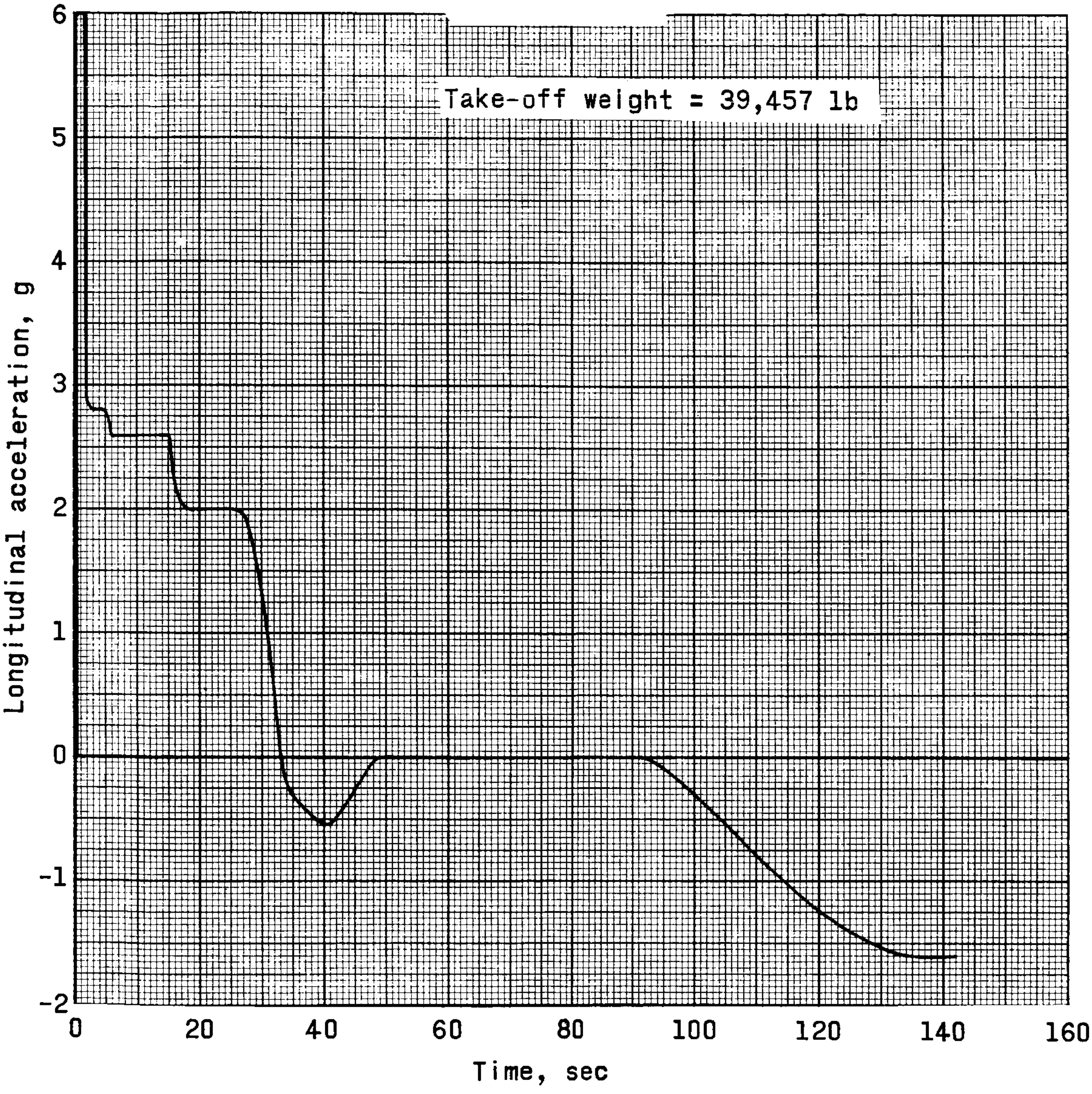

Figure 38.- Longitudinal acceleration time history of Little Joe flight 5.

[redacted]

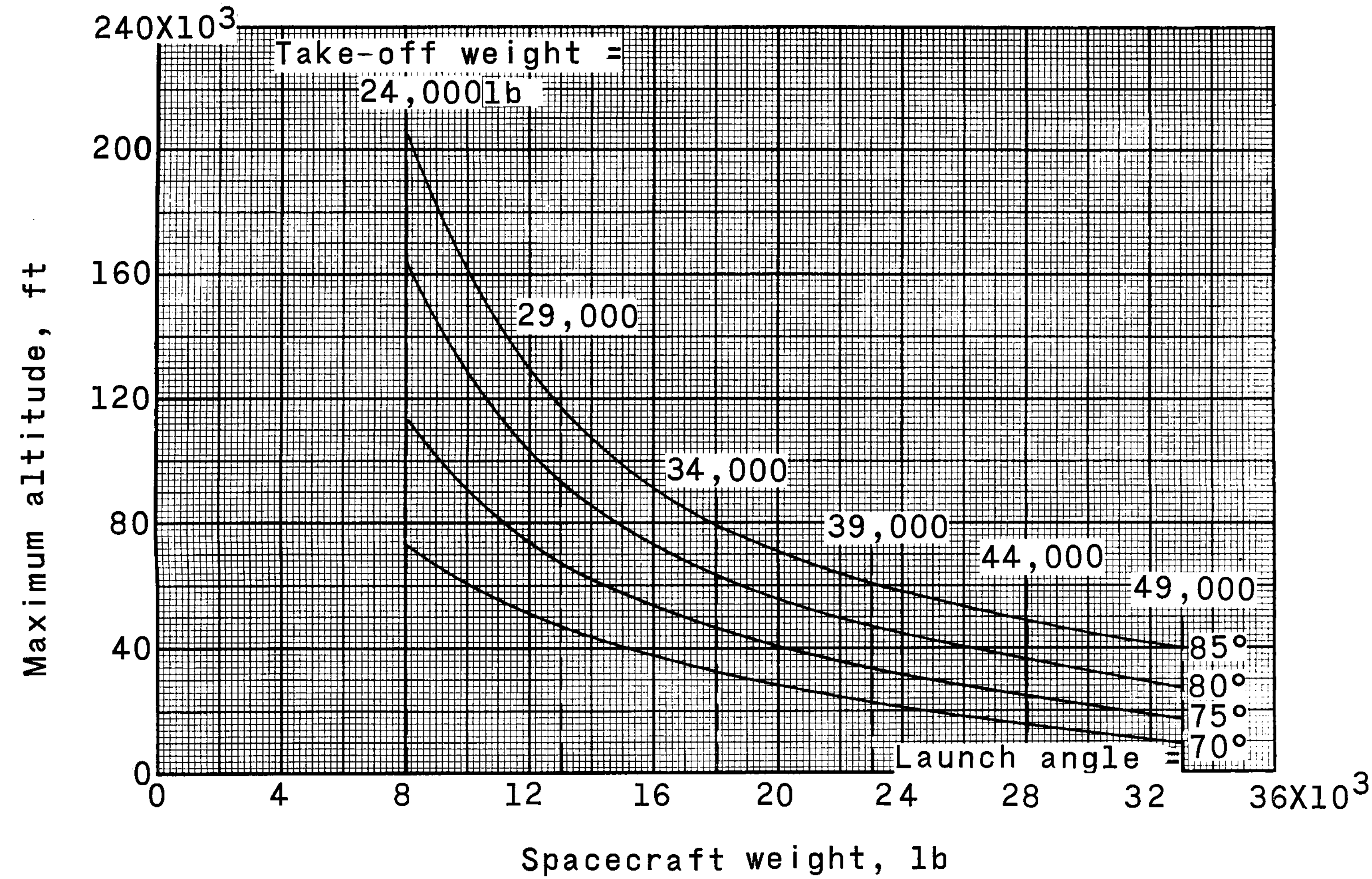

Figure 39.- Maximum altitude plotted against spacecraft weight as a function of take-off weight and launch angle for type I launch vehicle.

[redacted]

S-22

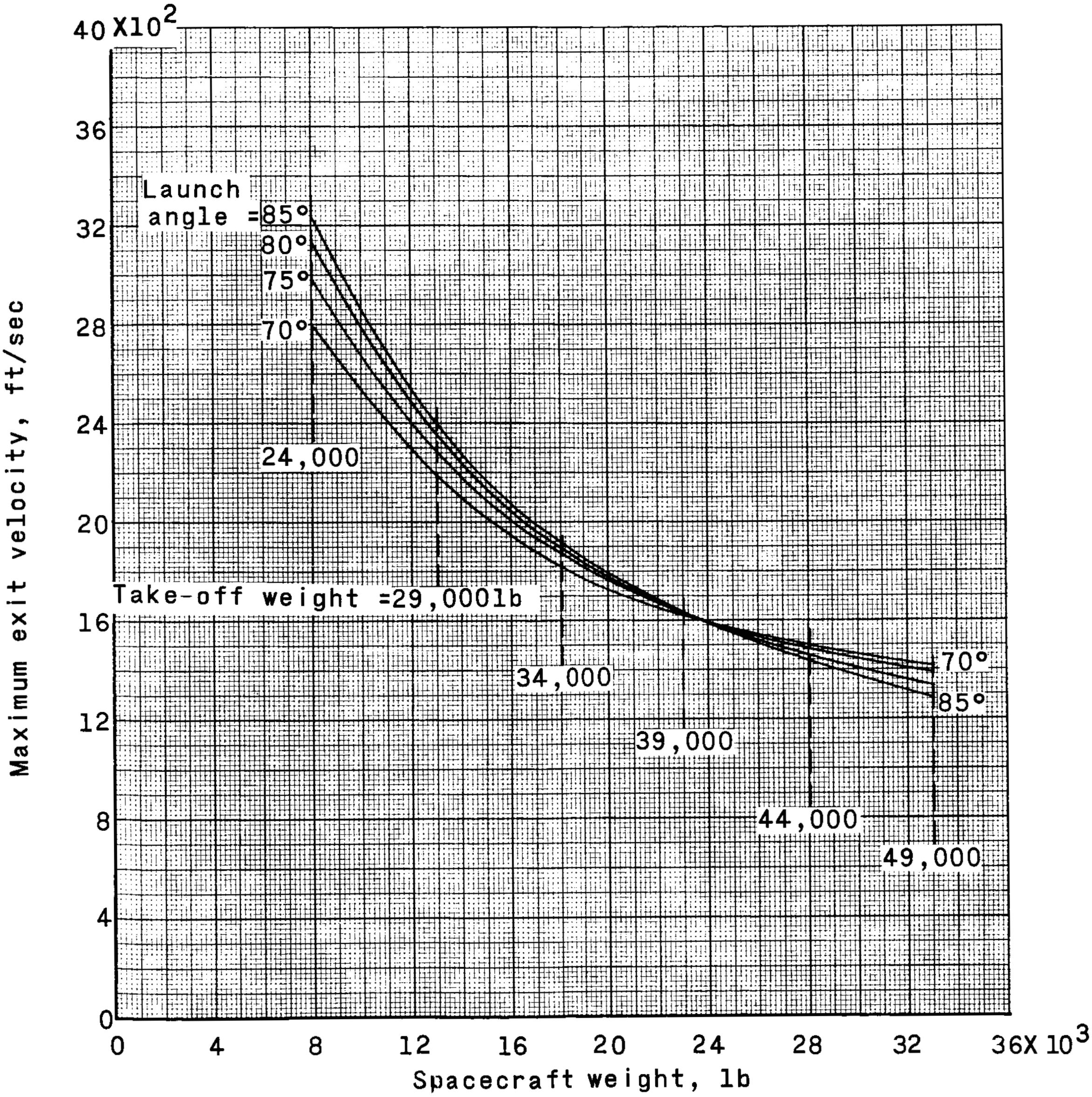

Figure 40. - Maximum exit velocity plotted against spacecraft weight as a function of take-off weight and launch angle for type I launch vehicle.

[redacted]

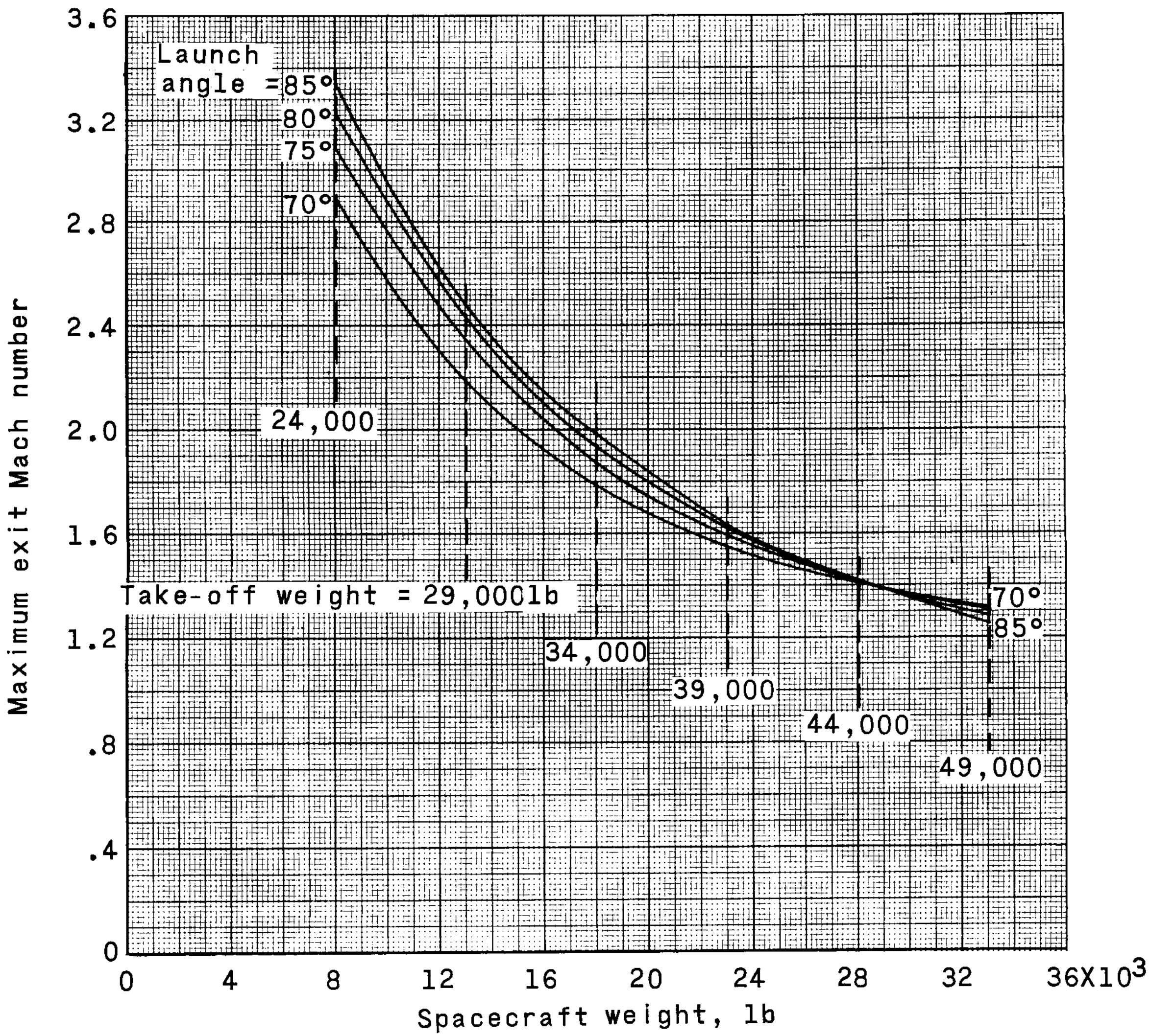

Figure 41.- Maximum exit Mach number plotted against spacecraft weight as a function of take-off weight and launch angle for type I launch vehicle.

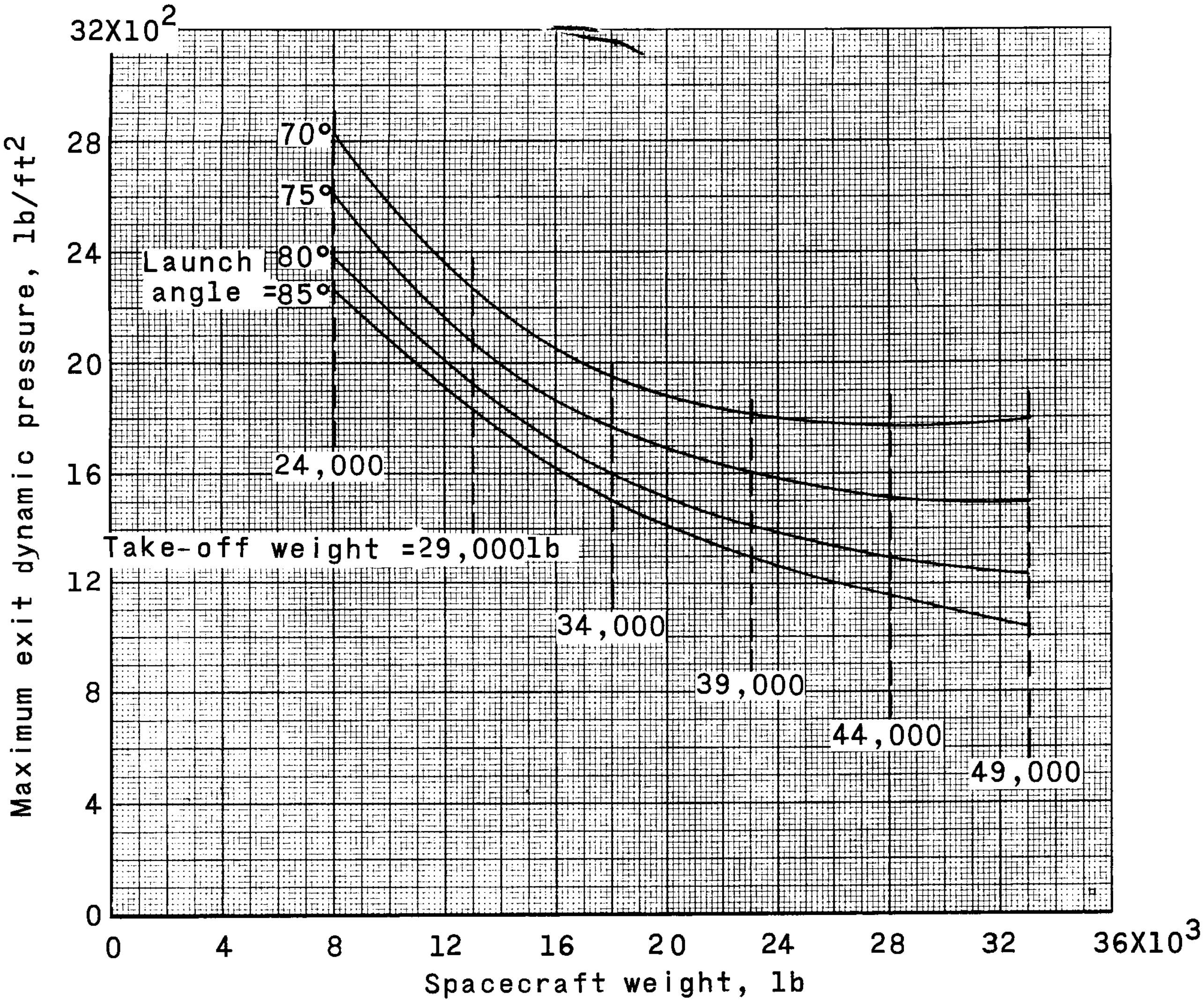

Figure 42.- Maximum exit dynamic pressure plotted against spacecraft weight as a function of take-off weight and launch angle for type I vehicle.

[redacted]

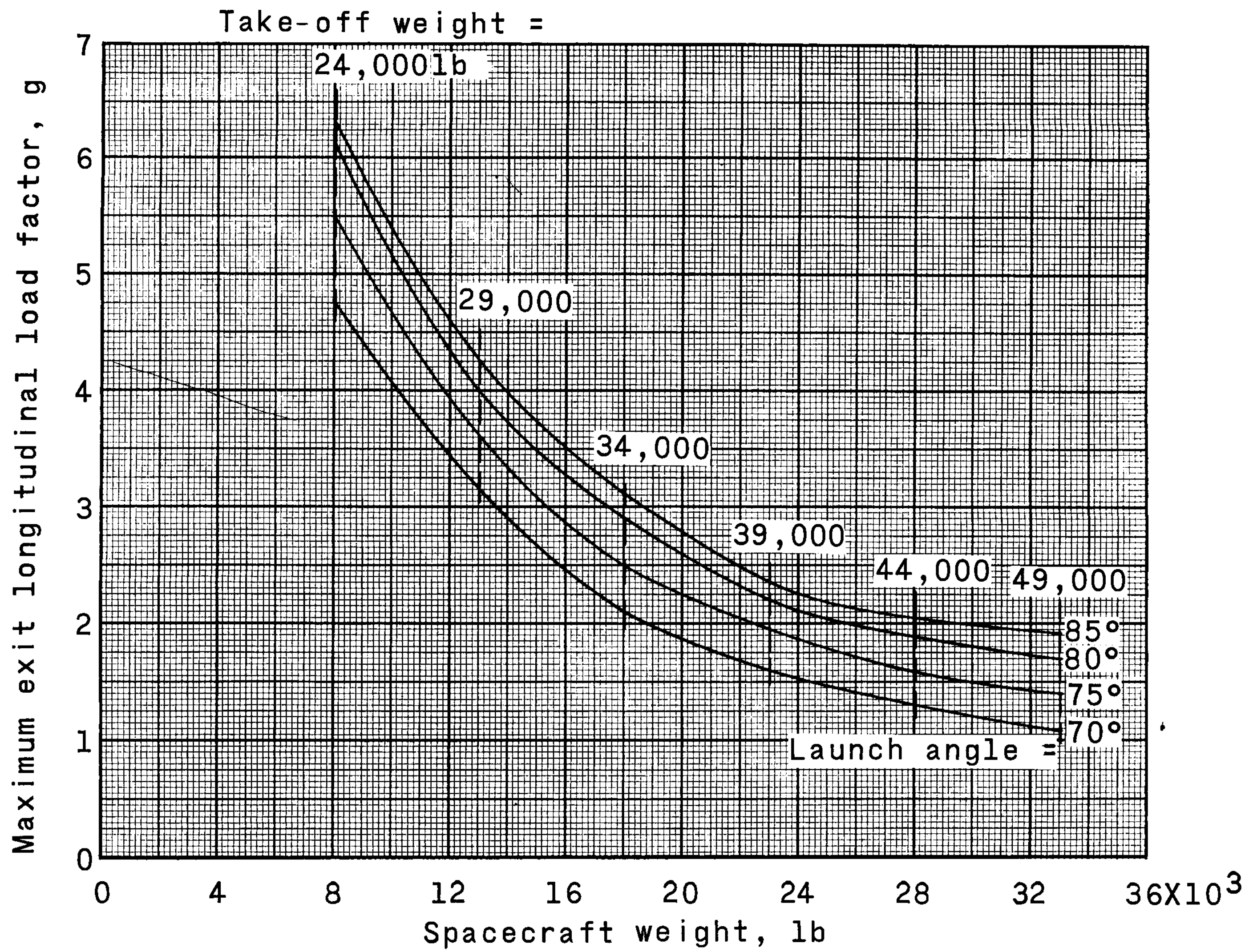

Figure 43.- Maximum exit longitudinal load factor plotted against spacecraft weight as a function of take-off weight and launch angle for type I launch vehicle.

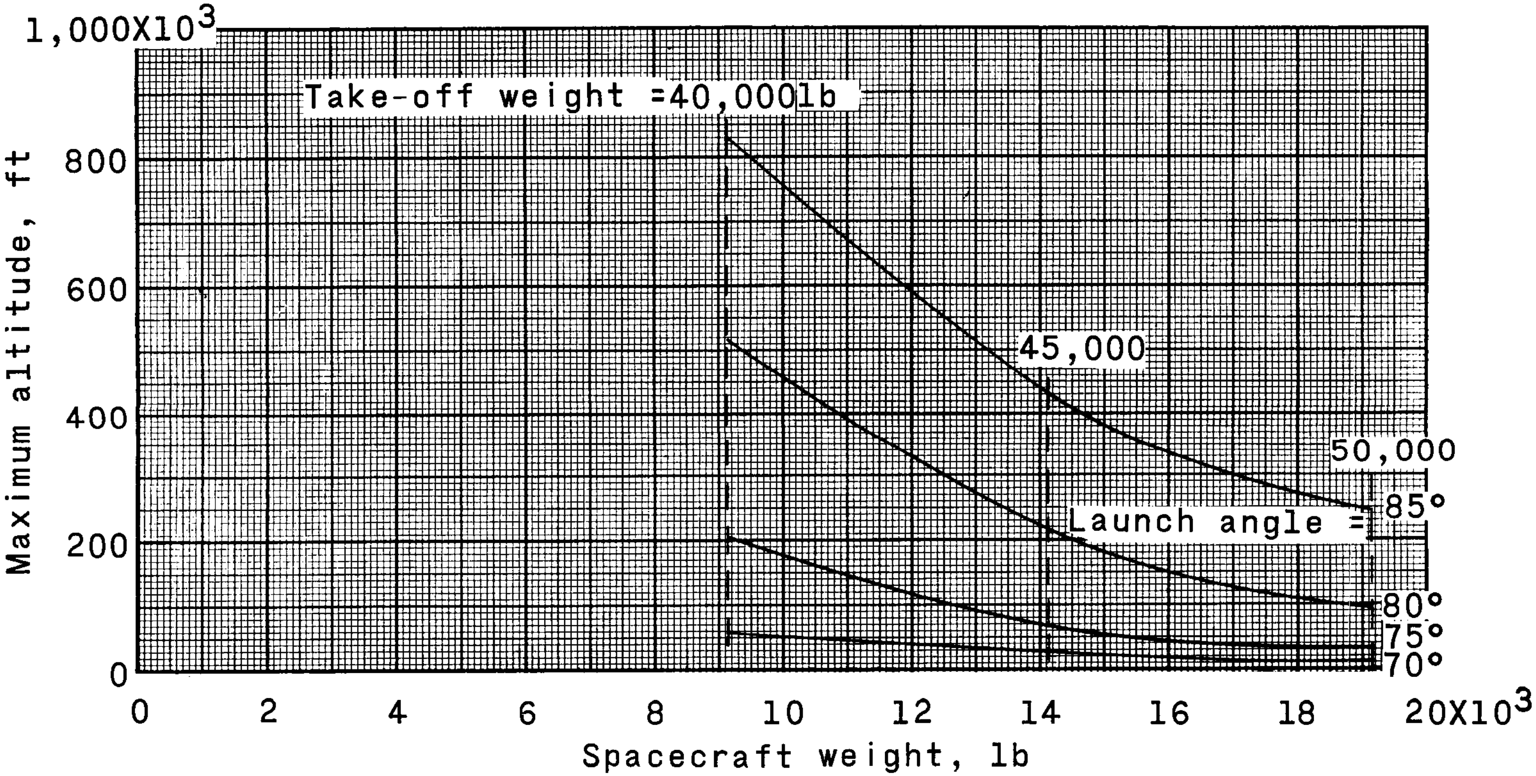

Figure 44.- Maximum altitude plotted against spacecraft weight as a function of take-off weight and launch angle for type II launch vehicle at a staging time of 19 seconds.

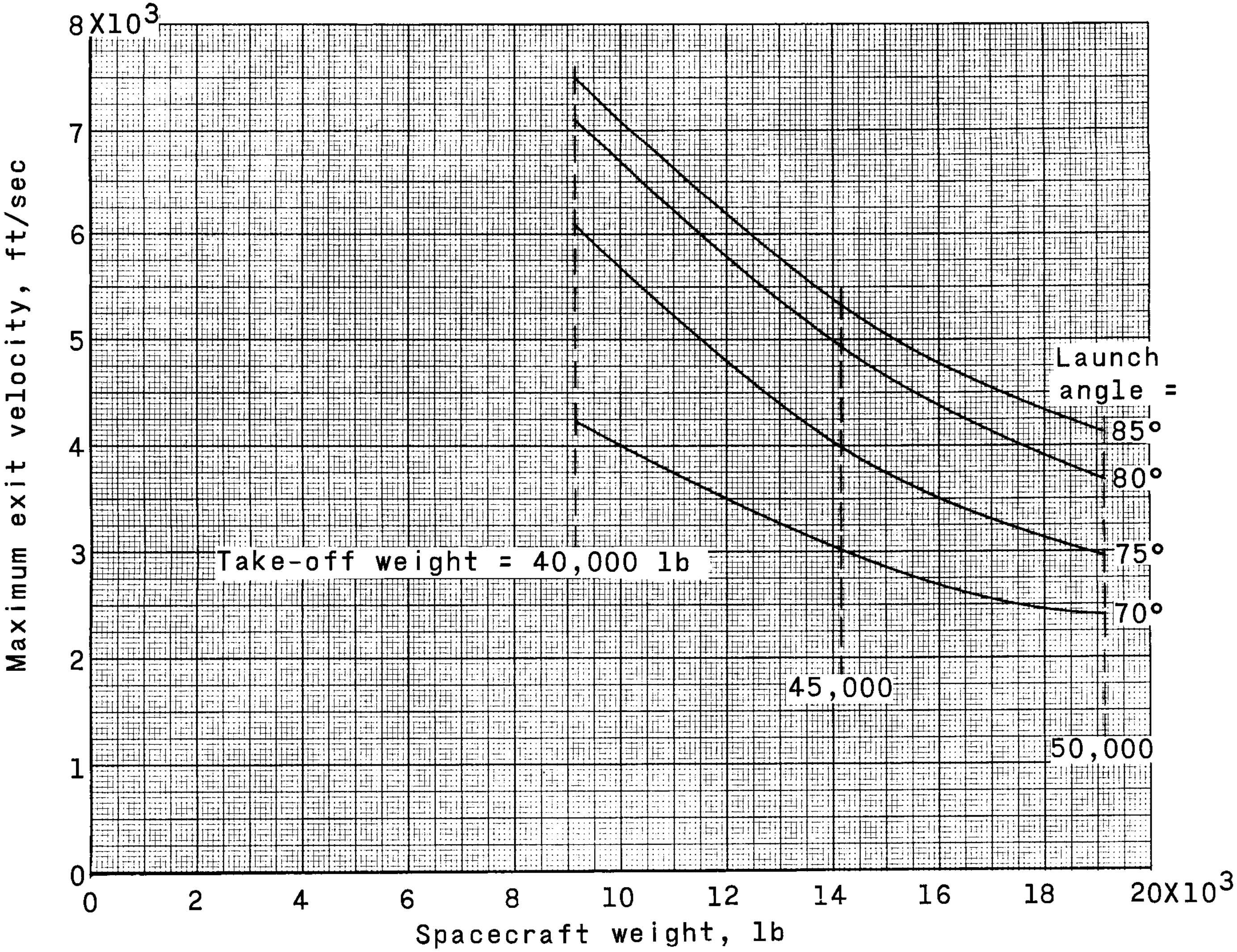

Figure 45.- Maximum exit velocity plotted against spacecraft weight as a function of take-off weight and launch angle for type II launch vehicle at a staging time of 19 seconds.

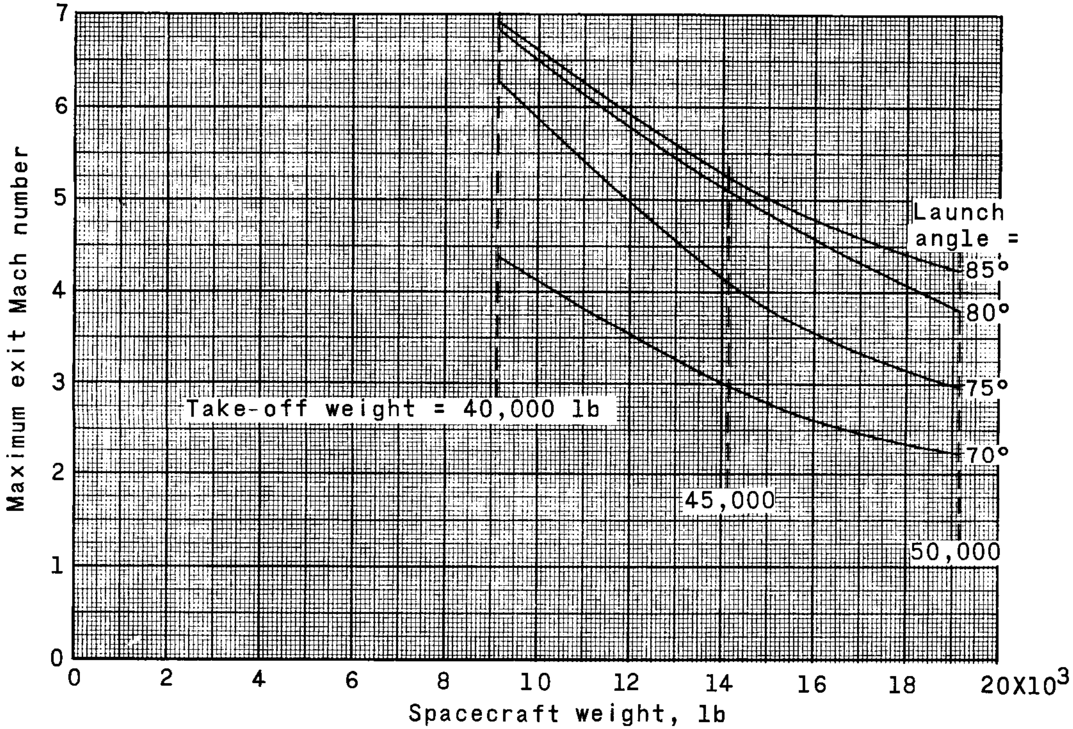

Figure 4[illegible].- Maximum exit Mach number plotted against spacecraft weight as a function of take-off we[illegible]ht and launch angle for type II launch vehicle at a staging time of 19 seconds.

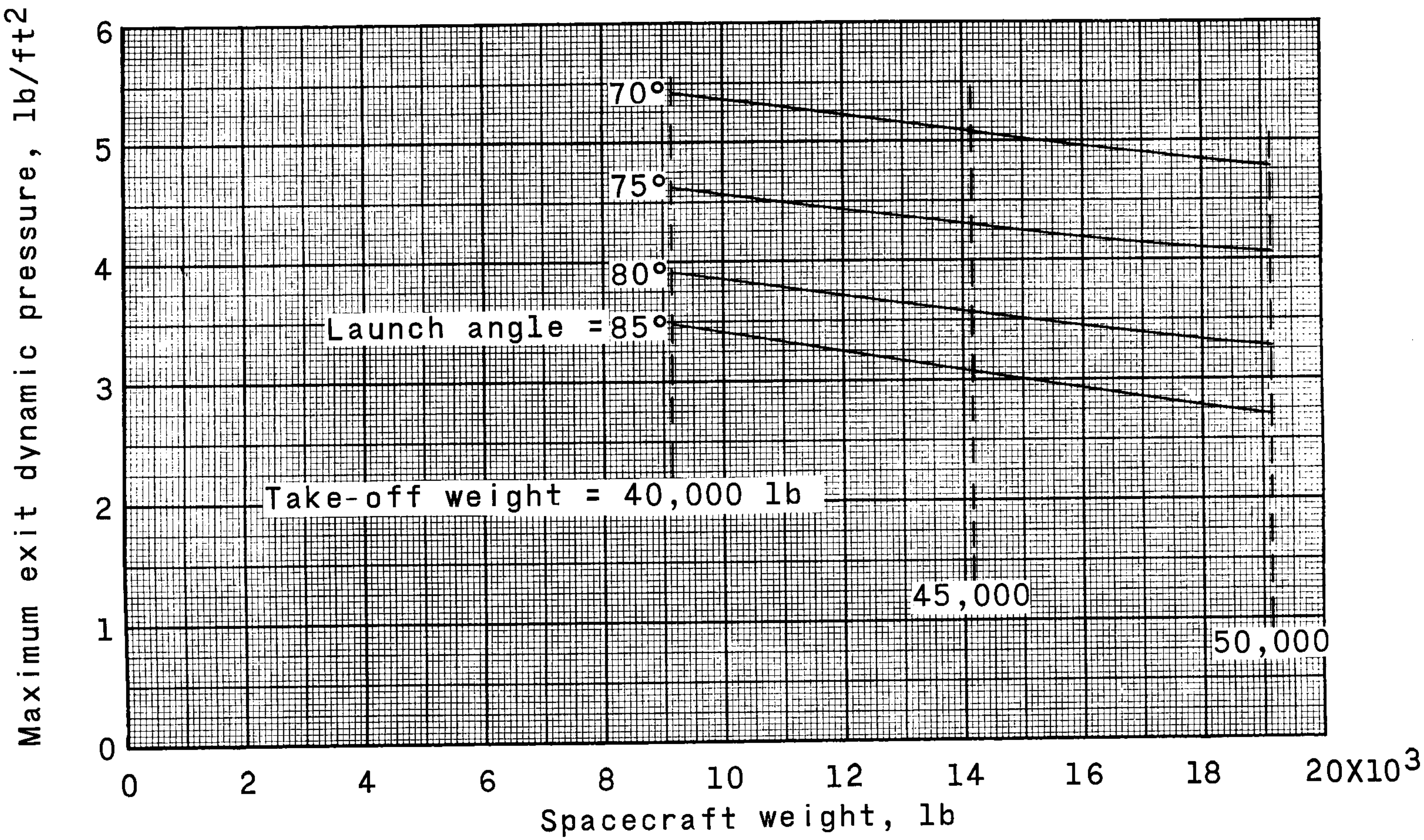

Figure 47.- Maximum exit dynamic pressure plotted against spacecraft weight as a function of take-off weight and launch angle for type II launch vehicle at a staging time of 19 seconds.

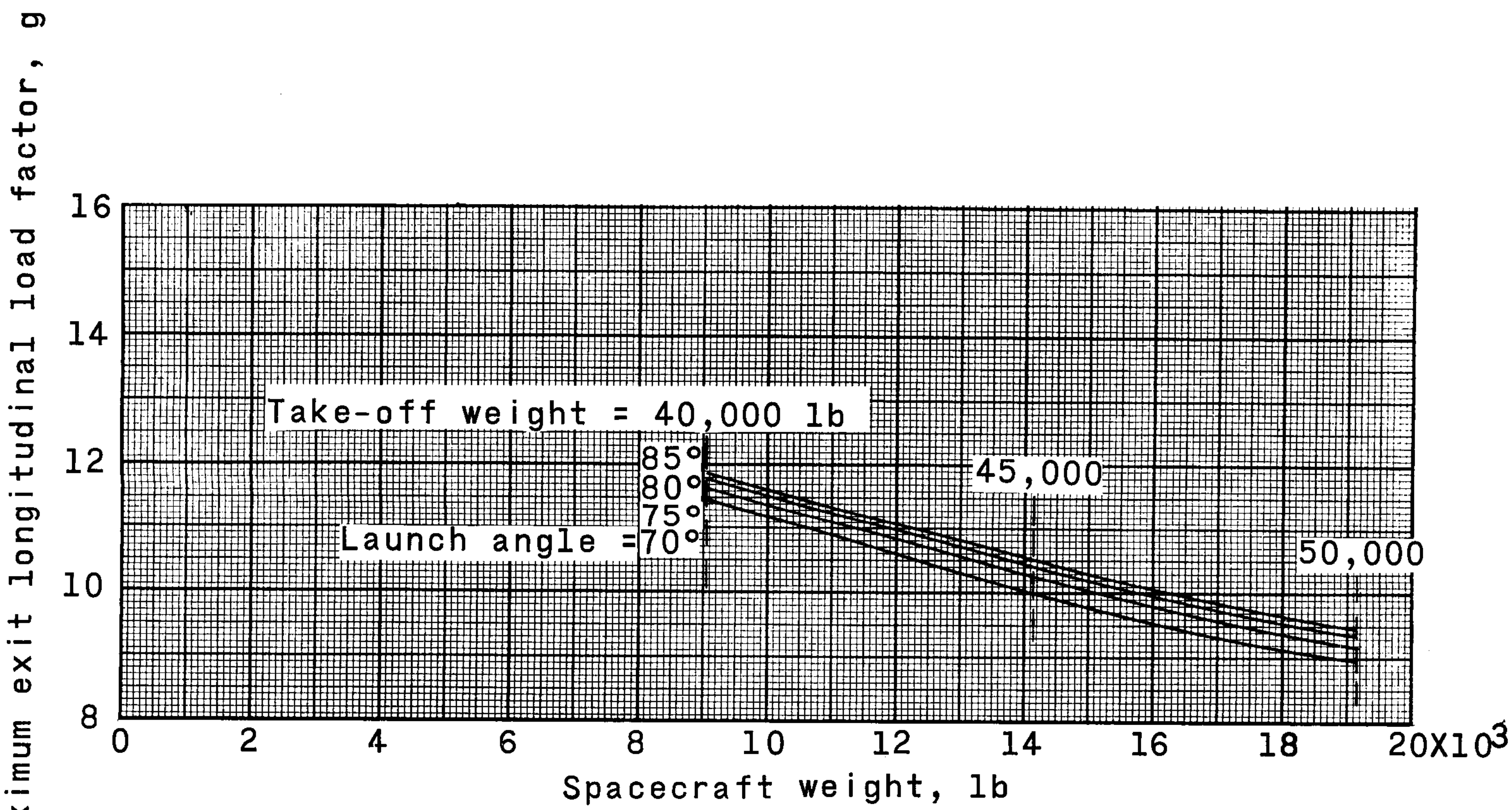

Figure 48.- Maximum exit longitudinal load factor plotted against spacecraft weight as a function of take-off weight and launch angle for type II launch vehicle at a staging time of 19 seconds.

[redacted]

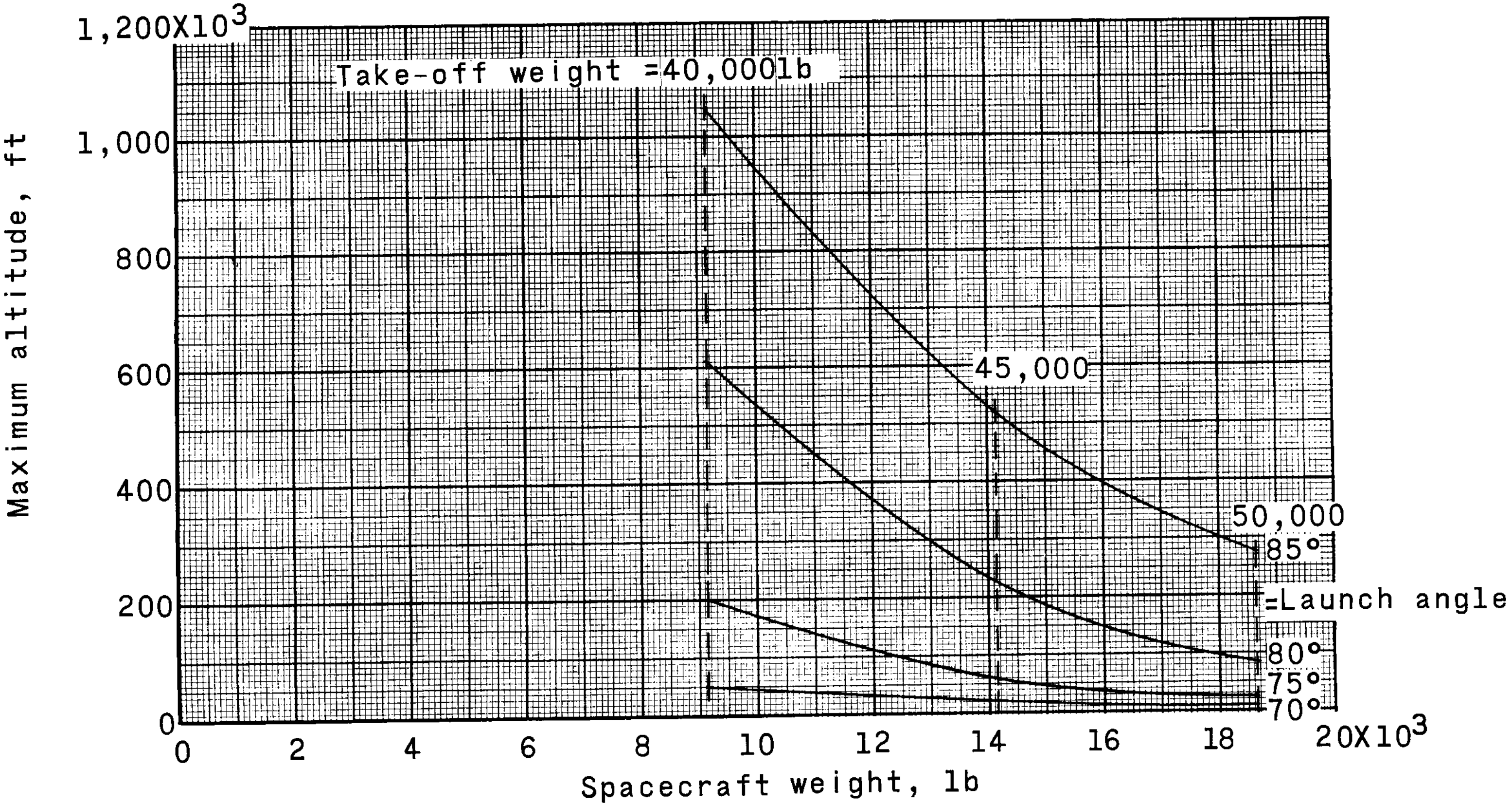

Figure 49.- Maximum altitude plotted against spacecraft weight as a function of take-off weight and launch angle for type II launch vehicle at a staging time of 23 seconds.

[redacted]

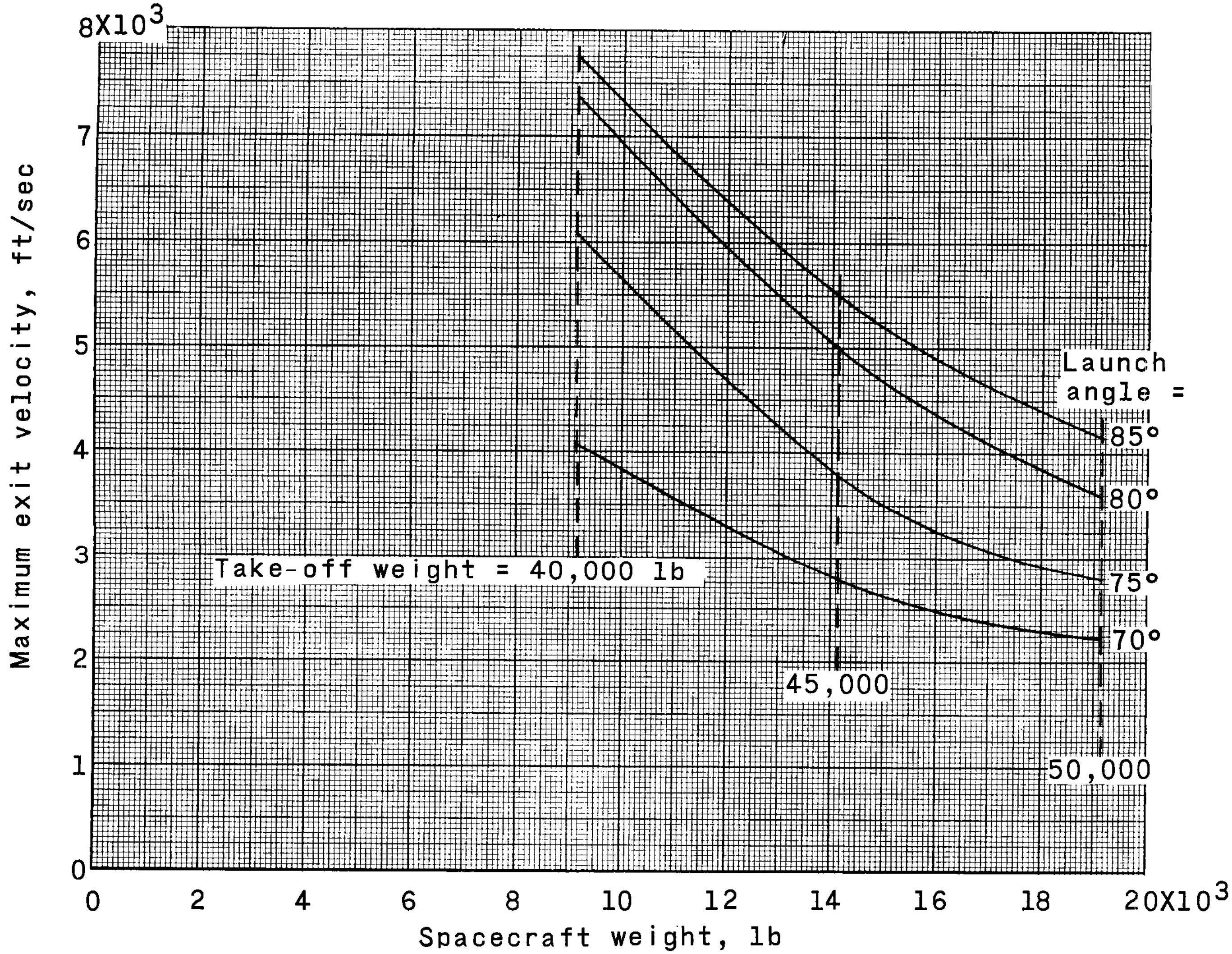

Figure 50.- Maximum exit velocity plotted against spacecraft weight as a function of take-off weight and launch angle for type II launch vehicle at a staging time of 23 seconds.

[redacted]

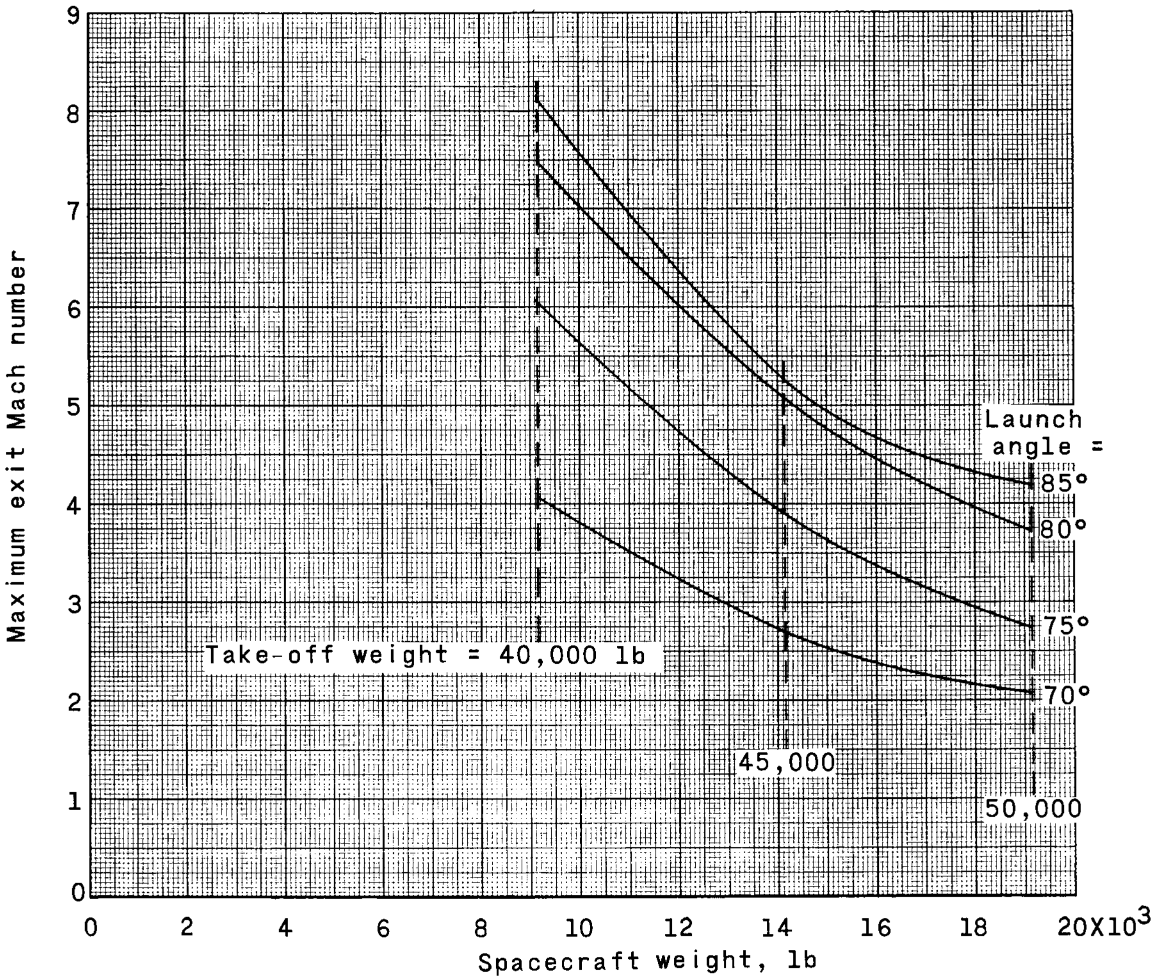

Figure 51.- Maximum exit Mach number plotted against spacecraft weight as a function of take-off weight and launch angle for type II launch vehicle at a staging time of 23 seconds.

S-22

[redacted]

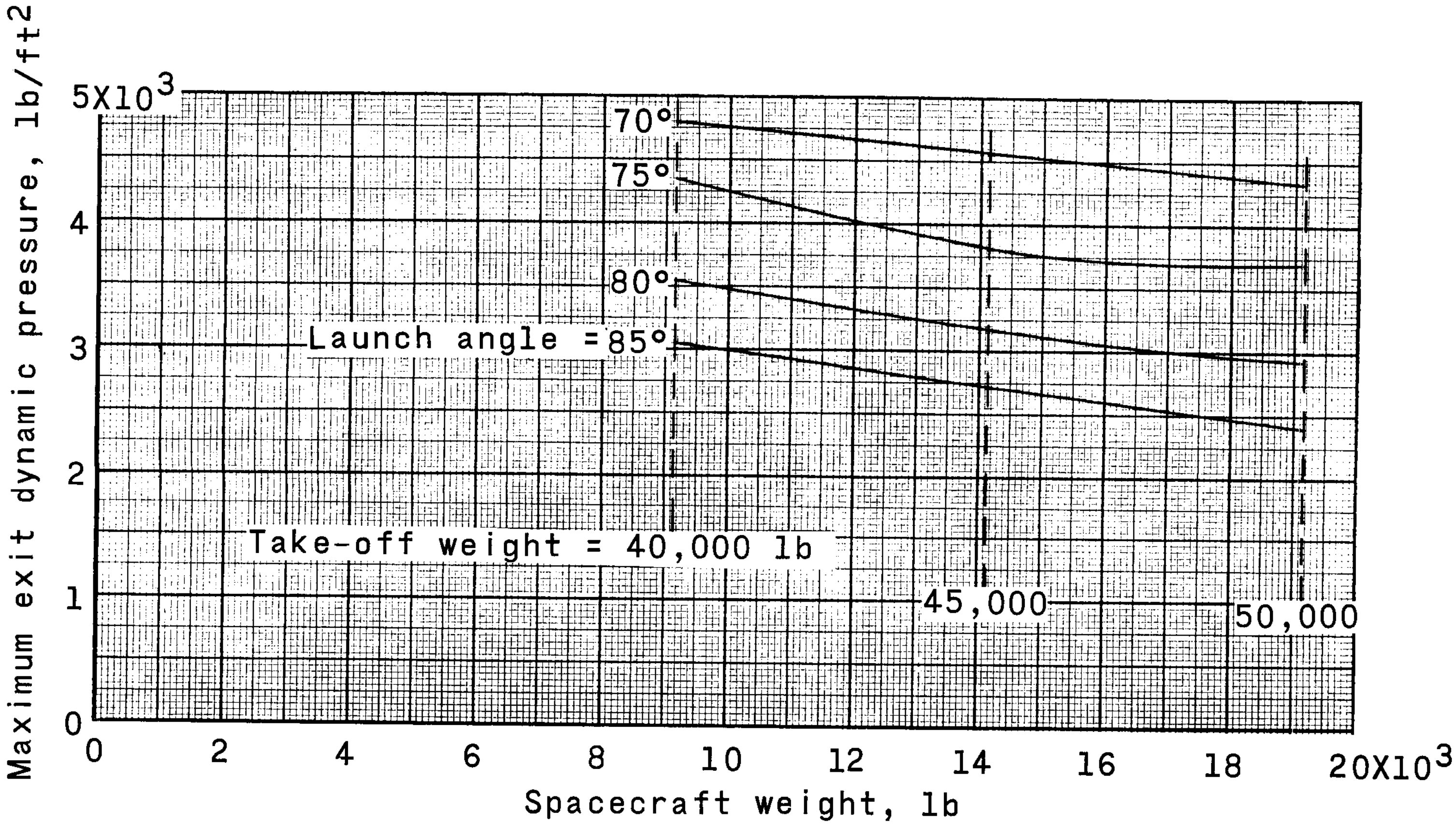

Figure 52.- Maximum exit dynamic pressure plotted against spacecraft weight as a function of take-off weight and launch angle for type II launch vehicle at a staging time of 23 seconds.

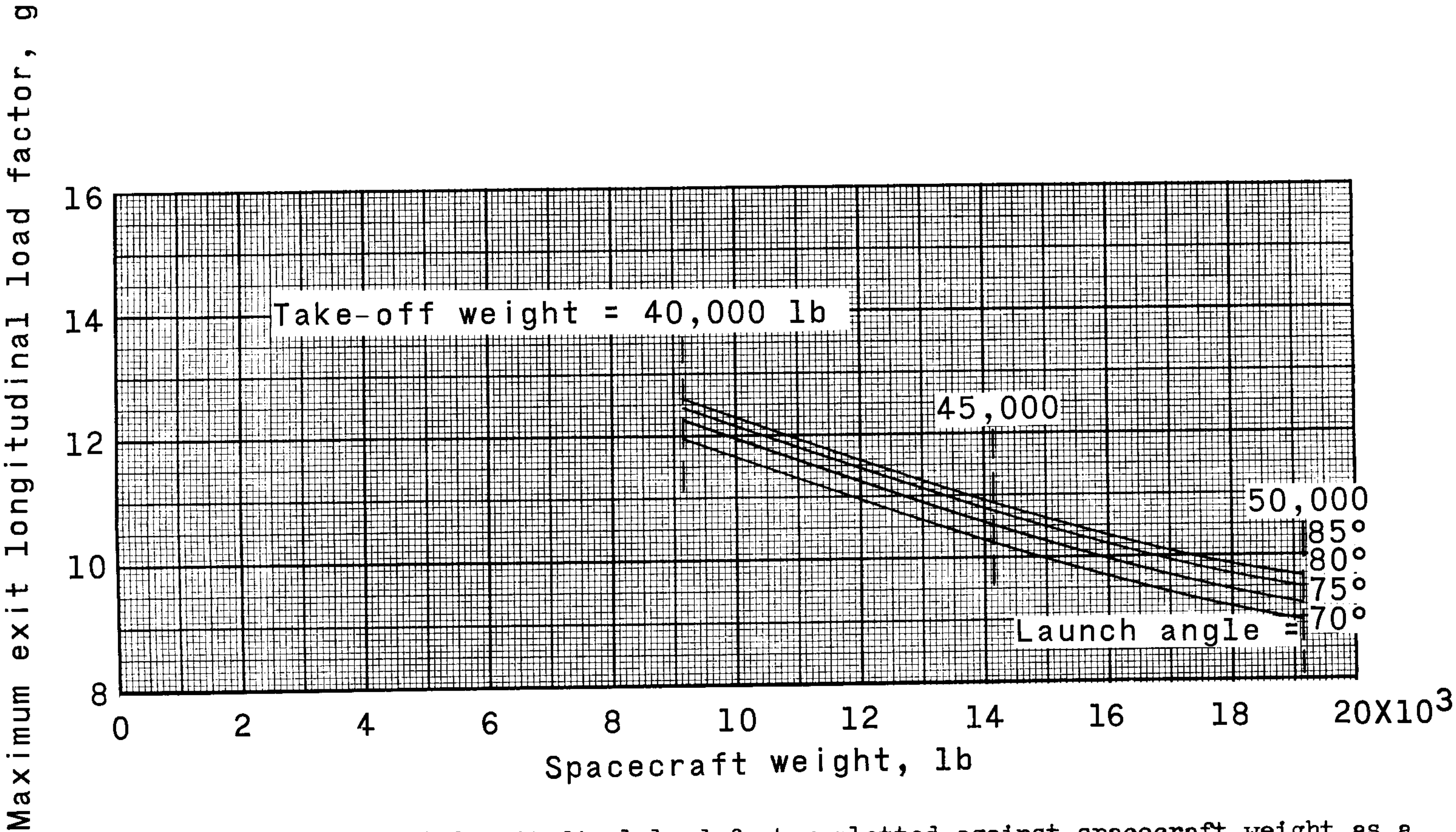

Figure 53.- Maximum exit longitudinal load factor plotted against spacecraft weight as a function of take-off weight and launch angle for type II launch vehicle at a staging time of 23 seconds.

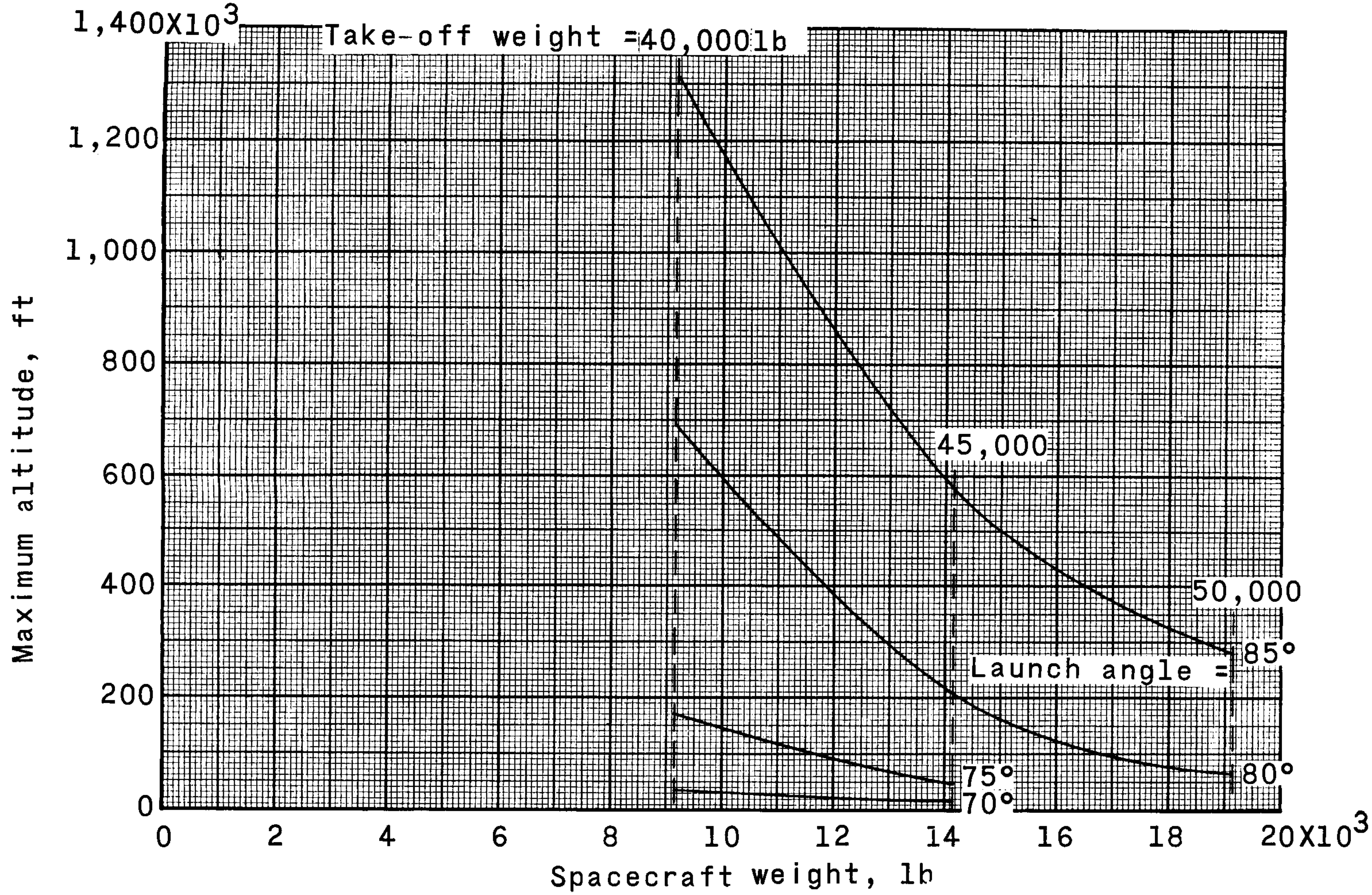

Figure 54.- Maximum altitude plotted against spacecraft weight as a function of take-off weight and launch angle for type II launch vehicle at a staging time of 27 seconds.

[redacted]

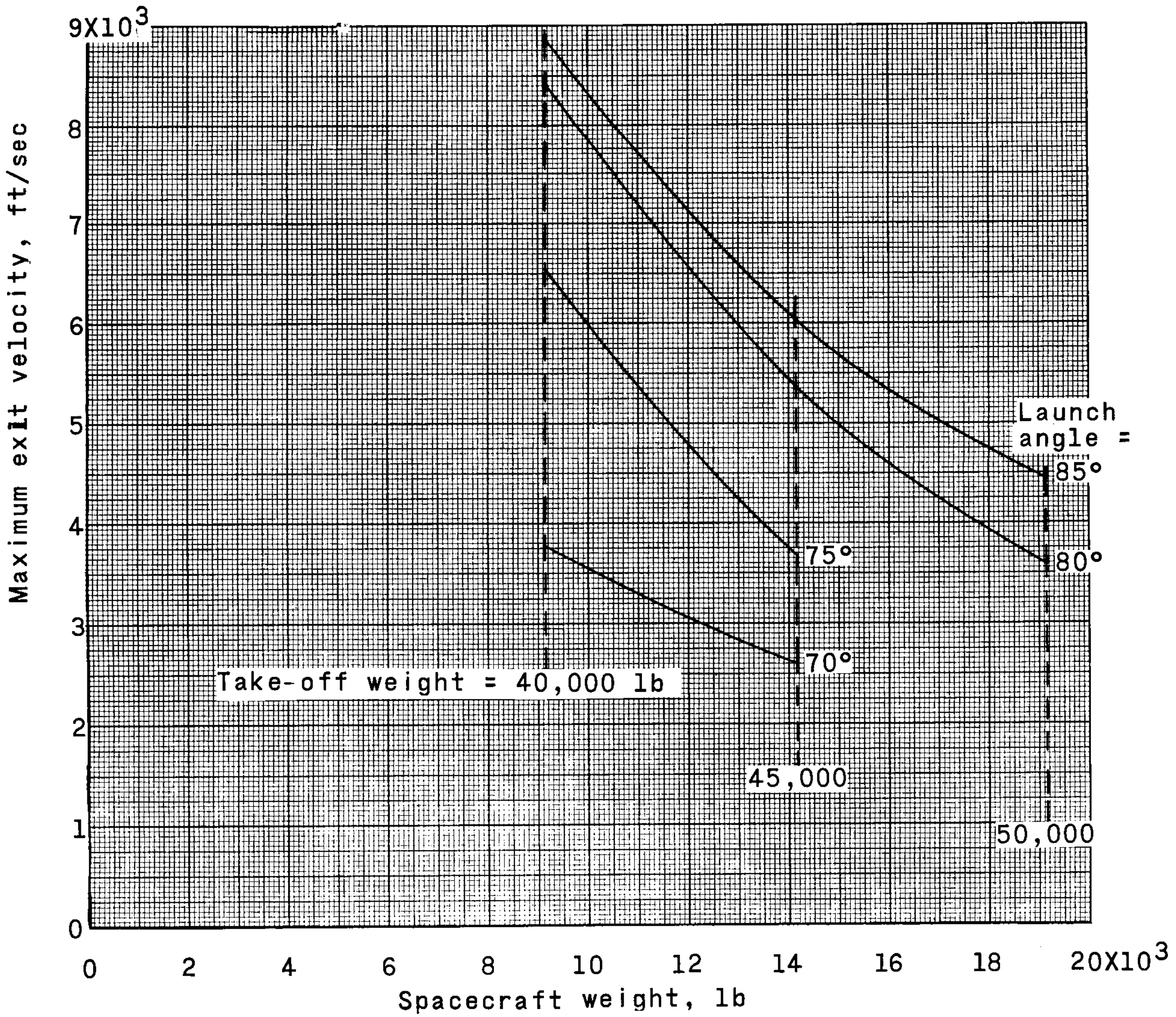

Figure 55.- Maximum exit velocity plotted against spacecraft weight as a function of take-off weight and launch angle for type II launch vehicle at a staging time of 27 seconds.

S-22

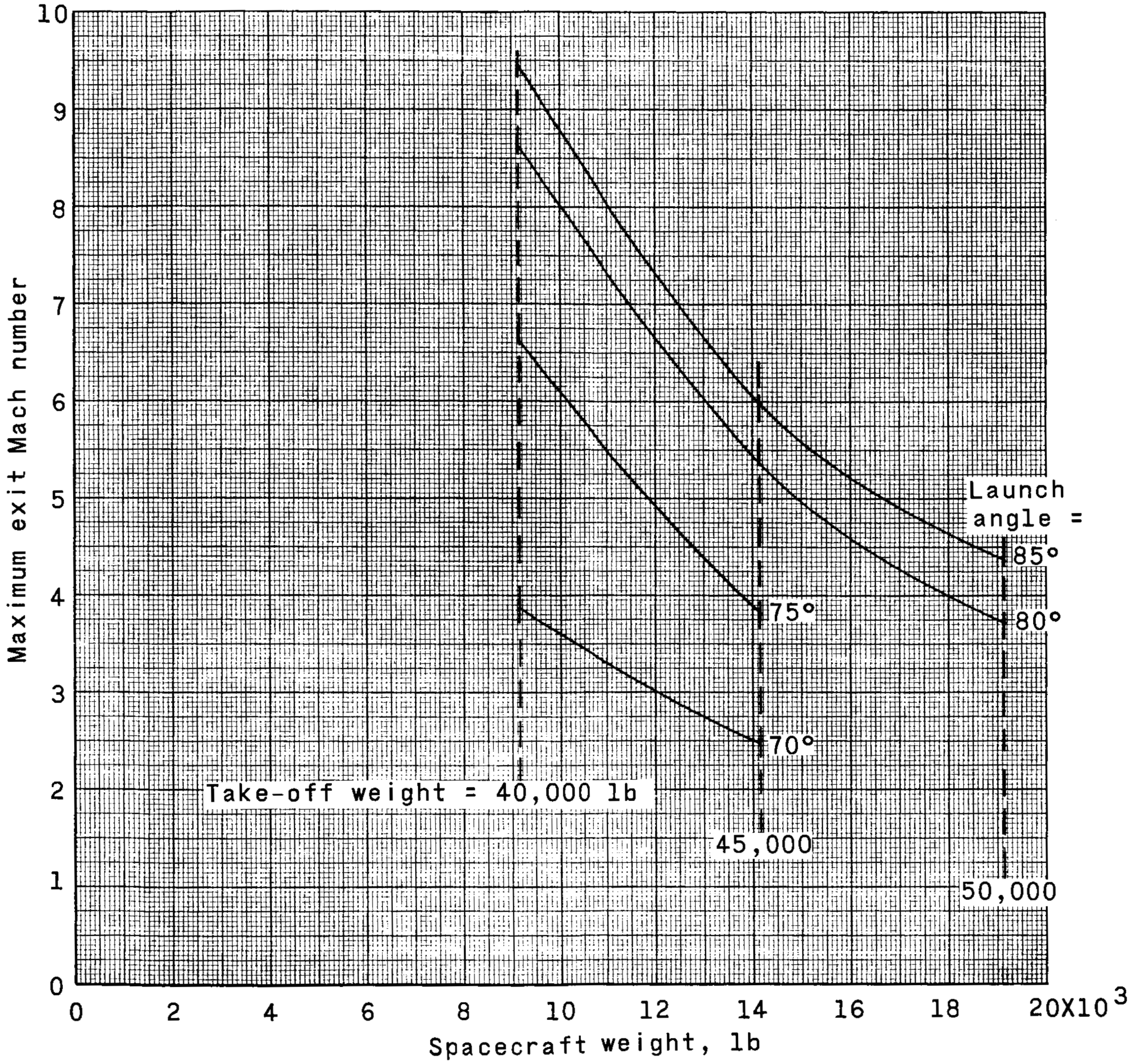

Figure 56. - Maximum exit Mach number plotted against spacecraft weight as a function of take-off weight and launch angle for type II launch vehicle at a staging time of 27 seconds.

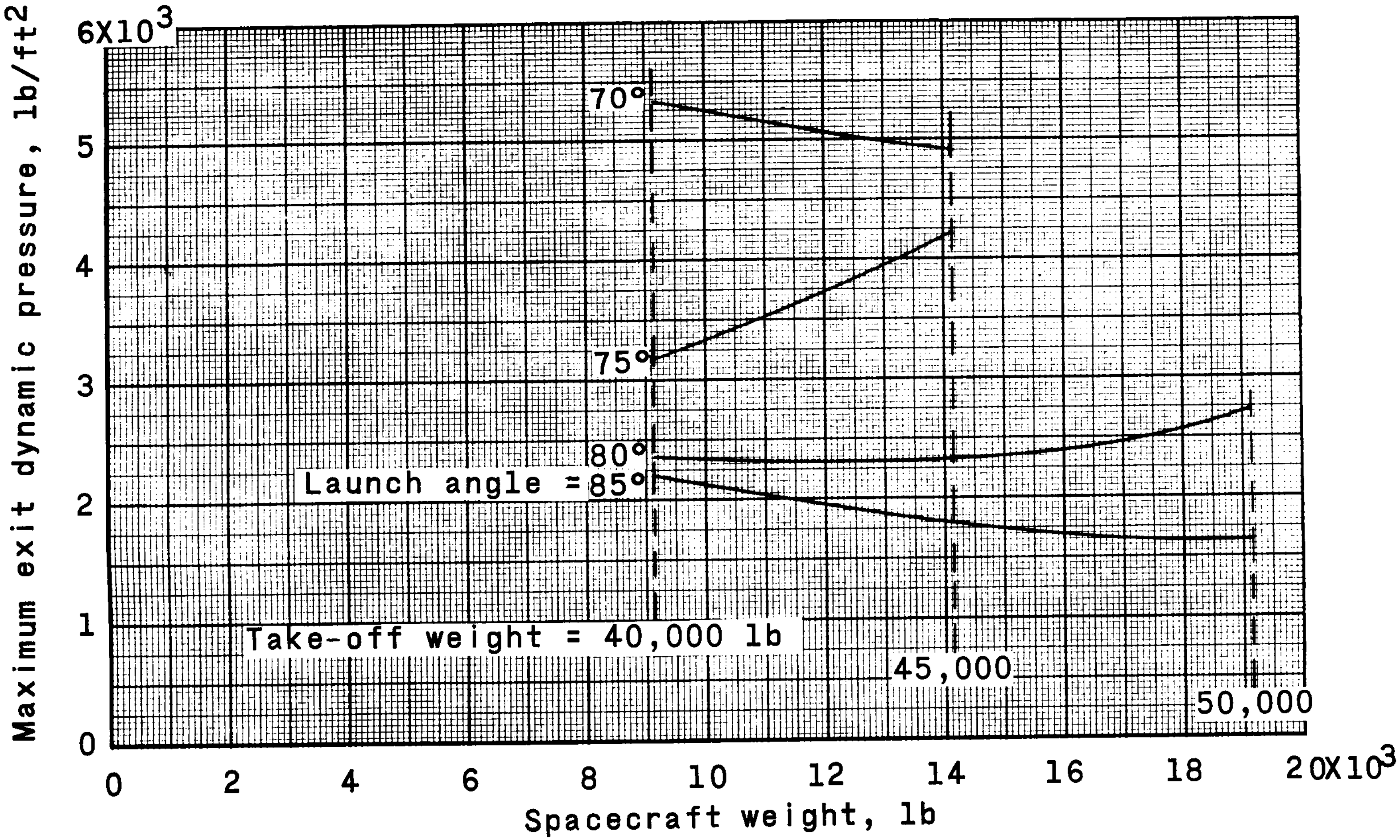

Figure 57.- Maximum exit dynamic pressure plotted against spacecraft weight as a function of take-off weight and launch angle for type II launch vehicle at a staging time of 27 seconds.

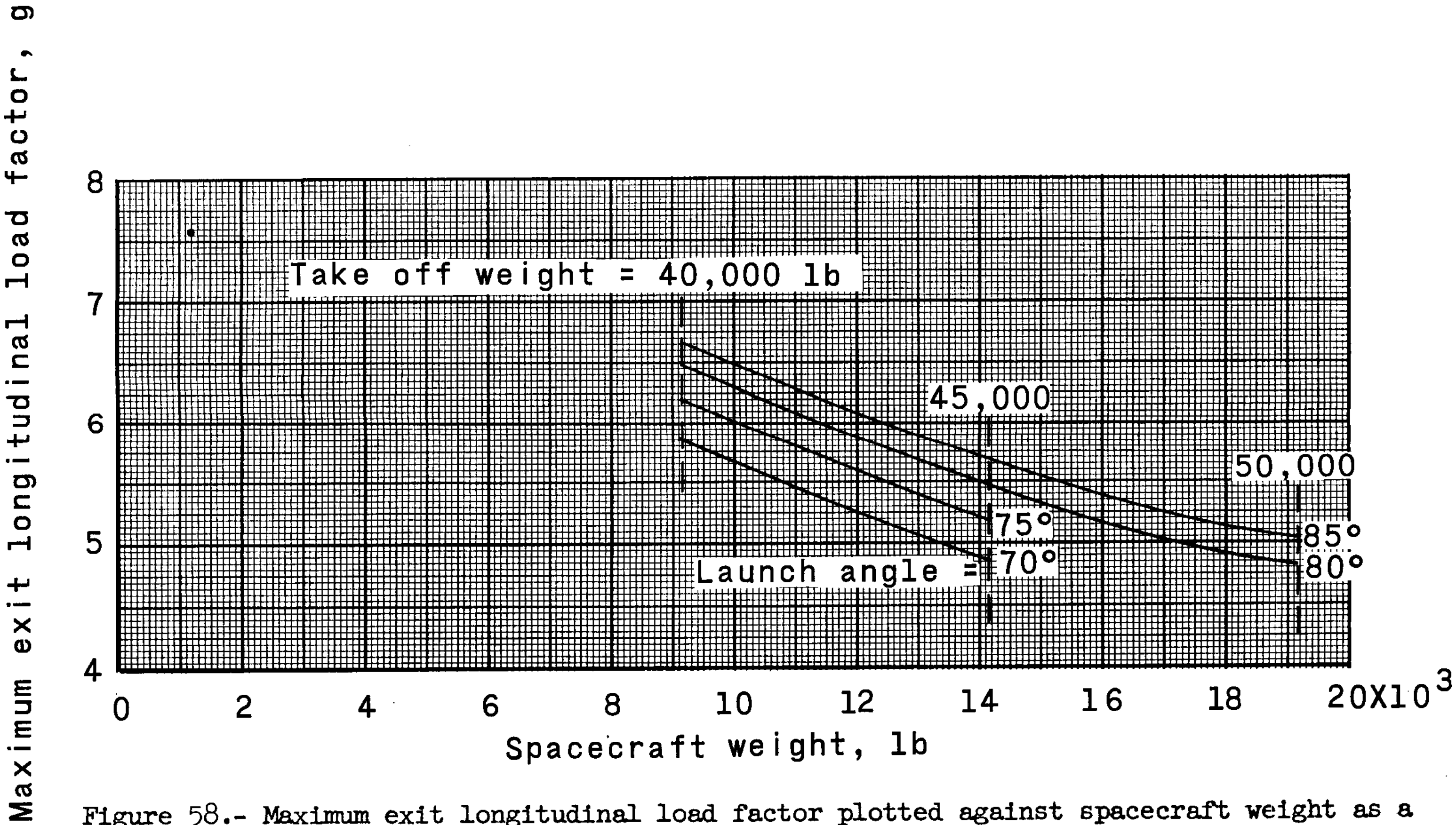

Figure 58.- Maximum exit longitudinal load factor plotted against spacecraft weight as a function of take-off weight and launch angle for type II launch vehicle at a staging time of 27 seconds.

[redacted]

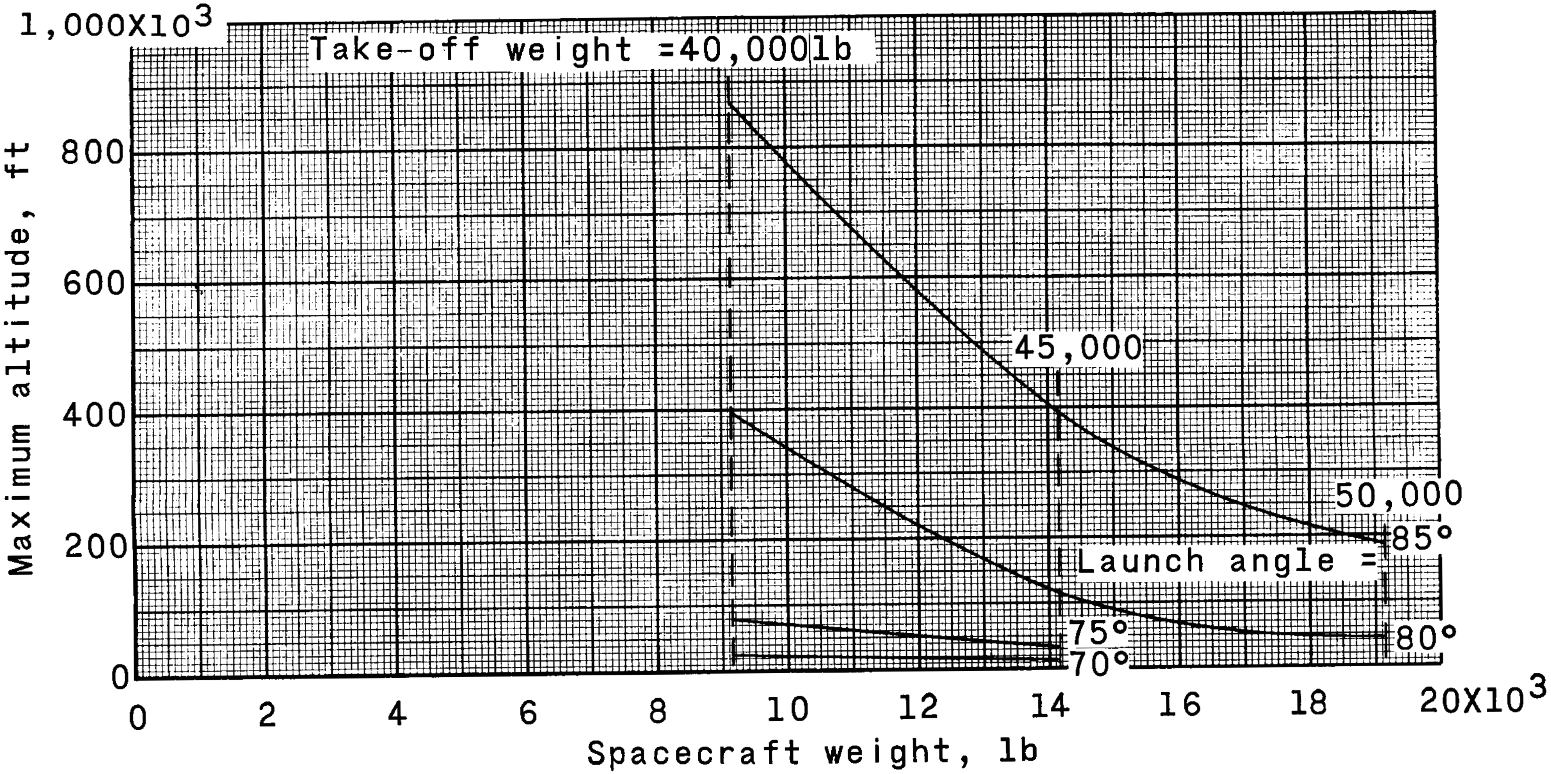

Figure 59.- Maximum altitude plotted against spacecraft weight as a function of take-off weight and launch angle for type II launch vehicle at a staging time of 31 seconds.

[redacted]

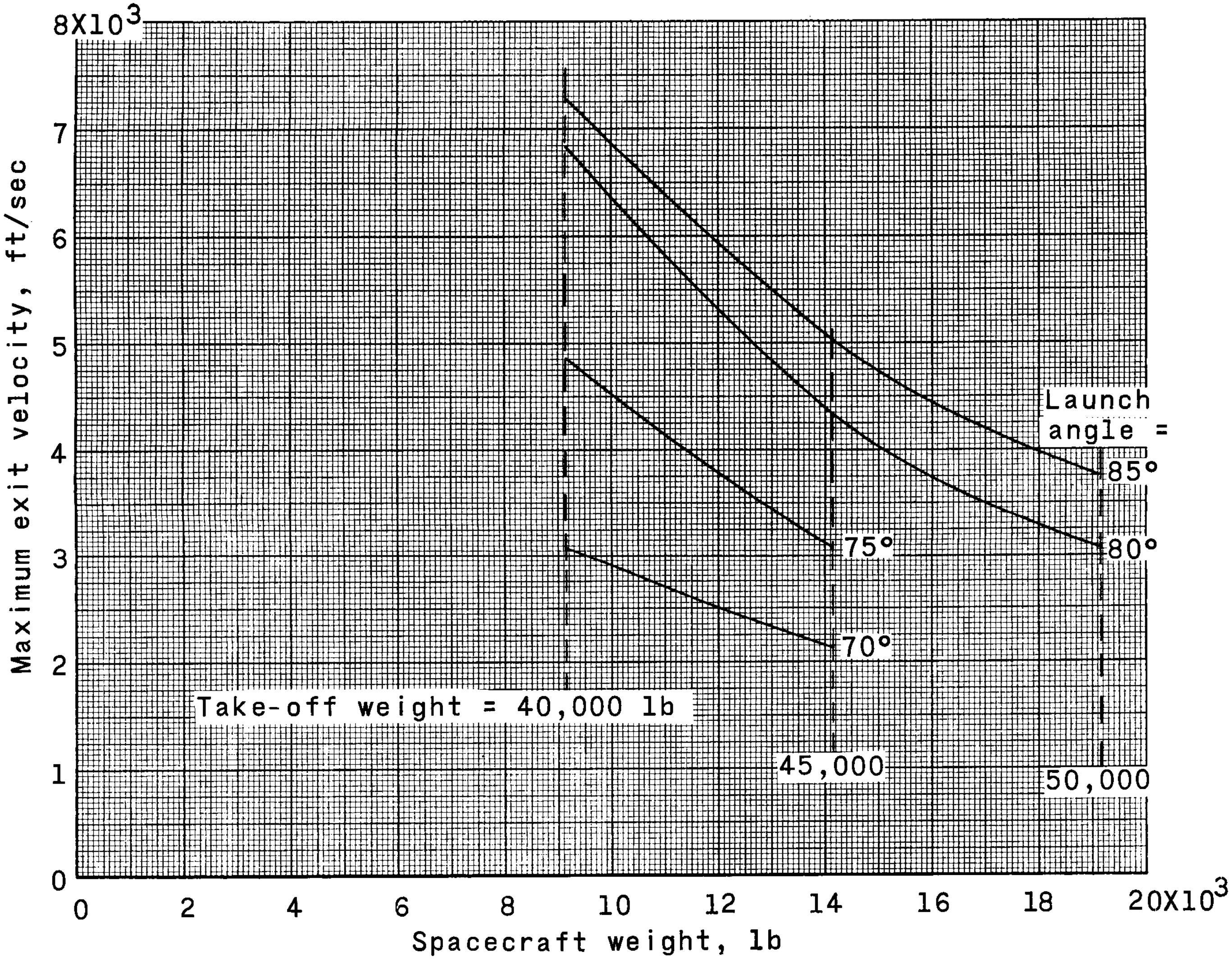

Figure 60.- Maximum exit velocity plotted against spacecraft weight as a function of take-off weight and launch angle for type II launch vehicle at a staging time of 31 seconds.

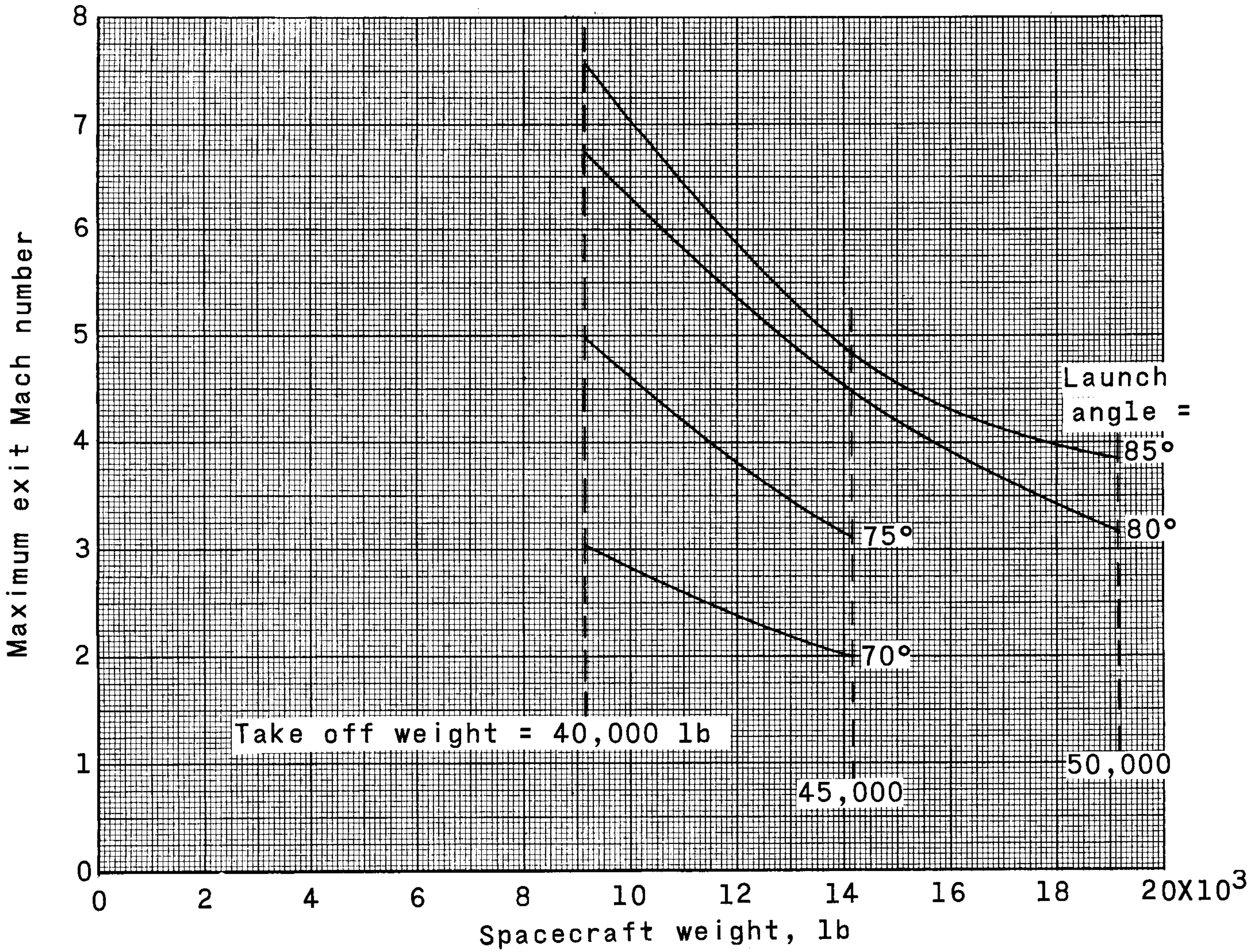

Figure 61.- Maximum exit Mach number plotted against spacecraft weight as a function of take-off weight and launch angle for type II launch vehicle at a staging time of 31 seconds.

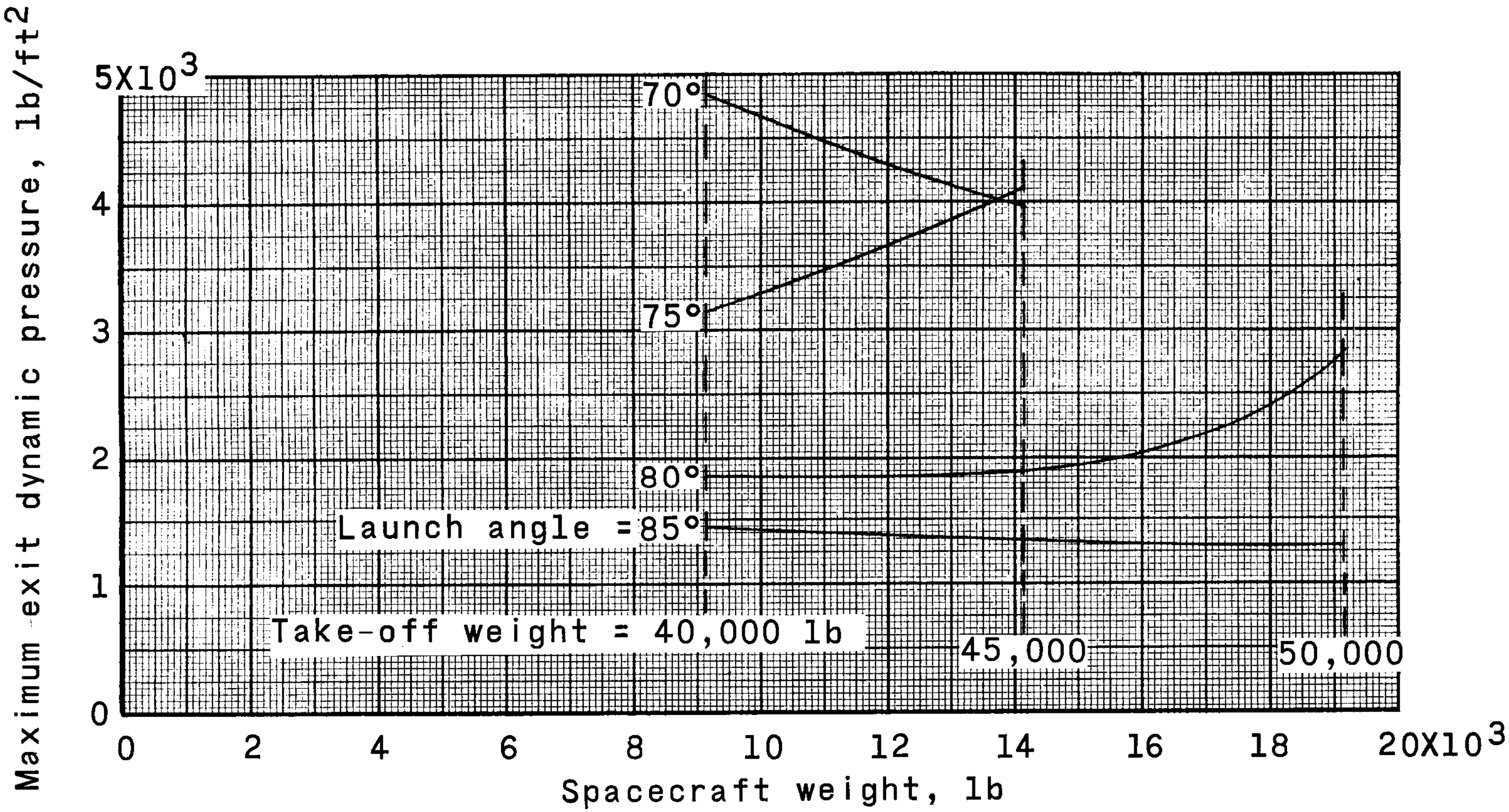

Figure 62.- Maximum exit dynamic pressure plotted against spacecraft weight as a function of take-off weight and launch angle for type II launch vehicle at a staging time of 31 seconds.

[redacted]

[redacted]

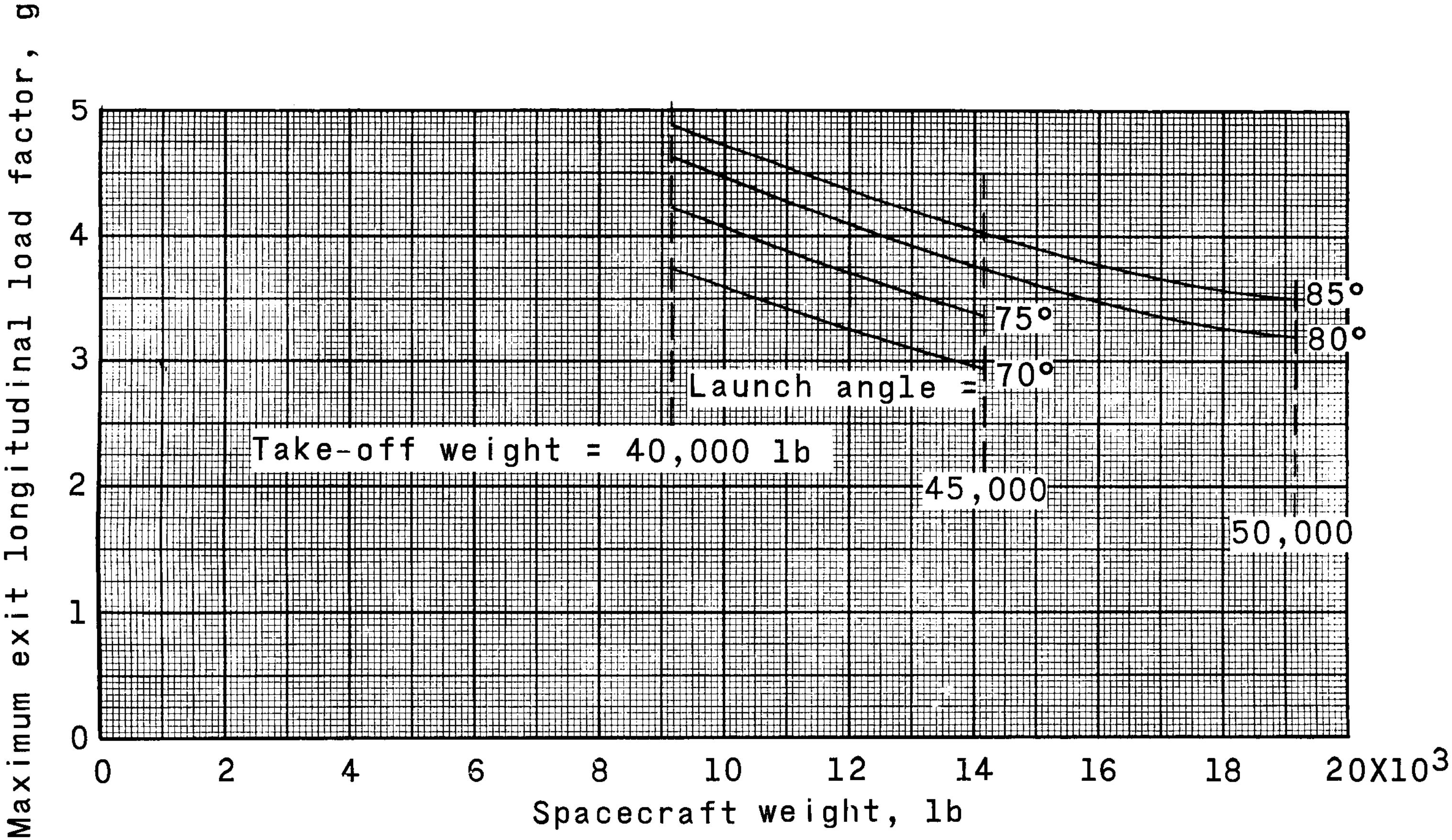

Figure 63.- Maximum exit longitudinal load factor plotted against spacecraft weight as a function of take-off weight and launch angle for type II launch vehicle at a staging time of 31 seconds.

[redacted]